INFORMATION TO USERS

This manuscript has been reproduced from the microfilm master. UMI films the text directly from the original or copy submitted. Thus, some thesis and dissertation copies are in typewriter face, while others may be from any type of computer printer.

The quality of this reproduction is dependent upon the quality of the copy submitted. Broken or indistinct print, colored or poor quality illustrations and photographs, print bleedthrough, substandard margins, and improper alignment can adversely affect reproduction.

In the unlikely event that the author did not send UMI a complete manuscript and there are missing pages, these will be noted. Also, if unauthorized copyright material had to be removed, a note will indicate the deletion.

Oversize materials (e.g., maps, drawings, charts) are reproduced by sectioning the original, beginning at the upper left-hand corner and continuing from left to right in equal sections with small overlaps.

ProQuest Information and Learning
300 North Zeeb Road, Ann Arbor, MI 48106-1346 USA
800-521-0600

UMI®

G-QUADRUPLEX DNA: A POTENTIAL TARGET FOR ANTI-CANCER DRUG DESIGN

by

YOSSRY HUSSEIN

A dissertation submitted to the Graduate Faculty in Biology in partial fulfillment of the requirements for the degree of Doctor of Philosophy, The City University of New York

2003

UMI Number: 3083674

ProQuest Information and Learning Company
300 North Zeeb Road
P.O. Box 1346
Ann Arbor, MI 48106-1346

This manuscript has been read and accepted for the Graduate Faculty in Biology in satisfaction of the dissertation requirement for the degree of Doctor of Philosophy.

2/13/03
Date

Chair of the Examining Committee

2/19/03
Date

Executive Officer

Prof. Richard Magliozzo

Prof. Zhen Huang

Prof. Jennifer Basil

Prof. He Qi

Supervisory Committee

The City University of New York

The City University of New York

Abstract

G-QUADRUPLEX DNA AS POTENTIAL ANTI-CANCER TARGET

by

Yossry Hussein

Advisor: Professor Lesley Davenport

Human telomeres contain many repeats of the guanine rich hexamer (TTAGGG), the oligonucleotides $(TTAGGG)_4$ form G-quadruplex DNA structures in the presence of physiological concentration of K^+ ions.

A new class of compounds has recently been identified that bind to and stabilize the quadruplex DNA structures found at the end of human chromosomes. These have been referred to as G-quadruplex interactive agents, or QIAs. Recent interest has focused on their potential application in cancer chemotherapy. Increasing the stability of the quadruplex region is expected to inhibit the progression of telomerase, the enzyme that adds

repetitive DNA sequence to the end of human chromosomes. About 90% of cancer cells are known to exhibit telomerase activity.

In the current study, the binding and selectivity of a series of porphyrin (polycyclic compounds) derivatives has been explored as potential G-quadruplex interactive agents using spectroscopic (absorption and/or fluorescence) and biological (gel electrophoresis) approaches.

A universal fluorescence-binding assay has been developed for measuring the binding and specificity of potential QIAs for the G-quadruplex structures. This approach is independent of the spectroscopic properties of the ligand, and involves use of a fluorescent DNA quadruplex sequence. $(TTAGGG)_4$ oligonucleotides have been synthesized using solid-phase synthesis where the 5^{th} and 11^{th} guanine residues of the human telomeric sequence have been replaced by a fluorescent pteridine derivative, 6-methyl-8-(2-deoxy-D-ribofuranosyl) isoxanthopterin (6MI), which serve as guanine analog.

From spectroscopic analysis, combined with dialysis studies and melting temperature measurements, we found that the N-substituted anionic porphyrins, N-methyl meso porphyrin IX (NMM) and Cobalt(III)

mesoporphyrin IX (Co(III)MPIX), are able to stabilize quadruplex structures and have a relatively high binding affinity and high selectivity for quadruplex DNA over single strand DNA, double strand DNA, and triple strand DNA. Attempts to increase selectivity of cationic porphyrin for quadruplex DNA by substitution of the TMP ring side chains showed little effect. Addition of saccharide moieties, for improved cellular uptake was also examined.

Porphyrins such as Co (III) MPIX which possess a high specificity for quadruplex over duplex DNA and relatively high binding affinity are predicted to be ideal agents for use in therapeutic approaches aimed to inhibit telomerase activity and thus inhibit the growth of cancer cells.

ACKNOWLEDGMENTS

I would like to express my gratitude to my mentors, Professor Lesley Davenport and Professor James Godde, for their help and excellent scientific guidance, and for being encouraging throughout the course of this work.

I would like to thank my committee members, Professor He Qi, Professor Jennifer Basil, Professor Zhen Huang, Professor Richard Magliozzo and Professor Richard Sheardy for their guidance.

I would like also to thank my laboratory members for stimulating conversation and their assistance during the course of this study.

This thesis is dedicated to my family, especially my parents for being encouraging and supportive during my graduate studies.

TABLE OF CONTENTS

LIST OF TABLES

LIST OF FIGURES

LIST OF ABREVIATIONS

TMPyP 4	5,10,15,20-tetra-(N-methyl-4-pyridyl)porphine
CD	Circular dichroism
NMM	N-methyl mesoporphyrin IX
MPIX	Mesoporphyrin IX
PPIX	Protoporphyrin IX
Tm	Melting temperature
hTR	Human telomerase RNA
hTERT	Human telomerase reverse transcriptase
Hsp90	Heat shock protein 90
TP1	Telomerase Protein 1
QIA	Quadruplex interactive agent
6MI	6-methyl-8-(2-deoxy-D-ribofuranosyl) isoxanthopterin
3MI	3-methyl-8-(2-deoxy-D-ribofuranosyl) isoxanthopterin
HT4	Human telomeric repeats
BPDE	Benzo [a] pyrene diol epoxide
PDT	Photodynamic therapy
ss-DNA	Single strand DNA

ds-DNA Double strand DNA

FI Fluorescence intensity

1. Introduction

1.1. Aims of the research

The overall goal of this study is to identify new agents that bind to and stabilize the four-strand DNA regions at the end of the human chromosomes with the hope of developing cancer treatments based on the inhibition of telomerase activity. The specific aims are as follows:

1. To test the specificity of commercially available porphyrins (both anionic and cationic) for quadruplex structure binding, and determine the most specific one by spectroscopic and biophysical methods.
2. To identify, through screening of libraries of porphyrins, potential new groups of compounds that bind to and stabilize quadruplex DNA structures.
3. To determine the effect of attached saccharide moieties on the DNA quadruplex binding affinity and selectivity.

4. To determine if coordination of central metal within the porphyrin ring will improve quadruplex binding affinity and selectivity.

5. To develop a fast, spectroscopic assay for screening libraries of potential drugs for DNA-quadruplex interaction.

1.2. Telomere Shortening and Replicative Senescence

Linear eukaryotic chromosomes are capped by a special DNA structure known as the telomere. In vertebrates, telomeric DNA consists of tandem repeats of the sequence $(TTAGGG)_n$ (1) (Figure 1). These specialized structures constitute the final 10-Kb of all human chromosomes, and up to 80 Kb of all mouse chromosomes (2). Recent studies have proven that telomeres are essential for maintaining chromosomal stability and integrity, preventing end-to-end fusion, and protecting against aberrant recombination and degradation (3-5). In the absence of a mechanism for telomere length maintenance, telomeres of most human cells shorten with each round of cell division because of the incomplete replication of linear DNA (6). The sequential loss of telomeric DNA limits the cell proliferation span of most human somatic cells to between 50-80 divisions before they enter a state of replicative senescence termed M1 (7).

Somatic cells of vertebrate show only a limited capacity to proliferate. This phenomenon, called replicative senescence, is controlled by a molecular counting mechanism (molecular clock),

which is thought to be related to a specific type of DNA reorganization occurring at the end of the chromosome or the telomeres. During proliferation of cells the chromosomes are replicated by conventional DNA polymerase, which is an enzyme that is dependent on an RNA primer to initiate replication. After removal of the primer, the newly replicated DNA strand is shortened at the 5'-end. This process (end replication problem) is repeated every cell cycle and is thought to be responsible for the observed time-dependent reduction in proliferation ability. Telomeric attrition continues until a critical telomeric length is reached (average: 5-7 kbp) at the M1 phase, which triggers the block of cell cycle progression. This affects the action of two main tumor suppressor genes, i.e., p53 and the retinoplastoma protein Rb.

Several conditions enable cells to bypass the M1 phase, such as: mutation(s) in the p53 and Rb genes, or the action of viral proteins such as E1A/E1B of adenovirus, the E6/E7 proteins of oncogenic human papilloma viruses or the large T-antigen of simian virus 40. This leads to a phase of extended life span, in which chromosomal instability gradually progresses until a second mortality phase (M2)

with telomeric length of 3-4 kbp, also called crisis, is reached (8). Approximately 1 in 10^{7} cells escape from crisis giving rise to immortalized cells with unlimited proliferative potential. Escape from crisis can only be accomplished by activation of a telomere maintenance system: either by reactivation of telomerase or by activation of alternative telomere restoration mechanisms (9), referred to as ALT-mechanism.

Cell types that proliferate indefinitely, such as unicellular eukaryotes, germ-line cells, and immortal cells, maintain their telomeres at constant length. In the majority of such cells, the enzyme telomerase appears to be the main mechanism for maintenance of telomere length (10). Telomerase is a reverse transcriptase that elongates telomeres by synthesizing TTTAGGG repeats onto the 3' end of chromosomes. Thus telomerase can compensate for the incomplete replication of telomeres. Telomerase, a ribonucleoprotein, consists of a complex of an RNA component and proteins. The RNA component contains an 11-base segment, which can be subdivided into an alignment domain and template domain. Telomerase docks to

telomere by base pairing between the RNA alignment domain and the terminal five nucleotides of the 3' end of the telomere. The template domain of the RNA, complementary to the TTAGGG sequence, then serves as a reading frame for *de novo* synthesis of a new TTAGGG repeat, resulting in elongation of the 3' end of the telomere with one repeat sequence (11). The telomerase complex is translocated and repositioned, and a new round of telomeric extension can be initiated. Since telomerase extends the telomere prior to replication, no net loss of telomeric sequence occurs.

1.3. Telomerase Components

Recently, the major components of human telomerase have been identified: Human telomerase RNA(hTR); the catalytic subunit of telomerase called human telomerase reverse transcriptase (hTERT); the telomerase associated protein (TP1/TLP1); and other accessory proteins.

Human telomerase RNA (hTR): although the primary sequence of telomeric RNA is poorly conserved among species, secondary

structure prediction strongly suggests the presence of a conserved three-dimensional folding and a number of conserved domains (12, 13). These include the template domain, a pseudoknot domain, a CR4-CR5 domain, and a box H/ACA domain flanked by a CR7 domain. The template domain consists of two functional parts essential for telomere extension: an alignment domain for binding to the very end of the 3' single strand of the telomere, and a template domain that is subsequently used as a reading frame for extension. The pseudoknot domain is essential for telomerase function *in vivo* and appears to be involved in telomerase assembly. The conserved box H/ACA small nuclear RNA motive in the vertebrate telomerase is likely to be required for proper 3'-end processing.

Human telomerase reverse transcriptase (hTETR): In 1997, the catalytic subunit of human telomerase was identified and cloned (10). Characteristics of the protein include seven conserved motifs and an additional telomerase-unique N-terminal T motif. Several reports indicate hTERT is the rate-determining component for telomerase activity (14, 15). In addition, numerous data demonstrate a close

correlation between hTERT expression and telomerase activity in human tumors. Interestingly, cells transformed with hTERT keep their primary characteristics and are not tumorigenic, indicating that transfection with hTERT *per se* is not sufficient to induce oncogenic transformation (16).

TP1/TLP1: This protein represents the human homologue of tetrahymena p80 telomerase-associated protein that specifically interacts with hTR (17). TP1/TLP1 is a closely associated with the telomerase complex, as demonstrated by co-purification with telomerase activity, and immunoprecipitation experiments using anti-TLP1 antibodies. TP1/TLP1 expression levels do not reflect telomerase activity level (18).

Until recently, these were the only three telomerase components identified; however, during the past year, a number of new telomerase-associated proteins, which appear to be essential for telomerase activity, have been identified (Figure 2).

p23 and Hsp90: The molecular chaperon p23 is an acidic phosphoprotein often associated with Hsp90. Together with Hsp90,

p23 has been implicated in mediating the formation of protein/RNA complexes. In a recent study (19), it was shown by immunoprecipitation with antibodies to p23 or Hsp90 precipitated telomerase from rabbit reticulocyte cell lysates (RRLs), that p23/Hsp90-immunodepleted RRL were severely impaired in their ability to stimulate the assembly of active telomerase. Pretreatment of RRL with geldanamycin, which blocks binding of p23 to Hsp90, completely blocked assembly of active telomerase. Geldanamycin treatment after the assembly step did not affect *in vitro* telomerase activity.

Dyskerin: Dyskerin is the human homologue of the yeast protein Cbf5p, which interacts with the H/ACA small nuclear RNA and is believed to be involved in the production of ribosomal RNA.

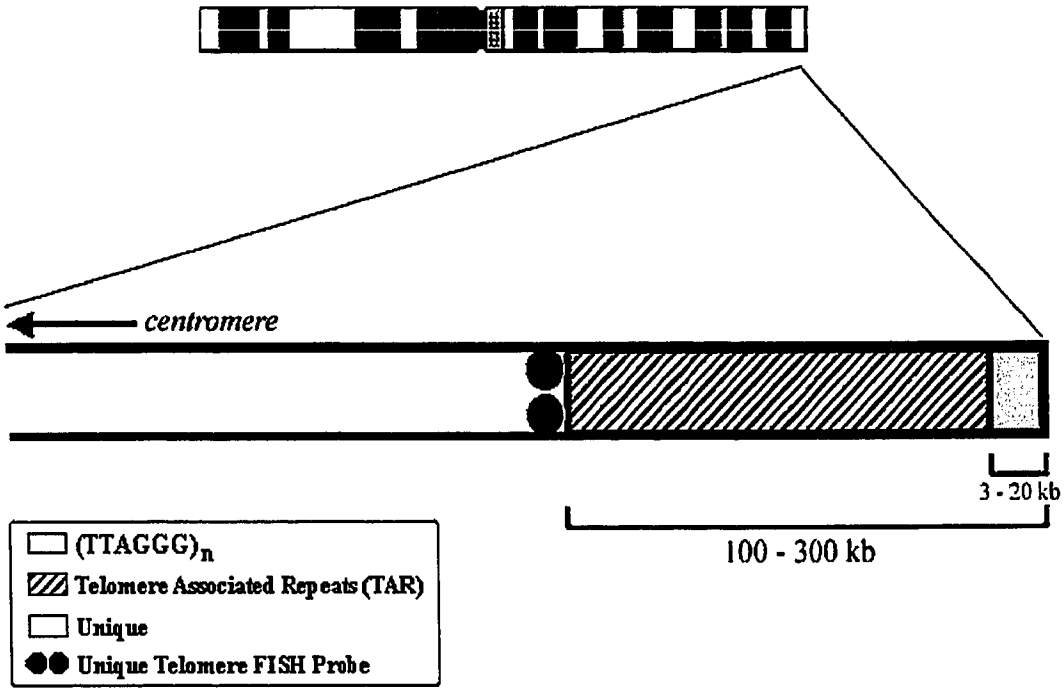

Figure 1. Human telomere.

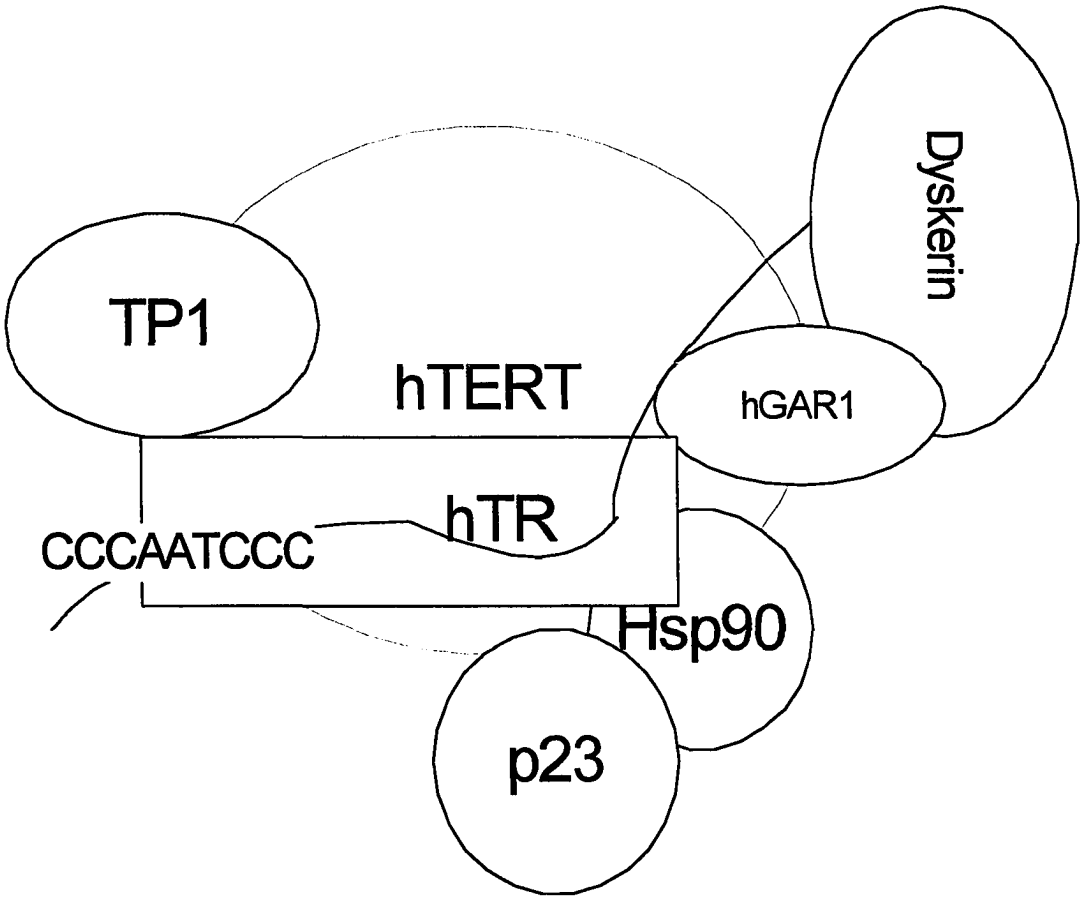

Figure 2. The Human Telomerase Components: The human telomerase is composed of the telomerase RNA (hTR) and a number of associated proteins. These include: the human reverse transcriptase (hTERT) catalytical subunit; telomerase associated protein (TP1); Heat shock protein 90 (Hsp90); the p23 protein (p23); and the H/ACA proteins including dyskerine and hGAR1.

1.4. Recent development of telomerase inhibitors for treatment of cancer

Telomerase activity has been detected in 85-90% of human tumors and tumor-derived cell lines, and there is a strong correlation between expression of hTERT, (but not hTR or TP1), and telomerase activity. Thus hTERT expression is suggested as the major determinant for telomerase activity and is known to be tightly regulated, chiefly at the transcription level. Furthermore, both hTERT expression and telomerase activity are largely absent in most human somatic cells.

Consequently, telomerase has been proposed to be a potentially highly selective target for the design of new anticancer drugs. Down regulation of telomerase activity should theoretically result in the resumption of telomeric attrition, potentially leading to tumor cell death and/or growth arrest. Inhibition of telomerase activity can be accomplished by interference with the assembly of telomerase holoenzyme, expression of telomerase components, or inhibition of telomerase accessibility.

1.4.1. Telomerase down-regulation

1.4.1.A. Reverse transcriptase (RT) inhibitors

RT inhibitors have been widely used to inhibit the RT of the human immounodeficiency virus (HIV) (20). A number of these compounds have also been evaluated for their capability of telomerase inhibition, including 3-azido-3 deoxythymidine (AZT), dideoxyguanosine (ddG) and 7-deaza-2-deoxyguanosine-5-triphosphate (7-deaza-dGTP) (21).

AZT and ddG are the RT inhibitors most intensively studied. These two compounds have proven to be the most potent inhibitors among other RT inhibitors examined to date *in vitro*. In human and animal studies, the effect of RT inhibitors on telomerase activity and/or telomeric erosion in tumor cells has not yet been thoroughly addressed. It remains to be determined whether the dosage needed to cause telomerase-mediated effects is compatible with maximal tolerable dosages.

A serious matter of concern arises from the efficacy of uptake by nucleoside transporters which vary widely between cell types (22).

Hence, this kind of treatment may well be ineffective in the cells to be targeted. Acquisition of drug resistance to nucleoside analogs is also a frequently occurring problem in anti-HIV therapy regimens. Together, these aspects make it less likely that blocking of telomerase action by RT inhibitors will be the method of choice, although its use in a combined setting with more classical anti-cancer agents may still be a valid approach.

1.4.1.B. Interference with transcription of telomerase components

Identification of modulatory elements on the transcriptional level can be accomplished by analyzing the promoter regions of telomerase genes for consensus transcription factor binding sites and/or by the induction/repression of the level of transcription factors. The hTERT gene promoter has been published recently (23, 24). The promoter region for hTERT is situated in a CpG island. It was concluded that hTERT CpG islands can undergo methylation but that no generalized pattern of site-specific methylation correlating with the expression of hTERT gene could be identified, and CpG island

methylation is not responsible for repressing hTERT expression in most cells (25). The hTERT promoter region contains numerous consensus binding sites, among which are sites for SP1, P1, AP2 and estrogen and progesterone receptors. Also binding sites for proto-oncogenes c-myc and p53 were identified (26). Telomerase activity was shown to be inhibited by repression of c-myc mRNA after exposure of leukemia cells to antisense c-myc oligomers (27). In the opposite situation, ectopic overexpression of c-myc resulted in an increase of telomerase activity, which was consequently linked to upregulation of hTERT (28).

Recent studies have identified other regulatory transcription factors: Mad1 is a factor which competes with c-myc for dimerization with Max, and upon heterodimerizing with Max forms antagonistic complexes, resulting in potent repression of transcription of hTERT (29). In addition, adenoviral expression of p53 was found to repress telomerase activity. Estrogen treatment appears to increase telomerase activity in estrogen receptor-positive (MCF-7) cells, whereas

telomerase inhibition in the same cell line was demonstrated after treatment with the anti-estradiol tamoxifen.

Sp1 cooperates with c-Myc to activate transcription of hTERT. The 3'- region of the hTERT promoter contains a GC-box, which binds Sp1 and is essential for transactivation. Overexpression of Sp1 leads to significant activation of transcription (30).

1.4.1.C. Antisense strategies

The successful cloning of the RNA component of human telomerase and the identification of the hTR template region provided an initial stimulus for the rational design of telomerase inhibitors (31). The hTR transcript comprises approximately 450 nucleotides and contains an 11-nucleotide sequence (5'-CUAAUCCCUAAC) template region complementary to the human telomeric repeat sequence 5'-d(TTAGGG). The RNA active site is functionally divided into two distinct domains. The 3' end of the active site acts as an alignment domain for binding of the substrate, while the 5' domain acts as a template for telomere elongation. The intrinsic accessibility of the

template region of hTR compared to that of other antisense-directed mRNA targets, due to the necessity to bind telomere ends, thus renders the RNA template an attractive target for enzyme inhibition.

The basic concept of the antisense (AS) strategy is straightforward: an AS molecule recognizes complementary mRNA or DNA by sequence-specific base pairing, and hence prevents translation or transcription, resulting in a selective inhibition of protein synthesis. Interference with gene expression at the molecular level in cells may be accomplished in two ways: either by *in situ* generation of mRNA from recombinant vector (AS RNA), or by the exogenous introduction of synthetic AS oligonucleotides (AS ONs). In case of hTR, AS ONs directed against the active site of the telomerase RNA may also inhibit telomerase functioning by preventing docking (alignment domain) and/or *de novo* synthesis of telomeric repeats (template domain) of the telomerase complex.

Antisense RNAs: Feng *et al.* (31) have described the effect of antisense hTR expression on telomerase activity, telomere length and cell viability in telomerase-positive HeLa cells, where cells expressing

an 185 nucleotide-long antisense RNA to hTR were monitored over a series of population doublings (PDs). In addition, HeLa cells transfected with the control expression vector lacking antisense hTR, and telomerase-negative cells with the hTR antisense expression, were included as controls. At 23-26 PDs after transfection, 33/41 antisense expressing cultures underwent crisis, whereas the control cultures were unaffected. Furthermore, of the antisense expressing cultures that underwent crisis, all colonies had a mean TRF length 27-31% shorter than those of the control cultures. Telomerase activity, as determined by telomeric repeats amplification protocol (TRAP) assay, was 20% of that found in vector controls after 23 PDs.

Other groups have subsequently reported similar findings. For example, Kondo *et al.* (32) demonstrated telomerase inhibition in antisense hTR-expressing human malignant glioma U251-MG cells. After 30 PDs, morphological analysis showed apoptotic cell death in 40 % of cells from each culture over one week period. No effects were observed for the cultures similarly treated with control vector.

A number of hammerhead ribozymes have been reported to selectively cleave telomerase RNA. Ribozymes are catalytic RNA molecules with endoribonuclease activity that can be designed to specifically cleave a target RNA sequences by incorporating the flanking sequence complementary to their target into their structure. Kanazawa *et al.* (33) have demonstrated telomerase inhibition with a hammerhead ribozyme molecule, teloRZ, designed to specifically cleave the 5' end of the hTR template. This ribozyme effected a dose-dependent inhibition of telomerase activity (IC_{50} = 1μM) in cells extracts from human hepatocellular carcinoma-derived cell lines.

To date, no studies on AS hTERT expression vector have yet been published.

1.4.2. Inhibition of assembly/activity of telomerase holoenzyme

Various purification protocols reveal that the telomerase enzyme exists as a large complex that acts as a dimer or a multimer (34, 35). Two separate, catalyically inactive TERT proteins can complement each other in *trans* to reconstitute catalytic activity. This

complementation requires the N-terminus of one hTERT and the reverse transcriptase and the C-terminal domain of the second hTERT. Moreover, the telomerase RNA templates in the active enzyme are interdependent and function cooperatively with each other.

Interference with the correct assembly of telomerase holoenzyme may provide a valid approach to inhibit telomerase activity. Pretreatment with geldanamycin, which interferes with the binding of p23 to hsp90 and blocks their ability to form active telomerase (19). Geldanamycin treatment after the assembly step does not affect *in vitro* telomerase activity, which means that this kind of treatment is only applicable for blocking the *de novo* assembly of functional telomerase complexes. Remarkably, assembly of the holoenzyme appears to be regulated by hsp90-related chaperones, as the concentration of these proteins is elevated during transformation as well as in advanced prostate carcinomas.

Whether this geldanamycin treatment will also be applicable *in vivo* will depend on the toxicity of the compound and the hTERT protein half-life, which has not been assessed yet.

1.4.3. Inhibition of telomerase accessibility

Another approach to inhibit telomerase is to inhibit telomerase action by blocking the accessibility of the telomere for the enzyme. Recently, the enzyme tankyrase showed ability to bind to TRF1 protein (quadruplex stabilizing protein) and release it from the telomeric end making the telomere accessible to telomerase (36). This implies that targeting tankyrase and/or its expression may prevent telomerase docking to the telomere and subsequently inhibit telomere elongation. However, no compounds inhibiting tankyrase expression have yet been described.

1.4.3.A.Quadruplex interactive agents as telomerase inhibitors

The G-rich sequence of the telomere can adapt a variety of conformations, such as an intramolecular fold-back (G-quadruplex) structure. G-quadruplexes have been shown to inhibit telomerase activity and hence, drugs that stabilize these tetraplexes could produce immediate anti-proliferation effects (37-41). Several compounds have

been tested, mostly in *in-vitro* assays. Although a number of compounds have been identified that bind G-quadruplex DNA and inhibit telomerase (diaminoanthraquinones and perylene diimides) most of these drugs also bind to double stranded DNA and are more or less cytotoxic at the concentrations required to inhibit telomerase.

There is now considerable interest in the development of chemotherapeutic agents capable of providing selective binding to quadruplex DNA over other DNA structures, with low cytotoxicity. This strategy has the advantage of targeting tumor cells over healthy cells; also there is no limitation to drug delivery methods as in antisense strategy (Figure 3).

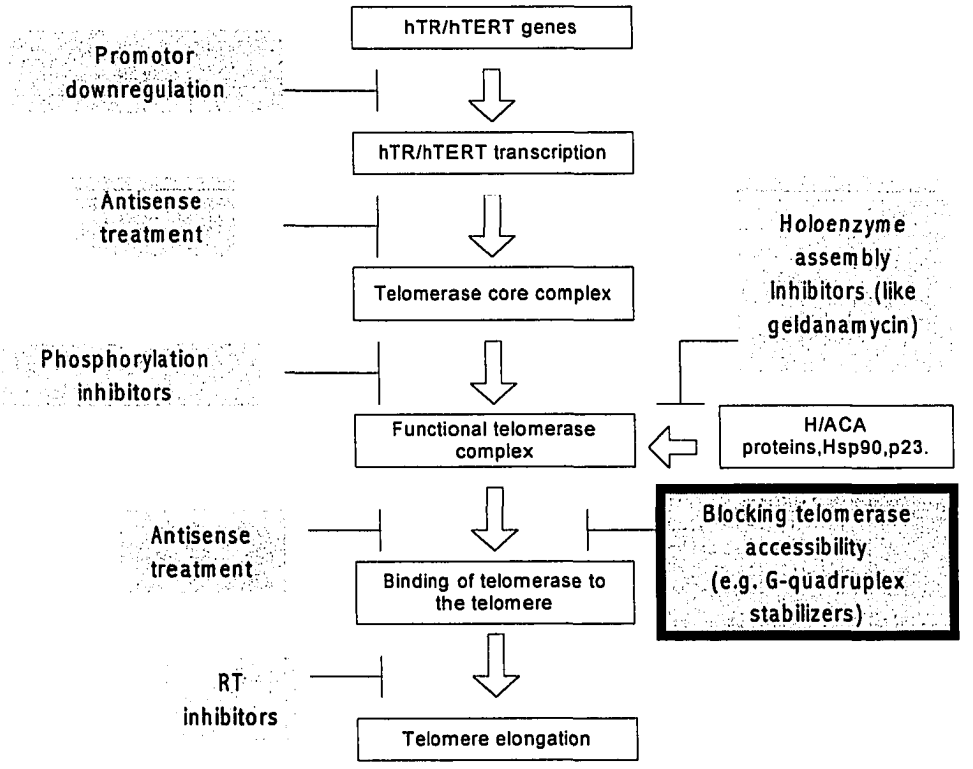

Figure 3. Overview of pathways for targeting telomere and/or telomerase activity.

1.5. Biophysical properties of telomeric DNA

1.5.1. The guanine tetrad

Oligonucleotides, corresponding to many terminal repeat sequence G-strands show unusual *in vitro* properties in that they can fold or associate to form both intramolecular and intermolecular structures stabilized by G-G base pairing (Figure 4). It is possible that some of these structures can form *in vivo* and play a role in telomere function. Polyguanosine and its derivatives tend to form viscous gels *in vitro*. X-ray fiber diffraction studies of these gels over 30 years ago revealed molecules arranged in what is now termed a G-tetrad structure. G-tetrads are stabilized by Hoogsteen G-G pairing (42); this is a different mode of pairing from that found for guanine in the more conventional Watson-Crick G-C pairing. Four atoms (H1, N7, O6 and one of the exocyclic amino protons) are essential for Hoogsteen G-G pairing. The ability to form a planar tetrad appears to be unique to guanosine and its derivatives, reflecting a fortuitous arrangement of multiple hydrogen bonding donor and acceptor sites. It is well-known

that G-tetrads are stabilized by certain cations, with K^+ ion being the most effective of the monovalent series and Sr^{2+} ion being the most effective of the divalent cations; both have a very similar ionic radii. The suggested model is a crown-ether like structure with a K^+ or Sr^{2+} cation sandwiched between two G-tetrads. One of the first clues that G-rich oligonucleotides are forming a secondary structure stabilized by G-tetrads arises from the fact that they run with an aberrant mobility on non-denaturing polyacrylamide gels. A number of biochemical methods can be used to study its structure. For example, N7 guanine methylation interferes with Hoogsteen G-G pairing but not conventional Watson-Crick G-C pairing. Therefore the sensitivity of a structure to N7 methylation by dimethyl-sulphate (DMS) implies the existence of G-G pairing. It is also possible to perform methylation protection assays in an analogous fashion; because when the N7 of guanine is involved in Hoogsteen G-G pairing it is not accessible to methylation.

1.5.2. G-quadruplexes

In DNA, two or more guanine tetrads can stack upon each other to form four-stranded structures with a guanine tetrad core. These are collectively referred to as G-quadruplexes or DNA tetraplexes. The term G-quadruplex refers to any four-strand DNA structure containing guanine tetrads without reference to strand connectivity. Despite a unifying origin, the most intriguing aspect of a G-quadruplex is their extensive polymorphism, which can be divided into a number of subclasses.

Sequences that exhibit G-quadruplex formation motifs are widely dispersed in eukaryotic genomes, but perhaps surprisingly, so far there is no evidence for occurrence of such structures in prokaryotes.

1.5.3. Strand stoichiometry

Strand stoichiometry variation allows G-quadruplexes to be formed by association of one (42), two (43) or four strands (44)

(Figure 5). In principle, three strand arrangements are conceivable but have yet to be substantiated. Moreover, if one strand has the ability to form a unimolecular structure it could also form bimolecular or quadrimolecular structures.

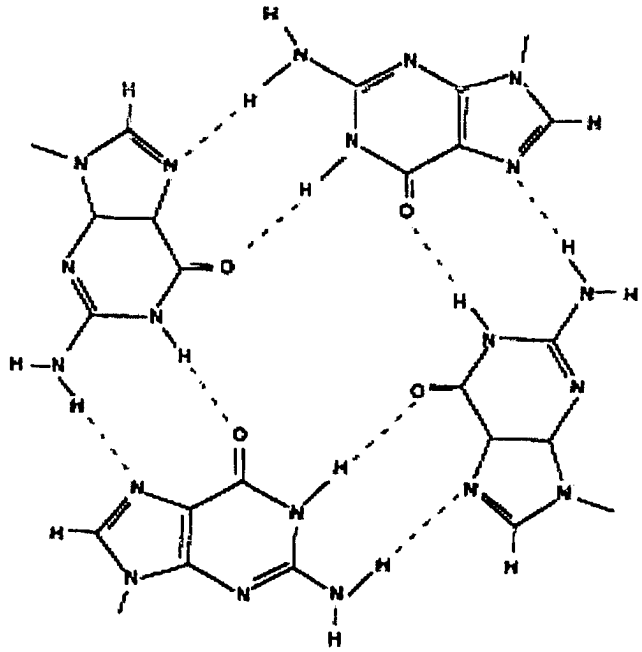

Figure 4. G-tetrad

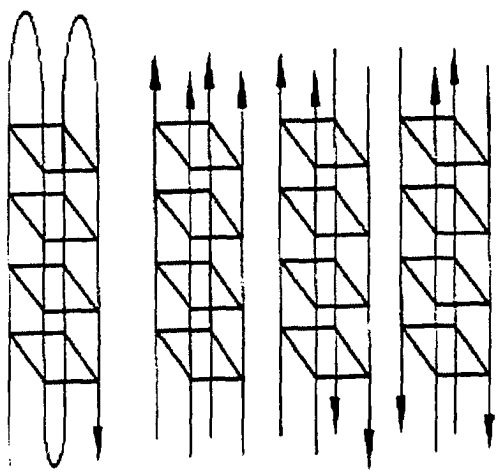

Figure 5. Quadruplex polymorphism

1.5.4. Strand polarity polymorphism

The next fundamental source of structural variation is the relative arrangement of adjacent backbones, which can have different polarities. Irrespective of whether they are part of the same molecule or not, the strand or strands that constitute a G-quadruplex can come together in four different ways. They can be all parallel, three parallel and one antiparallel, adjacent parallel or alternating parallel. Strand polarity configurations have been determined for various sequences. Many short oligonucleotides with guanine tracts have been found, by either NMR spectroscopy or crystallography, to adopt G-quadruplex structures in which all strands are parallel (45, 46). NMR spectroscopic determination of the *Tetrahymena* and *Oxytricha* telomere repeats sequences are examples of G-quadruplex structures that have three parallel strands and one antiparallel strand (47).

1.5.5. Glycosidic torsion angle variation

The bases in normal B-DNA are found exclusively in the anti conformation, whereas guanines involved in formation of guanine tetrads are observed both anti and syn conformation. However, restrictions apply to adjacent guanines involved in the same tetrad. If they are on parallel strands, they must have the same glycosidic torsion angle, and conversely if they are on antiparallel strands they must have the opposite glycosidic torsion angle. The glycosidic conformation changes the relative orientation of the bases in contiguous guanine tetrads, and affects the stacking energy. In a chair or edge type structure the dG residues of each quartet alternate syn-anti-syn-anti while in crossover or basket type structure the dG residues alternate syn-syn-anti-anti within each quartet and both intra- and intermolecular basket type structures are observed (Figure 6).

While normal B-DNA has one minor and one major groove, the stacking of guanine tetrads produces four grooves that are not necessarily identical, but can be wide, medium, or narrow. If all four

strands that participate in the guanine tetrad core are parallel, the four grooves are all of a medium size. However, if the guanine tetrad core has antiparallel strands it can result in wide, medium, and narrow grooves. In the first case, for a guanine tetrad core that is built from two pairs of adjacent parallel strands, the following applies: guanines that belong to adjacent strands and have the same glycosidic torsion angles produce medium grooves, whereas guanines that belong to adjacent antiparallel strands and have the opposite glycosidic torsion angles produce one narrow groove. In the second case, for a guanine tetrad core that is built from alternating antiparallel strands exclusively, two wide and two narrow grooves are produced. This phenomenon extends the polymorphism of G-quadruplexes further since loops that connect adjacent strands may produce grooves of any size. Theoretical calculations suggest that tracts of guanines favor formation of G-quadruplex with four parallel strands in which all guanine adapt the anti conformation and that alternating *anti/syn* arrangements were restricted to intramolecular G-quadruplex with antiparallel strands (48). It is easily realized that any G-quadruplex

structures that contain antiparallel strands must have bases in both *anti* and *syn* conformation in order to maintain the tetrad base-pairing scheme. There are examples of virtually any combination of glycosidic torsion angles. Several structures with exclusively *anti* or *syn* conformation have been characterized, as well as structures with alternating *anti/syn* conformations or mixture of *anti/syn* within the guanine tetrads (49-51).

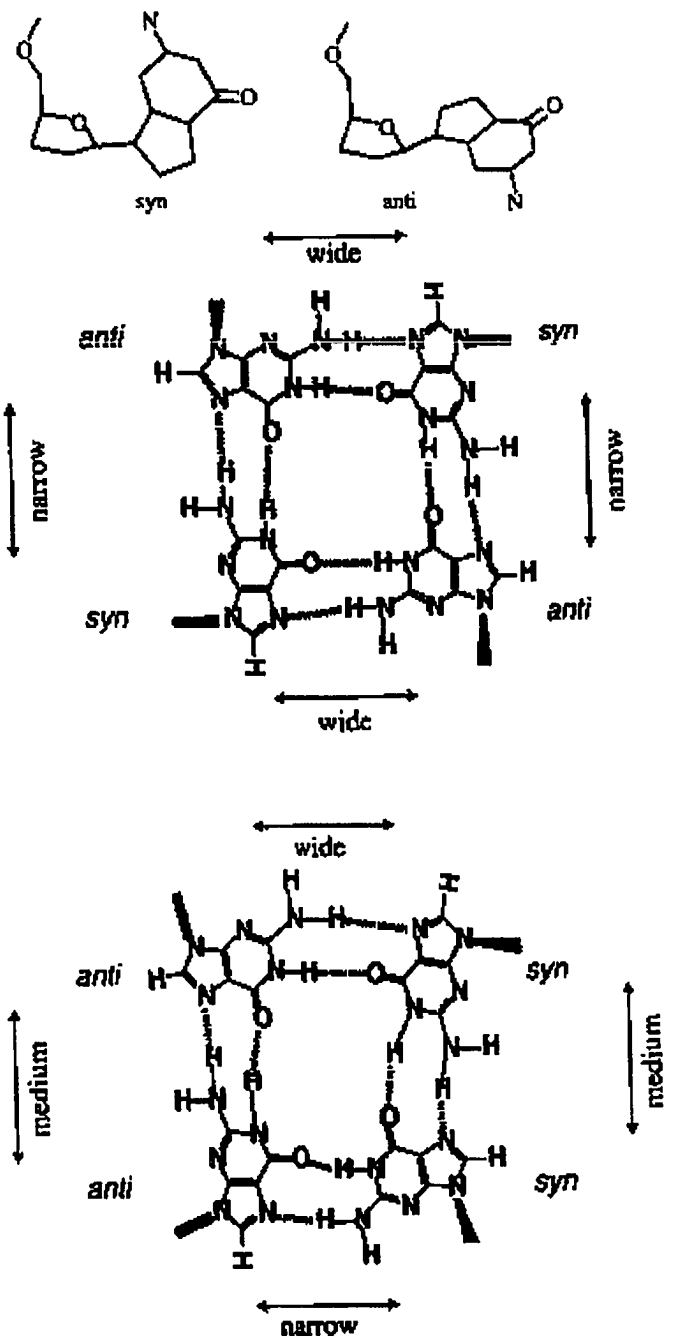

Figure 6. Glycosidic torsion angel variation

1.5.6. Connecting loops

The loops that connect guanine tracts participating in the formation of unimolecular or bimolecular G-quadruplexes can run in a number of different ways. The two strands involved in bimolecular G-quadruplex can have loops that connect guanine tracts either diagonally or edgewise. Diagonal loops are expected to protrude on opposite ends of the guanine tetrad core (52). Although bimolecular G-quadruplexes with two diagonal loops on the same side are conceivable, their formation is highly unlikely due to both steric hindrance and electrostatic repulsion between the two negatively charged backbones. If instead the two loops connect the guanine tracts edgewise, they can protrude either on the same or on opposite sides of the tetrad core. Loops protruding on the same side of the core can be either parallel or antiparallel. When the two loops protrude on opposite sides of the core they can run in two different directions.

For unimolecular G-quadruplexes the alternatives are probably fewer. In order to avoid the clash of two diagonal loops on the same

side, the three loops can join either in the order adjacent-adjacent or adjacent-diagonal-adjacent. On the other hand, there is at least one example of a parallel strand connecting *via* loops running on the outside of the guanine tetrad core, which indicates that the unimolecular structures may be more complex (45).

1.5.7. Inclusion of other bases

The perfect sequence motif required for the formation of intra-strand fold-back G-quadruplex DNA structure can be written $G_xN_{y1}G_xN_{y2}G_xN_{y3}G_x$, where x states the number of stacked guanine tetrads and y1, y2, and y3 dictate the loop lengths. However, a number of variations on this motif have been reported. Inclusion of adenine bases has been reported for human telomeric repeats (53). A number of base-pairing schemes have been suggested, but so far the details of the tetrads built from two adenines and two guanines remain to be elucidated.

Length polymorphism in d(CGG) tracts is associated with numerous diseases (54). *In vitro* such sequences can adopt a G-quadruplex structure with a core of guanine tetrads and loop-out cytosines. Under acidic conditions, the structure is further stabilized by formation of hemi-protonated cytosine$^+$-cytosine base pairing. Another G-quadruplex forming element in the chicken ß-globin promoter

described earlier has been suggested to involve bases other than guanine in the core structure, but no details are known (55).

1.5.8. Precise coordination of cations

The most interesting characteristics of G-quadruplex structures are their selective interaction with certain cations that fit well in the cavities formed by the stacking of guanine tetrads (Figure 7). The cavities between the guanine tetrads planes are lined by eight carbonyl oxygen atoms that can all participate in precise coordination of cations. The ability of potassium ion to stabilize guanine tetrads was first observed when it was found that the melting temperature of guanosine gels correlated well with the ionic radii of the coordinated cations (56). It is now well established that coordination of potassium ion, and more rarely sodium or strontium ions, adds both thermodynamically and kinetically to the stability of G-quadruplexes. Potassium and strontium ions have similar ionic radii of approximately 1.3 Å, and are believed to fit exceptionally well in the cavities between guanine tetrads. More

generally, the ionic radius is a parameter that mainly describes how well guanine tetrads are stabilized by various cations. In the alkali series the order is $K^+ >> Na^+ > Rb^+ > Cs^+ > Li^+$ and for the earth alkali series the order is $Sr^{2+} >> Ba^{2+} > Ca^{2+} > Mg^{2+}$ (56).

The perfect fit model does not stand undisputed. It has been argued that the preferred coordination of potassium over sodium ion is driven by relative free energies of hydration. Furthermore, the observation that Tb^{3+} promotes G-quadruplex formation may not be attributed to the perfect fit model, since its ionic radius is even larger than that of Cs^+.

Except for the earth alkali series, little is known about the ability of multivalent cations to stabilize G-quadruplex. In live cell nuclei the free cations are dominated by four species whose approximate concentrations are as follows: K^+ (150 mM), Na^+ (5 mM), Mg^{2+} (0.5 mM), and Ca^{2+} (0.2 μM). All other cations have normal physiological concentrations in the sub-nanomolar range. Since G-quadruplex formation greatly prefers potassium ions, it is doubtful that their formation in the living cell is affected by the presence of other ions.

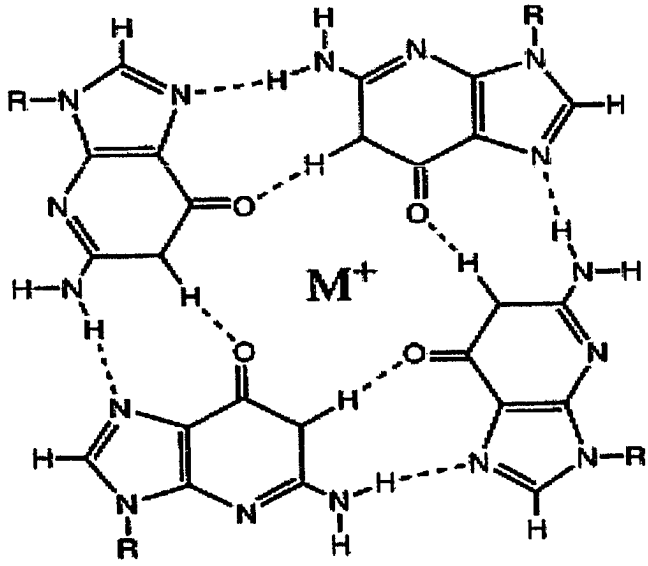

Figure 7. Interaction of potassium with quadruplex DNA

1.5.9. Proteins that stabilize G-tetrad structures

The argument that G-tetrad structures can form *in vivo* is strengthened by the identification of proteins such as Quad, which bind only to these structures. Although most of these proteins are not likely candidates for having a role in telomere function their existence suggests that G-tetrad structure can form and have a role *in vivo*. Another example of a protein that recognizes structures containing G-G base-pairs is MyoD, a vertebrate transcription factor involved in the initiation of myogenesis. MyoD can bind molecules terminating in (TTGGGG) when assembled into an intermolecular G-tetrad structure with high affinity ($K = 10^{10} M^{-1}$) (57). Another example is an avian protein termed MF3, which binds to TTAGGG sequence with high affinity ($K = 10^{9} M^{-1}$). The common feature among these oligonucleotides, which are recognized some four orders of magnitude better than unrelated oligonucleotides (non-G-rich sequences), is that they can form higher-order structures involving G-G bonds. N7 guanine methylation or inosine substitution abolishes factor binding.

These observations are consistent with the factor binding to structures stabilized by G-G base pairs.

Proteins that promote and stabilize the formation of G-quadruplex have been isolated. The ß subunit of the *oxytricha* telomere-binding protein promotes G-quadruplex formation of telomeric DNA. The protein seems to act by binding to the single-stranded form of telomeres and facilitates their association into G-quadruplex structures, thus acting as a DNA chaperone (58). In a similar way RAP1, the telomere binding protein from *Saccharomyces cerevisiae,* selectively binds to and promotes the formation of G-quadruplex in the presence of potassium ions (59). Intriguingly, the human topoisomerase I was recently implicated in the formation of certain G-quadruplex structures (60).

G-quadruplexes are exceedingly stable entities that do not fall apart spontaneously. If there are proteins that promote their formation, a class of enzymes that catalyze their disintegration must also exist. For a number of years, the absence of such a protein disputed the biological significance of G-quadruplexes. However, human proteins

that actively resolve G-quadruplex DNA structures have recently been discovered. The first G-quadruplex resolvase was identified in placental tissue (61). The genes, which are defective in Bloom's syndrome and Werner's syndrome, have been shown to encode proteins that work in a similar fashion. Both belong to the RecQ family of helicases and which are important to ensure precise genetic recombination and chromosome segregation (62). Finally, the SV40 large tumor antigen helicase appears to specifically unwind a variety of G-quadruplexes (63). The presence of all these proteins supports the argument that G-tetrads can form and have a role *in vivo.*

1.5.10. Types of quadruplex structures

There are two kinds of quadruplex DNA structures: intramolecular quadruplex and intermolecular quadruplex (Figure 8).

1.5.10.A. Intramolecular quadruplex

Complexes that migrate more quickly than single-strand molecule were detected when a range of oligonucleotides corresponding to a variety of terminal repeat G-strands were run on non-denaturing gels. The formation of these more rapidly migrating complexes is independent of concentration and suggests some form of fold back intramolecular structure. Other evidence also points to a model where a single molecule is folding back on itself to form a four-strand structure containing G-tetrads (42). This includes NMR data, indicating the presence of guanines in both syn and anti conformation, and UV crosslinks between thymines in different repeats on the same molecule. Furthermore, the more rapidly migrating complexes of $(TTGGGG)_4$, form in the presence of Na, K, and Cs ions but not Li

ion. This is consistent with a model where the cation is sandwiched between two stacked G-tetrads, the cation forming electrostatic bonds with the keto groups of the four guanines both above and below it. Atomic sizes are such that the central pocket between the G-tetrad can accommodate Na, K, and Cs cations and allow them to form bonds with guanines. However, Li ion does not fit, as it is too small to be able to form stable bonds with all the guanines simultaneously. These steric constraints explain why Li does not stabilize the fold-back structure. Similar fold-back intramolecular G-quartet structure can also be formed by oligonucleotides corresponding to the human $(TTAGGG)_4$, *Chlamydomonas* $(TTTTAGGG)_4$ and Arabidopsis $(TTTAGGG)_4$ terminal repeat sequences.

1.5.10.B. Intermolecular quadruplex

Many regions of the human genome, such as some promoters or the immunoglobulin switch regions, contain G-rich sequences. These oligonucleotides can form secondary structures that migrate more

slowly on non-denaturing gels compared to corresponding single strands. The guanines are protected from N7 methylation by DMS when formed into such structure, suggesting Hoogsteen G-G pairing. The model proposed, G4-DNA, containing four parallel strand of DNA held together by G-tetrads. One of the earliest suggestions that telomeric sequences could form intermolecular four-stranded structure came from the observation that purified Oxytricha macronuclear DNA aggregated at high concentration in a Na-dependent manner. A four-stranded association was suggested (47) since it is known that 3' overhangs are not complementary and hence could not arise from straight-forward Watson-Crick pairing. Oligonucleotides at the end of chromosomes of *Tetrahymena* (TTGGGG), or *Oxytricha* (TTTTGGGG) form a variety of dimerization or tetramerization products that are believed to be in dynamic equilibrium with each other. The formation of these intermolecular structures appears to be promoted by Na and K ions. Once formed these structures are strongly stabilized by K ions against thermal denaturation.

Intermolecular structures stabilized by G-tetrads can have a number of roles *in vivo*. For example, a parallel guanine quadruplex association could initiate the alignment of four sister chromatids during meiosis. These associations have significance for understanding the behavior of purified *Oxytricha* genomic DNA. The macronuclear genome is composed of short molecules, and *in vitro* these slowly cohere at high concentration to form multimeric complexes. This requires the presence of Na, or K ion. The macronuclear telomeres, which terminate in (TTTTGGGG) single stranded overhangs, is all that appears to be required for coherence. Oligonucleotides that form four stranded structures can also form higher-order structures under the appropriate conditions.

Both kinds of G-tetrads are found in the promoter regions of certain genes suggesting that G-quadruplex structures may play a role in the transcription regulation of genes (65). Alternatively, another possible role for G-quadruplex DNA is the regulation of telomere length, since a telomere overhang that forms a G-quadruplex structure would not be a good substrate for telomerase enzyme.

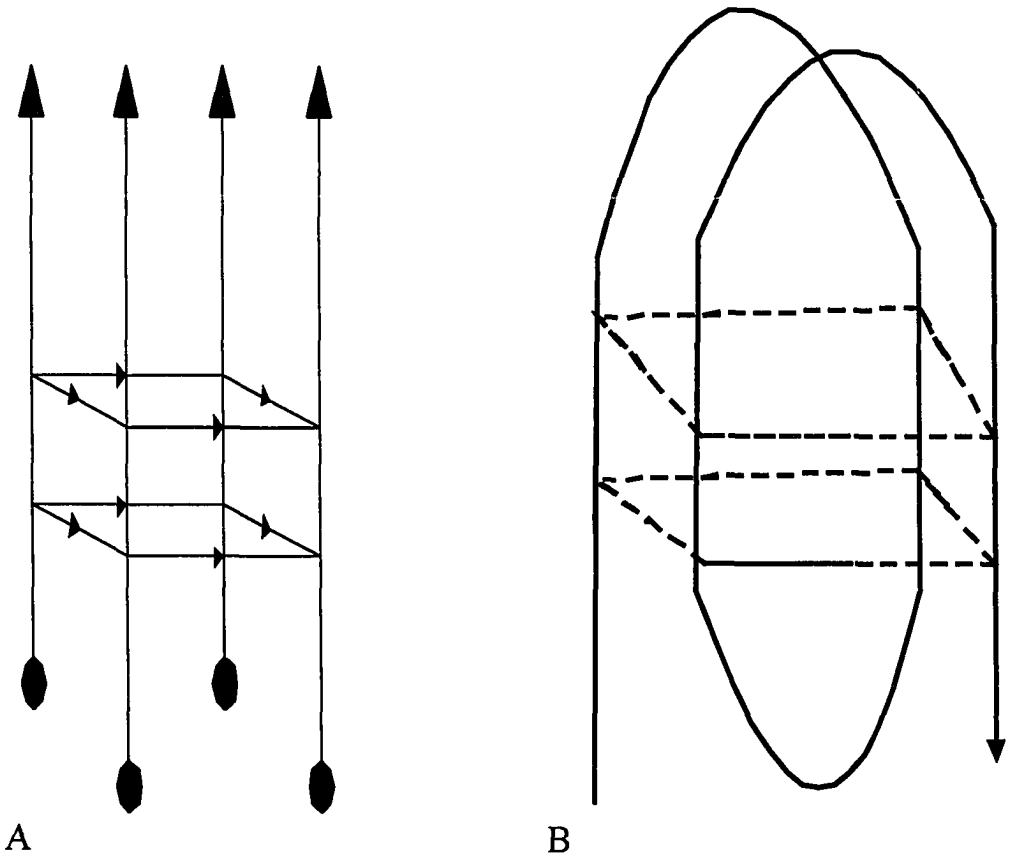

Figure 8. A) Intermolecular quadruples DNA structure.
B) Intramolecular quadruplex DNA structure.

1.6. G-quadruplex interactive agents

1.6.1. G-quadruplex stabilizing agents

An approach to telomerase inhibition that has been the focus of much attention is the design of small molecules that can bind to the G-quartet structure. This strategy is based on the assumption that the single-stranded G-rich region at the telomere ends will form a quadruplex structure, and that these structures are essential for telomerase inhibition. It is believed that the stabilization of quadruplex structures will prevent telomerase binding to the telomere.

The first quadruplex-interactive agent reported to be a telomerase inhibitor was a symmetric 2, 6-disubstituted aminoalkylamido anthraquinone molecule (66). Importantly, this study by Jenkins demonstrated the involvement of an intermolecular DNA tetraplex-ligand complex as the stalling of telomeric elongation appeared with a periodicity that corresponds to four G-repeat units. Confirmatory support for this model was provided by enhancement of DNA polymerase arrest in the presence of K^+ ions.

The polycyclic aromatic compound PIPER, (N, N"-bis[2-(1-piperidino)ethyl)]-3,4,9,10-perylenetetracarboxylic diimide, has been shown to accelerate the formation of intermolecular hairpin dimer G-quadruplexes some 100 fold using nondenaturing gel electrophoresis. This suggests that PIPER acts in a chaperone-like manner with telomeric DNA and can to promote G4 complex formation. This significant finding provides support for the hypothesis that targeting telomerase via quadruplex-ligand complexes does not require the presence of preexisting of quadruplexes. Rather, the ligands are able to facilitate quadruplex folding of telomeric sequences downstream of template binding.

PIPER has been shown to induce a duplex → quadruplex transition in a 27-mer sequence corresponding to c-myc promoter gene (40). It has been suggested that this duplex to quadruplex transition can serve as a model for quadruplex formation in nontelomeric sequences, suggesting that the quadruplex interactive ligands might have a role in targeting those few genes with such sequences (G-rich).

Earlier molecular modeling and structure activity studies of amido-anthraquinones and acridines have been applied in recent times to a more systematic approach in the design of selective and potent inhibitors. Such studies have exploited the inherent differences between duplex and quadruplex DNA structures, in terms of number of grooves and the localization of negative electrostatic potential at the center of the G-quartets. For example, acridines have been synthesized with a third aniline substituent at the 9-position, to fit into a narrow third groove of the human intramolecular quadruplex. This molecule has a quadruplex binding affinity over 30-fold greater than duplex affinity. The parent disubstituted-acridine has equivalent affinity for quadruplex compared to duplex DNA (67). Other molecules that have been reported recently to bind and stabilize quadruplex DNA structures include telomestatin, isolated from *Streptomyces anulatus*, porphyrins and carbocyanine dye (68).

1.6.2. G-quadruplex destabilizers

Agents that cause destabilization or destruction of quadruplexes can lead to the binding of telomerase to the single-stranded 3' overhang at the end of the telomere. We suggest that most of these compounds should be considered carcinogenic in nature. For example, benzo[α]pyrene is a polycyclic aromatic hydrocarbon present widely in the environment as in automobile exhaust, tobacco smoke, and as a contaminant in food such as vegetable oils. It is metabolically activated to highly reactive diol epoxides, which can bind chemically to cellular DNA and cause mutations in oncogenes and tumor suppressor genes ultimately leading to tumor formation. Among the metabolic activation products of benzo [α] pyrene are a pair of mirror image diol epoxides, (+) -7R, *8S*-dihydroxy - 9S, 10R- epoxy -7, 8, 9, 10 tetrahydrobenzeno[α]pyrene and the corresponding (-)-7S,8R,9R,10S enantiomer known as (+) and (-)-*anti*-benzo[α]pyrene diol epoxide (BPDE) (69,70).

The (+) enantiomer is more mutagenic than the corresponding

(-) form in mammalian systems. Both (+) and (-) *anti*-BPDE react with DNA principally at the exocyclic amino group of guanine to form covalent adducts. *Cis* and *trans* additions are possible in each case. Mutation to a lesser extend at adenines has also been reported. That higher frequency rates of mutation are observed in some sequence contexts over others is well established. For example, mutation hotspots have been found at the middle base pair of GGG triplets with six other hotspots located at GC sequences of the *supF* gene. Most of the G→T transversions occurs in purine-rich sequences. One possible explanation for observed mutation hot spots is that these sequences provide sites (hotspots) for covalent binding.

2. Chapter I

Porphyrin-DNA Interaction:

Spectroscopic Studies

2.1. Introduction:

2.1.1. Porphyrin as probe for DNA secondary structure

The basic porphyrin structure consists of four pyrrole units linked by four methene bridges. Porphyrins and metalloporphyrins are found widely in nature, and are used by organisms as cofactors for a variety of enzymes and other specialized proteins: they play important roles in various biological processes.

Metalloporphyrins are extraordinarily versatile and participate in oxygen transport, electron transfer, and a variety of redox reactions such as those associated with catalases, peroxidase, and monooxygenases. Heme, [iron (II) protoporphyrin-IX-complex] is the prosthetic group in hemoglobins and myoglobins, which are responsible for oxygen transport and storage in living tissues.

Although a variety of protein-porphyrin complexes and conjugates exist in nature, no role *in vivo* has yet been attributed to porphyrin-nucleic acid complexes; indeed, naturally occurring anionic porphyrins have not been yet found to associate with double-helical DNA or RNA either *in vivo* or under experimental conditions *in vitro*.

Recently, however, a class of synthetic cationic porphyrins, including mesotetra (4-N-methlpyridyl) porphine (TMPyP4), containing two or more positive charges has been found to bind double-helical DNA (73) (Figure 9).

The highly conjugated porphyrin macrocycle shows intense UV-visible absorptions with a peak around 400 nm (the "Soret" band), followed by several weaker absorptions (Q-bands) at higher wavelength (470-650 nm). Variation of the peripheral substituents on the porphyrin ring often result in minor changes to the intensity and wavelength of these absorptions. Protonation of two of the inner nitrogen atoms or insertion of a metal into the porphyrin cavity can also change the visible absorption spectrum.

The interaction of porphyrins with DNA appears to follow, under different conditions, one of three modes: intercalation between the DNA base pairs, outside binding, and outside binding reinforced by self-stacking interactions between the porphyrins (Figure 10). Intercalation of porphyrin between the base pairs of DNA is typically indicated by large red shift of Soret band, substantial hypochromicity

of the Soret band, and a negative induced CD band in the Soret band. On the other hand, outside binding without stacking is typically characterized by small red shift of the Soret band, and a small hypochromicity (or even hyperchromicity) of the Soret band, and a positive induced CD band in the Soret region (74).

The cationic porphyrin-DNA interactions have been studied extensively, using a wide variety of spectroscopic and footprinting techniques, and have been subject to kinetic and thermodynamic analysis. Such interactions have potential for:

a) *In vivo* photodynamic therapy [a variety of porphyrins have been found to photosensitize DNA strand cleavage, and this property has been used and is currently being developed for the treatment of certain cancers (reviewed by Marzilli, 1990)].

b) Use as an analytical probe for investigating higher-order structures formed by nucleic acids, particularly branched DNA and RNA.

The use of porphyrins for probing DNA-quadruplex structures appears appropriate for the following reasons:

1) The dimensions of porphyrin are roughly similar to those of the G-tetrad, which is responsible for quadruplex formation.

2) Porphyrins have constituents that can hydrophobically and electrostatically (cationic porphyrins) interact with the G-tetrad.

3) Porphyrin-DNA interactions can be readily monitored by optical spectroscopy.

4) Low cytotoxicity.

5) Porphyrins by themselves are novel drug delivery vehicles (75).

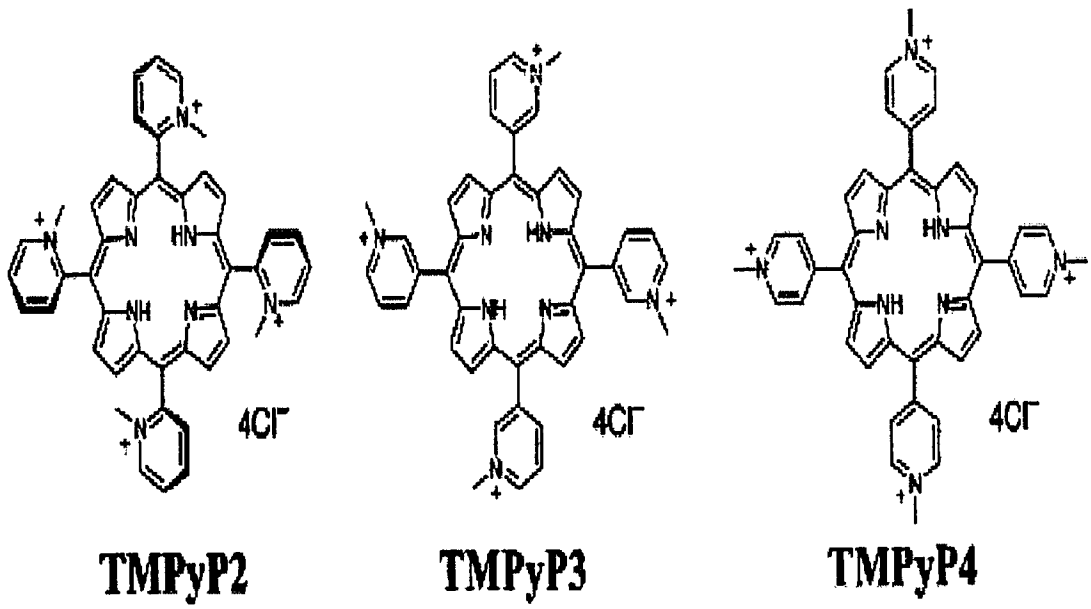

Figure 9. Structure of cationic porphyrins

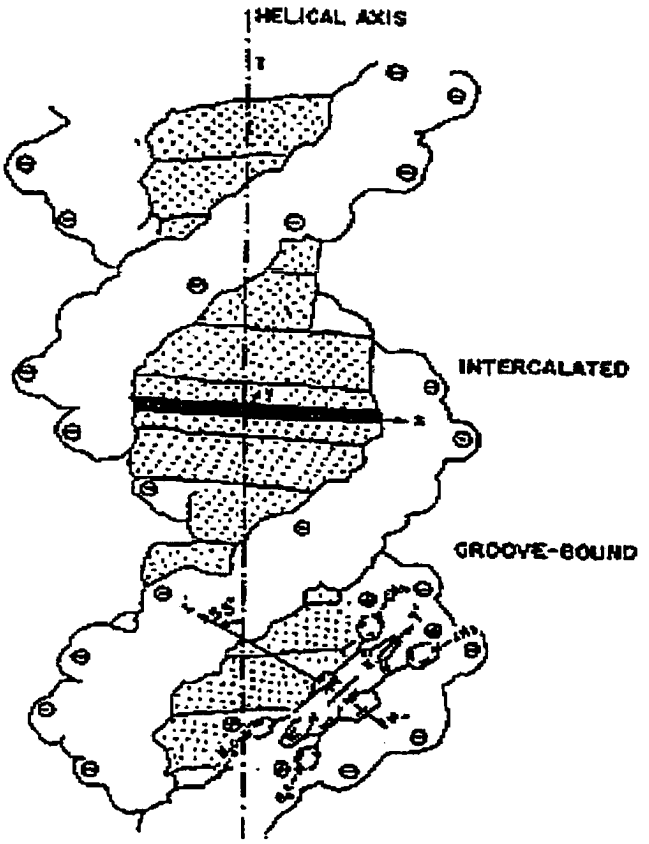

Figure 10. Porphyrin-DNA modes of interaction

2.1.2. Porphyrin interaction with duplex DNA

Several lines of experimental evidence were offered by Fiel and coworkers for the intercalation of TMPyP4 with duplex DNA of which perhaps the most compelling are: the increase in viscosity with increasing drug load; the unwinding of circular DNA; and the increase in melting point temperature. The hypochromism of the porphyrin Soret absorption band and the avidity of the binding were also noted as being consistent with an intercalation model (76). Two induced circular dichroism (CD) features were observed in the Soret region for TMPyP4-DNA complex: a negative band at 440 nm and a positive band at shorter wavelength. The profile of the CD spectrum is roughly independent of drug load and presents two distinct binding modes, reported as intercalation and external, electrostatic binding. Metal complexes of the (TMPyP4) 'T4 porphyrins' exist as (or can easily be converted to) four-coordinate species that are capable of intercalation. Other metal derivatives containing axial ligands are blocked from intercalation and instead form external complexes in which the metalloporphyrin nestles into a DNA groove. This model is consistent

with the earlier observation that, unlike TMPyP4, FeT4 does not intercalate into DNA (76). It points out that the key factor in preventing intercalation of this latter derivative is the presence of axial ligands at the metal center.

Based on work with synthetic DNAs, it was demonstrated that intercalation is favored at GC-rich regions of DNA while external binding is more favorable at AT-rich regions. Theoretical studies later showed that intercalation is indeed favored over groove binding by about 100 kJ at GC base pairs while outside binding is more favored at AT base pairs by some 40 kJ (77). In addition, it was proposed that there is a very convenient spectroscopic signature for these interactions; a negative induced CD band in the Soret band is diagnostic of intercalation while a positive feature indicates external groove binding. A number of studies employing other techniques helped to confirm and extend this model. Nuclear magnetic resonance (NMR) investigations, particularly those by Marzilli, Wilson, and coworkers, have contributed to the understanding of porphyrin-DNA interactions. Their initial report, combining NMR and viscometric

titration techniques, confirmed that NiT4 and H2T4 intercalate while axially liganded ZnT4 does not. Geacintov and coworkers using linear flow dichroism techniques also concluded that five-coordinate Zn-T4 is an outside binder, with the plane of the porphyrin core making an angle of 62-67° with respect to the two-fold DNA helical axis, whereas H2T4 (TMPyP4) is perpendicular to this axis as expected for an intercalator.

Reactions of porphyrins and metalloporphyrins with poly (dA-dT)$_2$ were shown to be much faster than intercalation into (dG-dC)$_2$, a result confirmed in studies by Marzilli and coworkers (73). External binding in the DNA groove is, as expected, much more rapid than insertion into the duplex DNA. Competition kinetic studies, in which H2T4 was distributed between the two synthetic polymers, poly (dA-dT)$_2$ and poly(dG-dC)$_2$, were completely consistent with the results obtained for the thermodynamic and kinetic studies of the binary systems involving the porphyrin and one of the polymers only. These studies led to the proposal that, in the mechanism of binding to natural DNAs, even intercalating porphyrins and metalloporphyrins first bind

externally, presumably in AT-rich regions and then redistribute to their intercalation binding sites *via* a direct internal transfer; in other words, a translocation along the duplex not involving dissociation. Evidence for such a kinetic process has been obtained by Strahan *et al*, and Sugimoto *et al* (78).

2.1.3. Porphyrin interaction with branched DNA

The binding of porphyrins to synthetic three-way or four-way junctions has been reported (79). Chemical footprinting techniques provide evidence that the region in the four-way junction near the branch point is a high-affinity binding site for H2T4, CuT4 and NiT4. On the other hand, the nature of the intercalation of ZnT4, CoT4, and MnT4, all of which contain axial ligands, is less well defined. These derivatives also bind to four-way junction DNA but in a manner different from porphyrins without axial ligands.

Similarly, binding of H2T4 and H2T3 (TMPyP3) occurs at a high-avidity site located in the three-way junction region. The data are consistent with a model in which, at low drug load, the porphyrins are

inserted almost exclusively at the location between the base pairs flanking the junction, a binding mode that is known as "inclusion" to distinguish it from "intercalation". As the drug load increases, binding to secondary sites occurs.

2.1.4. Porphyrin interactions with G-quadruplex

Because the G-quadruplex exhibits structural polymorphism, different G-quadruplex typologies may be associated with different cellular processes. Therefore, to achieve therapeutic selectivity using G-quadruplex as design targets, it was necessary to differentiate between different types of G-quadruplexes using appropriate selective quadruplex interactive agents. Recently, Hurley and coworkers compared the interaction of three cationic porphyrins TMPyP2, TMPyP3, and TMPyP4, with parallel and antiparallel types of G-quadruplexes using gel mobility shift experiments and a helicase assay (80). They found that structurally similar porphyrins showed dramatic differences in their ability to facilitate the formation of G-quadruplexes. The gel shift data showed that, among the tree

porphyrins, only TMPyP3 was able to promote the formation of a parallel telomeric G-quadruplex. Under the buffer conditions (1x TE, pH 8.0, and 100 mM K^+ ion) used in the gel shift experiments, DNA oligomers containing four repeats of (TTAGGG) are contained in equilibrium of at least four different types of G-quadruplexes. According to the mobility gel shift assay, most of the G-quadruplexes are in the form of intramolecular antiparallel quadruplexes, while the amount of dimeric and tetrameric quadruplex conformations is very small. The fact that TMPyP3 is able to dramatically increase the proportion of parallel tetrameric G-quadruplexes may be due to the preferential stabilization of the parallel G-quadruplexes by TMPyP3, in contrast to TMPyP4. This conclusion is supported by the observation in the helicase assay that TMPyP3 prevents unwinding of parallel G-quadruplex by Sgs 1 p (helicase enzyme) to a much greater extent than TMPyP2 and TMPyP4. TMPyP2 showed no activity in either the facilitation of G-quadruplex or the inhibition of unwinding in helicase assays, indicating that this porphyrin does not appreciably interact with either parallel or antiparallel G-quadruplexes. In

contrast, TMPyP4 showed some facilitation or inhibitory activity in both assays. In the helicase assay using antiparallel dimeric G-quadruplexes as helicase substrate, TMPyP4 showed higher Sgs 1 p inhibitory activity that TMPyP3, suggesting that TMPyP4 might be more specific to antiparallel G-quadruplexes.

TMPyP2, TMPyP3 and TMPyP4 are all positional isomers. The only structural difference among these three porphyrins is the position of the N-methyl group on the pyridyl ring relative to its connection to the porphine core. The different position of the N-methyl group determines the free rotation of the pyridyl rings at the meso position and the relative dihedral angles of the porphine core and the pyridyl groups. In turn, this must affect their interaction with the G-quadruplexes. It is possible that TMPyP3 fits the pocket between the end G-tetrads and the loops in a parallel G-quadruplex considerably better than TMPyP4, whereas TMPyP2 does not fit any site in the parallel G-quadruplex (81).

Two models have been proposed for the interaction of porphyrins with G-quadruplex structures. One is the tetrad

intercalation model, which postulates that the porphyrin molecules intercalate between two successive G-tetrads. This model is mainly based on the stoichiometry data obtained from isothermal titration calorimetery and molecular modeling studies. The second model, which is based on photocleavage data of antiparallel monomeric G-quadruplex DNA, proposes that porphyrins externally stack to the two ends of the G-tetrad. The photocleavage data on parallel G-quadruplex DNA reported by Hurley show that when single-stranded molecules associate together to form a G-quadruplex structure, TMPyP3 and TMPyP4 cleavage at the inner G-tetrads is almost completely diminished. This result suggests that the TMPyP3 and TMPyP4 molecules do not appreciably interact with the inner G-tetrads under these experimental conditions, which is consistent with an external stacking model. Time course incubation experiments also suggest that the intercalation of porphyrin molecules between two G-tetrads is neither kinetically not thermodynamically favored. This finding would therefore apparently argue against the intercalation model, which would predict the cleavage of guanines located in the

inner G-tetrads. Regardless of the binding mechanism, TMPyP4 was reported to bind to and stabilize G-quadruplex DNA and thus inhibit telomerase with IC_{50} of 6.5 μM.

The effect of TMPyP4 on intact MCF7 human breast carcinoma cells was examined by Izbicka *et al.* (39) to determine the effect of TMPyP4 on the whole cell, MCF7 carcinoma cells were cultured in the continuous presence of 1, 10, and 100 μM TMPyP4. The porphyrin solution was freshly added to the medium from the concentrated stock at each passage of the cells (every 3-4 days). On day 4, 8, and 15, the cells were lysed and telomerase activity was measured in the extracts. A clear concentration-dependent loss of telomerase activity in the presence of TMPyP4 was observed. The inhibition of the telomerase activity was also time dependent.

2.1.5. Selectivity to quadruplex DNA:

There is a clear requirement for a quantitative assay to determine the relative tetraplex, triplex, duplex DNA and single stranded (DNA/RNA) binding affinities for a candidate ligand. To satisfy this need, a rapid technique has recently been developed and refined by Chaires (82), using a thermodynamically rigorous competitive equilibrium dialysis method using therapeutically sensible concentration of agents. In the assay, solutions of different nucleic acid structures, each of identical concentration, are dialysed against a common ligand solution using suitably buffered solution conditions. After equilibrium is reached the amount of ligand bound to each DNA structure is measured by an optical assay. More ligand will accumulate in the dialysis tube containing the structural form of the highest binding affinity and, since all of the DNA structures are in equilibrium with the same free ligand concentration, the amount of bound ligand is directly proportional to the binding constant. Thus, comparison between the DNA samples gives a rapid and reliable indicator of structural selectivity for any ligand. In this study, this

technique was used to study the selectivity of different porphyrins to telomeric quadruplex structures.

2.1.6. Saccharide-coated porphyrins

Oligosaccharides play essential roles in various cellular activities such as antigen recognition, growth signals, and glues in cell adhesion, where the saccharide-receptor interactions are usually specific and multivalent. This specificity suggests a potential utility of synthetic, mostly polymeric, multiantennary saccharide derivatives as carriers in directed drug delivery and as blockers or inhibitors of undesired saccharide-receptor associations. However, saccharide-receptor interactions are by no means the sole access routes to the cells. Cells, especially tumor cells, show nonspecific affinities to hydrophobic molecules. This is the basis of photodynamic therapy of tumors by the use of porphyrin and related sensitizers.

It has been reported that saccharide-coated porphyrins with masked hydrophobicity was very important for cell recognition (83). The incorporation of galactose to porphyrin makes porphyrin

hydrophilic and electrically neutral and more accessible to the cell than the hydrophobic porphyrins. Under these circumstances, the identity of the saccharide moieties plays a crucial role; the correct sugar (galactoside) can undergo specific saccharide receptor interactions with the right (hepatic) cells, while the wrong (glucoside) saccharide is completely rejected by the cell. The included guest molecules are thereby either delivered to the target cells or protected (in solution) and excluded from the cells.

Since saccharide-receptor interactions are ubiquitous, well defined/well designed synthetic saccharide clusters may serve as a new tool in glycoscience and glycotechnology of cell communication and drug delivery.

In this study we investigated the impact of the incorporation of glucose and galactose molecules to porphyrin and whether or not the presence of the sugar moiety will affect the affinity of binding of such saccharide-coated porphyrin to DNA. Also, we studied the effect of the presence of these sugars on porphyrin selectivity for different DNA structures.

2.1.7. Functional porphyrin libraries

Combinatorial libraries have proven to be a powerful method for examining structure-function relationships, and the synthesis and screening of small molecule libraries is emerging as an important strategy for drug discovery (84). Although the binding mode is still controversial, the ability of 5, 10, 15, 20-tetrakis (4-N-methypyridinium) porphyrin to strongly bind to duplex DNA has been known for over 20 years. In contrast, negatively charged tetrabenzoate porphyrins do not bind as strongly. The mechanism of action of these compounds is also under debate, but probably arises from the formation of singlet oxygen and subsequent damage to the nucleic acid. Synthesis of such a library is important for the development of photodynamic therapeutics (PDT), such as photofrin, which is a mixture of monomers and ester-linked multimers of protopophyrin IX (85).

In this study we have screened combinatorial libraries of meso-tetraphenylporphyrin derivatives, (core structure libraries) where the largest library contains 1540 compounds (including isomers). The

purpose of the development of such libraries was to identify new combinations of functional groups that enhance porphyrin binding to quadruplex structures relative to homo-substituted parent molecules. Since porphyrins have been shown to congregate in a variety of cell structures, it is likely that different substitution patterns will target different tissues or cellular components. *In vivo* experiments have shown that the greater the amphipathicity of a compound, the greater the selectivity toward tumor cells (86). Therefore, a directed porphyrin library was made and modified in order to cross the cell membrane (which generally contains negatively charged lipids), be reasonably soluble under physiological condition, and bind nucleic acids. Thus, the members of the libraries should be amphipathic with some positive charge (Figure 6).

2.2. Materials and methods

2.2.1. Oligonucleotides DNA and porphyrins

Human telomeric $(TTAGGG)_4$ and *Oxytricha* telomeric (TTTTGGGG) sequences, were purchased from Oligos etc, (HPLC purified). ss-DNA (polyA), ds-DNA {poly (dA)-poly (dT)} and triplex DNA {poly (dA)-[poly $(dT)_2$] } were purchased from Amershem Inc. Quadruplexes were formed by heating the DNA at 90 °C for 10 minutes then cooling slowly to room temperature in a buffer containing 100 mM KCl and 10 mM cacodylate. Porphyrins were purchased from Porphyrin products (Logan, UT) and were used without further purification.

2.2.2. Non denaturing gel electrophoresis

Oligonucleotides were radiolabeled at the 5' end using ^{32}P with polynucleotide kinase. Labeled oligonucleotides were fully denatured by heat at 95° C in TE buffer and 0.1M KCl buffer, respectively. The sample was slowly cooled to room temperature and the loading dye

(0.2% w/v bromophenol blue, Xylene cyanol) was added. Samples were loaded onto preequilibrated (for one hour) gels (12% acrylamide, 0.6% bisacrylamide, 0.5x TBE buffer). The gel was dried and visualized with autoradiography.

2.2.3. Visible absorption titration

The binding of different porphyrins to human telomeric sequence was monitored by visible spectroscopy using an Ultra Spec 2000 UV/Visible spectrophotometer (Pharmacia Biotech). A solution of DNA was titrated into a solution of free porphyrin and the spectra were recorded from 300 to 500 nm after incubation in the dark for 5 min after each addition. The spectra of porphyrin solution were also recorded.

2.2.4. UV thermal melting studies:

Melting temperature profiles of quadruplex structure were monitored at 295 nm using an Ultra Spec 2000 UV/Visible

spectrophotometer (Pharmacia Biotech), attached to a Tm programmable Peltier heated cell holder equipped with SWIFT-Tm software. A control DNA sample comprised a single stranded DNA sequence was used as a control to confirm that the signal measured at 295 nm was due to the dissociation of G-quartet DNA. DNA at 1.5 μM was suspended in a buffer containing 10 mM sodium cacodylate (pH 8.0) and 100 mM KCl. Appropriate amounts of stock solution of the particular porphyrins were added sequentially and incubated in the dark for 5 min to increase the molar concentration ratio of porphyrin to DNA from 1:1 to 2:1, 3:1, 4:1. The melting temperature was determined after each porphyrin addition as the temperature was ramped from 30 to 80 °C at the rate of 1 °C/min. The temperature corresponding to the maxima in the first derivative plots was selected as the DNA melting temperature (T_m).

2.2.5. Competition dialysis assay

Competition dialysis assay was carried out as described by Chaires (82). Briefly, a buffer consisting of 6 mM Na_2HPO_4, 2 mM NaH_2PO_4, 1 mM Na-EDTA, and 185 mM Na Cl (pH 7.0) was used for all dialysis experiments. For each competition dialysis assay, 200 mL of dialysate solution containing 1 μM ligand (different porphyrins) was placed into a beaker. A volume of 0.5 mL of either single stranded DNA (poly A), double stranded DNA [poly (dA)-poly (dT)], triplex DNA poly (dA)-[poly (dT)2], or quadruplex DNA, was pipeted into separate DispoDialyzer units (Spectrum, CA). Dialysis units were then placed in a beaker containing the dialysate solution. The beaker was covered with Para film and wrapped with foil, and its contents were allowed to equilibrate with continuous stirring for 24 hours at room temperature. At the end of the equilibration period, DNA samples were carefully removed to microfuge tubes. The drug concentration was determined spectroscopically. The total concentration of the drug (Ct) within each dialysis unit was determined using the appropriate absorption wavelength (424 nm for TMPyP4, 400 nm for NMM, and

415 nm for Co(III)MPIX), and extinction coefficient for each ligand (ε_{424} of 2.2 x 10^5 M^{-1} cm^{-1} for TMPyP4, ε_{400} of 1.45 x 10^5 M^{-1} cm^{-1} for NMM, and ε_{415} of 1.5 x 10^5 M^{-1} cm^{-1} for Co(III)MPIX).

The free ligand concentration (Cf) was also determined spectrophotometrically using aliquots of the dialysate solution. The amount of bound drug (Cb) was determined from the difference (Cb = Ct – Cf). Data were plotted as a bar graph.

2.2.6. Screening libraries of porphyrins:

Four libraries of meso-substituted porphyrins [LA (1540 compounds), L1A (120 compounds), L2A (120 compounds) and L3A (21 compounds)] were provided by Dr. Charles M. Drain (Hunter College of CUNY) and were screened for their ability to bind quadruplex DNA with high selectivity.

Briefly, a portion of these libraries which had previously been passed over, and found not to bind to a column consisting of calf–thymus duplex DNA attached to glass beads (i.e., void volume fractions), was placed on one side of a specialized dialysis cell which

holds one milliliter of solution (Spectrum, CA) with an equal volume of quadruplex DNA being placed on the other side. The two chambers of the dialysis cell were separated using a dialysis membrane. After equilibrium for 24 hours in the dark, the library was replaced with buffer containing no porphyrin and the dialysis was repeated.

2.3. Results and Discussion

2.3.1. Quadruplex formation

Intramolecular quadruplex structures were detected by gel electrophoresis (Figure 11), and were found to migrate more quickly than single stranded DNA with similar base sequences, and a 24-mer double-stranded DNA. Quadruplex structures were more evident in the presence of 100 mM KCl.

A range of spectroscopic methods, including ultraviolet absorption, can produce detailed information regarding the conformation of quadruplex DNA structures. Absorption profiles, measured at 260 nm, for guanine-rich oligonucleotides *versus* temperature, in most cases do not provide a precise determination of the melting temperature. This observation has led several laboratories to record absorbance at different wavelengths. Absorption spectra derived from quadruplex structures exhibit an isobestic point around 280 nm, and a net hyperchromism is observed upon G-quartet formation at 285nm or higher wavelength. This effect is maximal at

295 nm. For these reasons, the formation of G-quadruplex structures can be followed at 295 nm (64).

For guanine-rich sequences, quadruplex formation was observed by drop in absorbance at 295 nm as the temperature increases. Observed high melting temperatures (60°C) supports the presence of a stable quadruplex. The spectra were compared to melting temperature curve of single stranded DNA of similar sequence [poly (A)] (Figure 12). However, there was no change in absorbance of single stranded DNA [poly (A)] with increasing temperature. Observing the quadruplex melting temperature at 295 nm was preferred to monitor the quadruplex formation (Mergny *et al* (64)), although measurement of the melting temperature at 260 nm was also conducted, but found to provide similar data to that recorded at 295 nm, and consequently, was used only for comparison purposes.

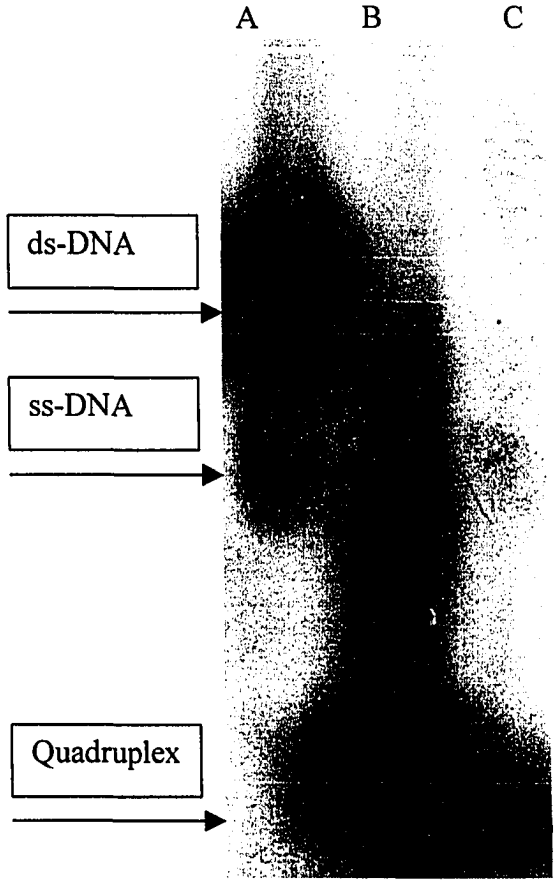

Figure 11. Quadruplex gel electrophoresis. Lane A is the double stranded DNA [$(CG)_2ATAT(CG)_2$]. Lane B is human telomeric sequence(HT4) which is able to form intramolecular quadruplex. Lane C is 8-mer single stranded DNA. All samples were labeled at the 5' end using ^{32}P. All samples were loaded into preequilibrated 12 % polyacrylamide gel and run in 0.5% TBE buffer.

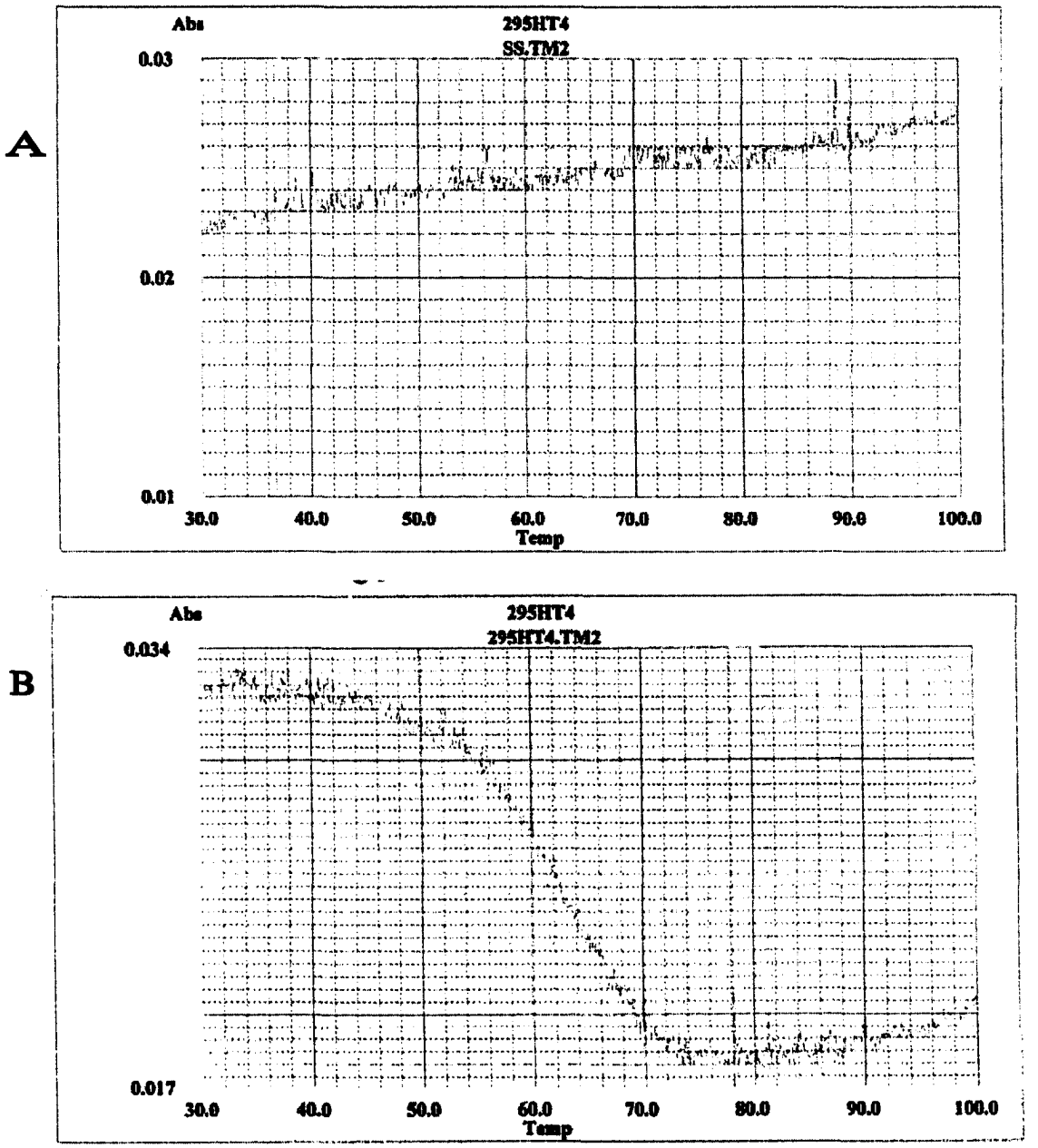

Figure 12. Melting temperature analysis of: A. ss-DNA and B. quadruplex –DNA. HT4 DNA at 1.5 μM was suspended in buffer containing 10 mM sodium cacodylate (pH 8.0) and 100 mM KCl. Melting curves were obtained by monitoring the absorbance at 295 nm as the temperature was ramped from 30 to 90°C at the rate 1°C/min.

2.3.2. Visible absorption titration:

Free porphyrin was titrated with DNA to construct Scatchard plots of r/Cf versus r, the binding ratio. "r" is defined as Cb/[DNA], where the molar concentration of bound porphyrin, Cb, is equal to $\Delta A/\Delta\varepsilon$ (ΔA is the difference in absorption of the free porphyrin and porphyrin in the presence of DNA at λmax) and $\Delta\varepsilon$ is the difference in molar extinction coefficients between the free and bound porphyrin, ($\varepsilon f - \varepsilon b$).

Figure 13 shows the visible spectra of porphyrin (TMPy4) in the absence and the presence of telomeric repeats. Changes in the Soret band of the porphyrin are observed in the presence of excess DNA; the spectra are characterized by a red shift and hypochromicity in this band. The magnitudes of these changes are quite different for different DNA forms; the quadruplex produces a larger shift in the Soret band, and a greater degree of hypochromicity for this band, compared to duplex DNA (87).

The absorption data were fitted to the simple Scatchard equation r/Cf =K(n –r), where Cf=Ct-Cb, K is the equilibrium constant, and n represents the number of ligand bound per DNA quadruplex (Figure 14). The high degree of linearity of the fit indicates a good correlation with a model where identical and independent binding sites are assumed.

Examination of binding data reveals that binding of the porphyrin, TMPyP4 to the quadruplex is about 2-fold stronger than for duplex DNA. The value of n indicates a binding of only one porphyrin for every quadruplex; these results are essentially in agreement with previously published data (87) (Table 1).

TMPyP4 represents a class of cationic (meso-substituted) porphyrins and has the advantage that it can electrostatically interact with the negative phosphate backbone of the DNA. However, its specificity for quadruplex over duplex DNA is not compelling. Also, spectroscopic studies showed that there is no significant difference in the hypochromicity of the Soret band of TMPyP in the presence of either duplex or quadruplex DNA. As a consequence, we chose to

explore the binding affinity and selectivity of N-substituted anionic porphyrins (Figure 15).

Anionic N-methyl mesoporphyrin IX (NMM) shows a significant difference in hypochromicity between duplex and quadruplex-DNA structure. The absorption spectrum of NMM is not changed by the presence of duplex DNA, whereas the wavelength of the maximal absorption shifts to longer wavelength in the presence of quadruplex structure (88). These results suggest that NMM has no appreciable binding affinity for duplex DNA and is specific for quadruplex binding.

A Scatchard plot was constructed for NMM/quadruplex absorption titration data to determine the porphyrin binding affinity (Figure 16). An equilibrium-binding constant of 2×10^6 for NMM was obtained compared to 2×10^7 for TMPyP4, with 3 binding sites compared to 1 binding site for TMPyP4. The binding affinity of NMM was tested for intramolecular and intermolecular quadruplex structures. NMM showed a somewhat greater binding affinity for

intramolecular quadruplex-DNA over intermolecular quadruplex structure (Table 2).

In summary, while our data reveal that NMM has a somewhat reduced binding affinity compared to TMPyP4, it does exhibit relatively high selectivity for quadruplex over duplex DNA.

Recently, it was reported that NMM is a highly specific inhibitor of RecQ helicase unwinding activity for G-quadruplex structures, but not for duplex DNA. This observation is in qualitative agreement with our binding data, which suggests that NMM can bind selectively to G-quadruplex DNA; this property undoubtedly contributes to substrate-specific inhibition of quadruplex unwinding (89).

It is unlikely that relative binding affinities of porphyrins to distinct DNA structures entirely account for the potency or specificity of inhibition. For example, NMM inhibits G-quadruplex unwinding somewhat better than does TMPyP4, but when binding of G-G paired DNAs by TMPyP4 and NMM was compared by equilibrium dialysis, TMPyP4 was shown to bind this nucleic acid species 3-fold better than

did NMM (82). Moreover, there is a 5-fold difference in inhibition constant for TMPyP4 inhibition of G-quadruplex unwinding relative to duplex DNA unwinding (89), but equilibrium dialysis and Scatchard analysis found that TMPyP4 showed little specificity for binding to G-quadruplex over duplex DNA (87). Further evidence that enzyme inhibition by small molecules is not a simple reflection of affinity of those molecules for nucleic acid substrates comes from a recent report, which tested the ability of a panel of reagents that interact with DNA to inhibit WRN and BLM helicase activity (90). The most potent inhibitor was distamycin, this compound inhibited the unwinding of duplex DNA substrate by BLM and WRN helicases with values for the inhibition constant (K_i) in the 1 μM range. In contrast, K_i values of other compounds that bind with higher affinity to duplex DNA were 10-fold higher. This report confirms that there is little direct relationship between ligand binding affinity to DNA substrate and their ability to inhibit certain enzymes. As a consequence, NMM is an attractive candidate for telomerase inhibition despite its relative low binding affinity to quadruplex DNA compared to TMPyP4.

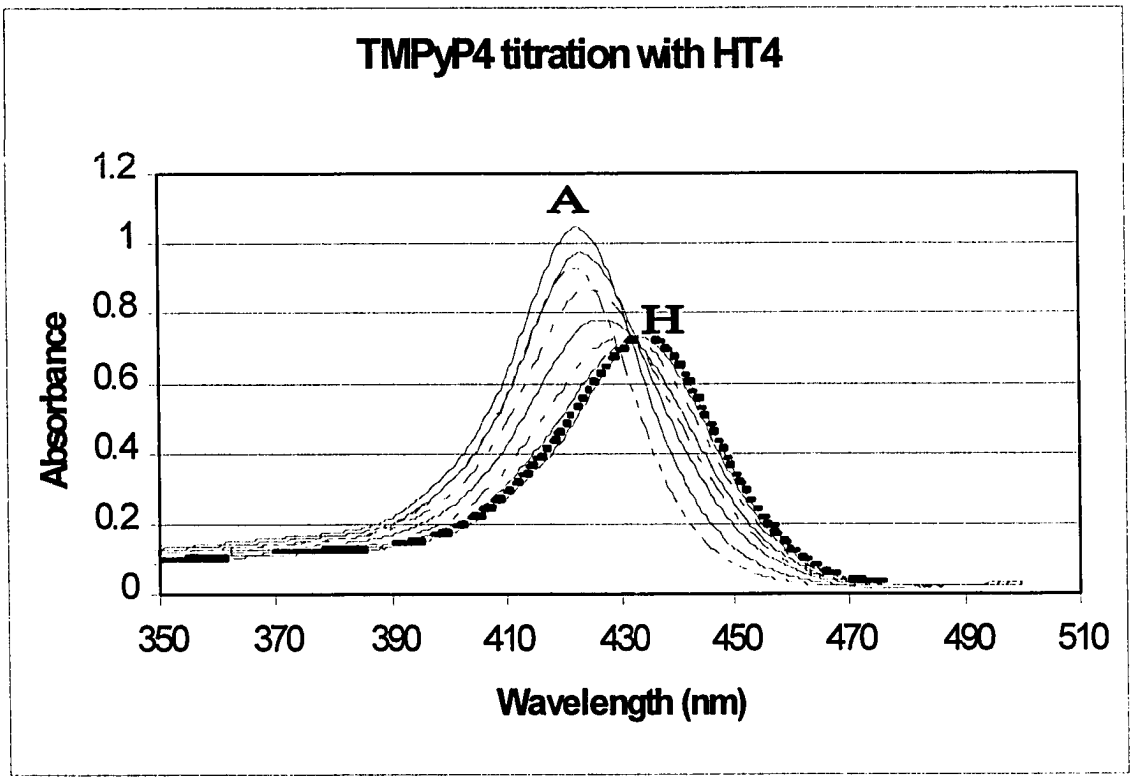

Figure 13. Visible spectrum of TMPyP4 in the absence of quadruplex DNA (A), and in the presence of quadruplex DNA at saturation (H). The concentration of porphyrin is 5mM. All titrations were performed at room temperature and in buffer containing 10 mM sodium cacodylate and 0.1 M KCl. Samples were incubated at the dark for 10 min after each addition.

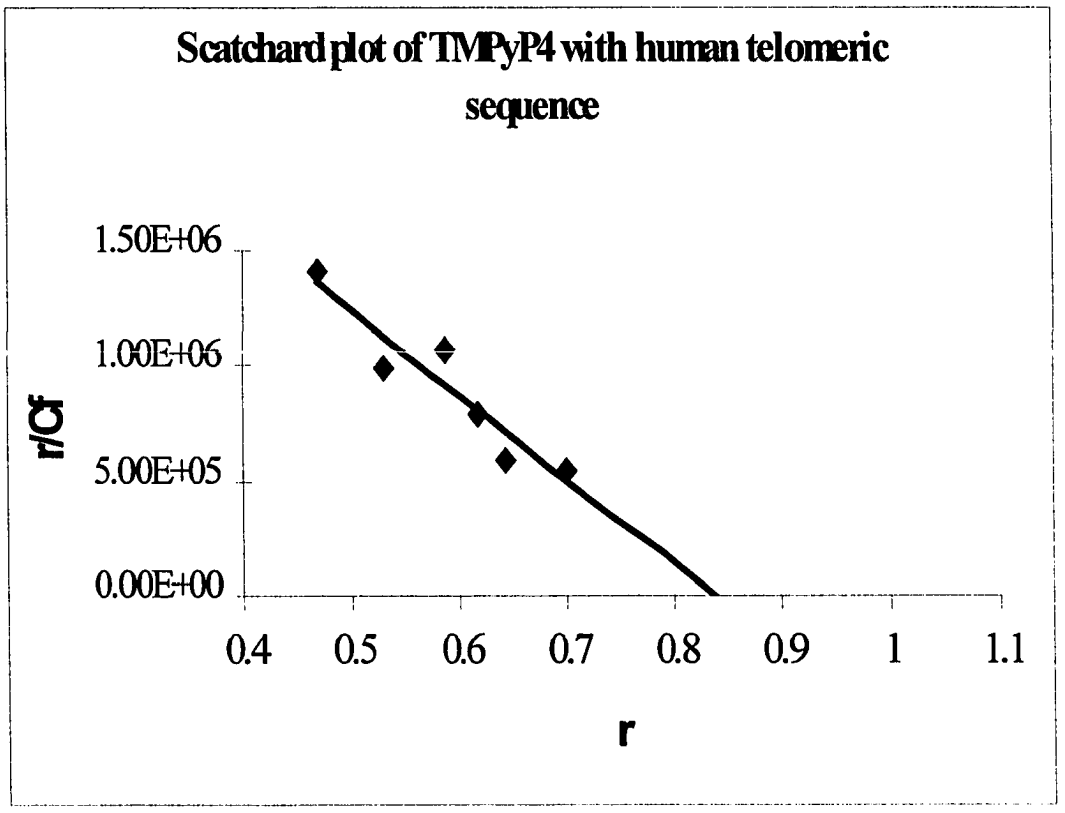

Figure 14. Scatchard plot analysis of TMPyP4 binding to HT4. The values of r were calculated in terms of the concentration of quadruplex DNA. The data are represented by the points, and the fits, calculated with Scatchard equation [$r/C_f = K(n-r)$].

Oligomers	K (mol^{-1})	n
ds-DNA	1.3×10^{7}	1.92
Intermolecular quadruplex (T4G4)	2.7×10^{7}	0.59
Intramolecular quadruplex (HT4)	6.0×10^{6}	0.67

Table 1. Equilibrium binding properties for various DNA sequences with TMPyP4. The binding constant K is calculated from the slope of the Scatchard plot, and n represents the number of porphyrin molecules bound by duplex or quadruplex DNA.
Results for intermolecular quadruplex are taken from Anantha *et al*, *Biochemistry*, 37(9):2709-2714.

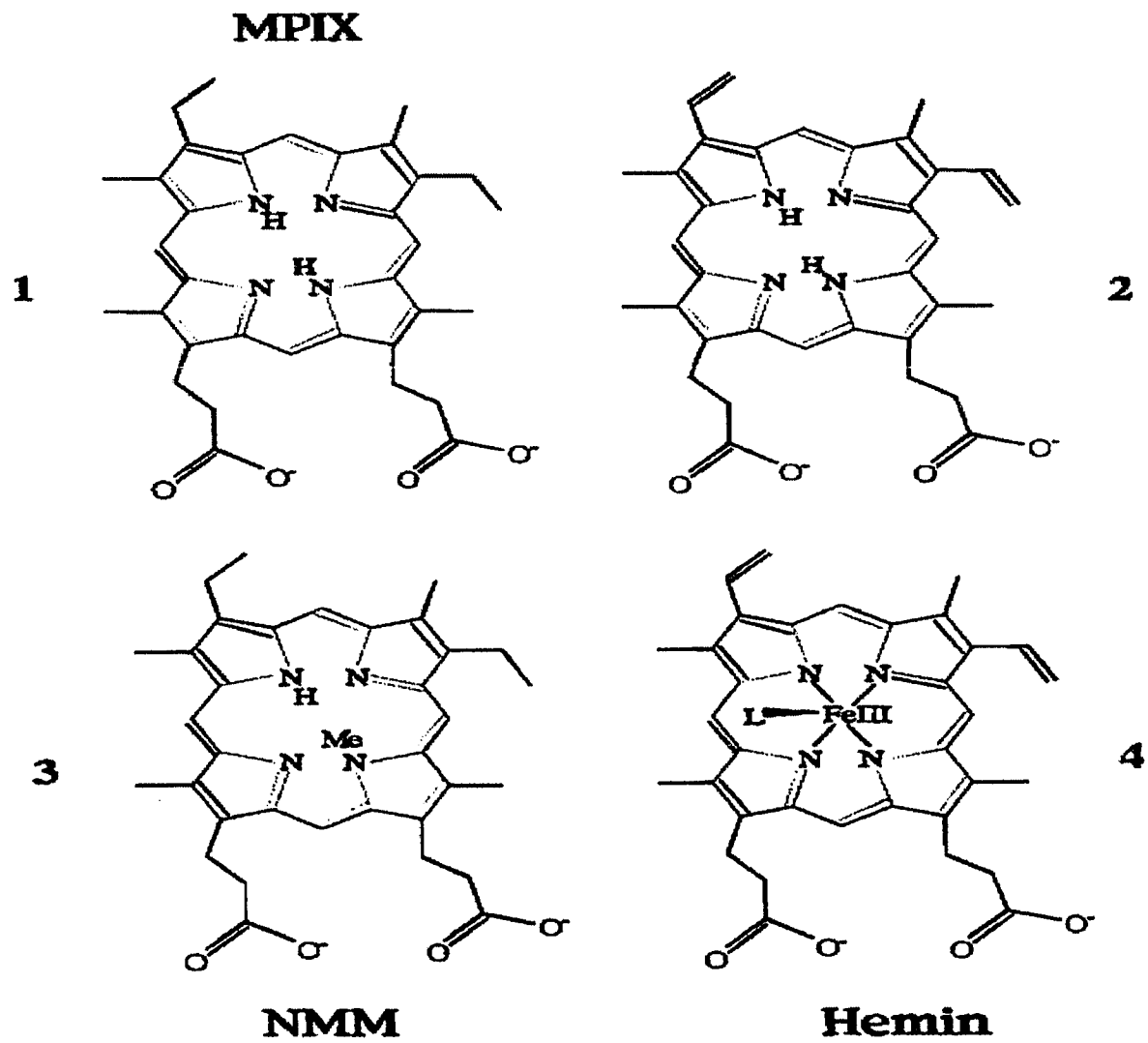

Figure 15. Structure of anionic porphyrins:

1- MPIX = Mesoporphyrin IX
2- PPIX = Protoporphyrin IX
3- NMM = N-methylmesoporphyrin IX
4- Hemin = Iron (III) protoporphyrin IX

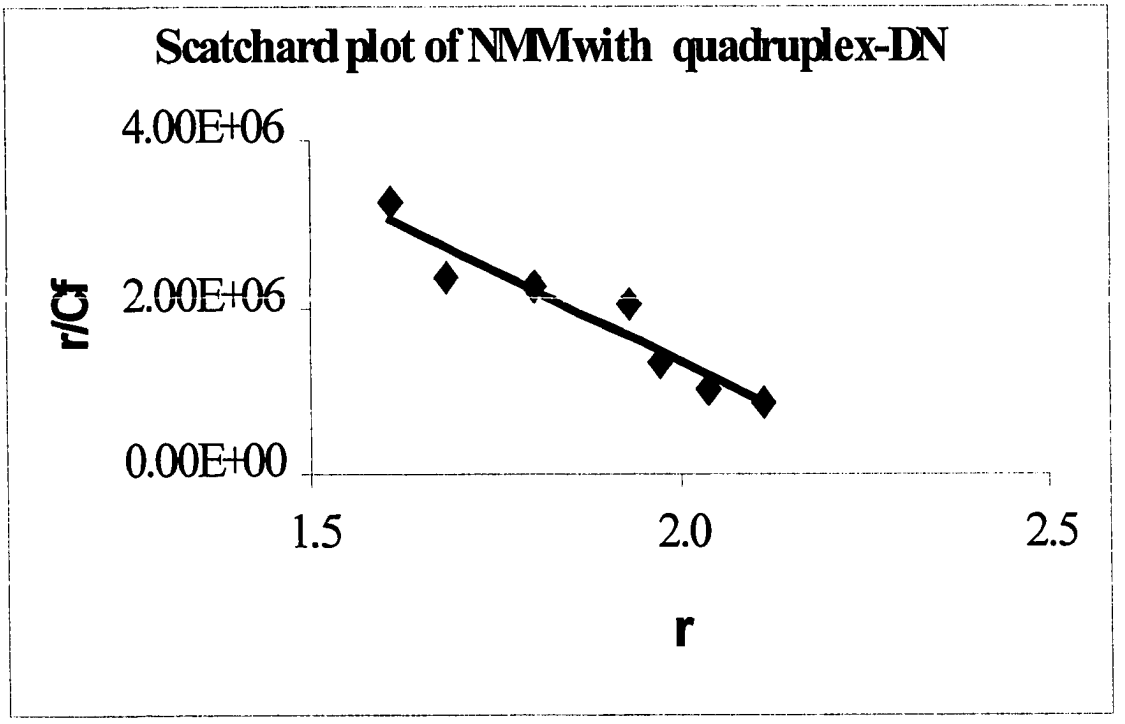

Figure 16. Scatchard plot analysis of NMM binding to quadruplex DNA.The values of r were calculated in terms of the concentration of quadruplex DNA. The data are represented by the points, and the fits, calculated with Scatchard equation [$r/C_f = K(n-r)$].

Oligomers	K (mol^{-1})	n
ds-DNA	No binding	No binding
Intermolecular quadruplex (T4G4)	1.0×10^{6}	2.3
Intramolecular quadruplex (HT4)	2.0×10^{6}	2.59

Table 2. Equilibrium binding properties for various DNA sequences with anionic NMM. The binding constant K is calculated from the slope of the Scatchard plot, and n represent the number of porphyrin molecules bound per quadruplex DNA. All titrations were performed at room temperature, and in buffer containing 10 mM sodium cacodylate and 0.1 M KCl. Samples were incubated in the dark for 10 min after each addition of the DNA.

2.3.3. Effect of central metal ion

The effects of a central metal atom, coordinated within the porphyrin ring, on binding affinity and selectivity for quadruplex DNA were investigated.

Scatchard plots from porphyrin absorption data were constructed from which the binding constants for Co(III)MPIX to intermolecular and intramolecular quadruplex structures were extracted (Figure 17). We found that Co(III)MPIX has a greater binding affinity for human telomeric sequence (HT4) than for intermolecular quadruplex structures formed by the *Oxytricha* telomeric sequence (T4G4), and requires only one molecule to stabilize the quadruplex structure (Table 3). Although the N-substituted anionic porphyrins bind to human telomeric sequences with a lower binding affinity than cationic TMPy, Co(III)MPIX was found to bind more tightly than corresponding anionic NMM and MPIX porphyrins. Furthermore, an increase in Co(III)MPIX: DNA molar ratio resulted in a corresponding increase in the quadruplex melting temperature, suggesting that Co(III)MPIX is able to stabilize quadruplex structures (Figure 18). The increased

melting temperature is an indication that the bonds between guanine residues participating in the G-tetrads are stronger in the presence of the drug compared to that of the quadruplex-DNA only. Comparison of the Co(III)MPIX stabilization effect with NMM revealed higher melting temperatures for Co(III)MPIX compared with the same molar ratio of NMM to DNA, suggesting a greater stabilization of the quadruplex by Co(III)MPIX.

Binding experiments were performed to determine whether the size or charge of the central cation (and hence the overall anionic character of the porphyrin) was important for improving the binding affinity of MPIX. Compared with Co(III)MPIX, we found that substitution of the central metal ion of MPIX with Sn(IV), Fe(III) or Zn(II) giving rise to porphyrins of differing overall net positive charge, does not significantly improve the binding affinity of the prophyrin for quadruplex DNA structures (Table 4). Substitution of the central Co(III) atom of MPIX with ions of larger ionic radii (Ru(II) or Yb(III)) resulted in significantly reduced binding affinity of the metal-MPIX porphyrin to quadruplex-DNA (Table 4). That size and overall net

positive charge of the bound ligand is not sufficient alone for quadruplex recognition has been previously noted (92) for binding of ethidium derivatives to quadruplex DNA structures.

In summary, coordination of a central metal ion within the porphyrin structure is important for improving the binding affinity of MPIX for quadruplex DNA. However, only Co(III)MPIX improves the binding affinity to quadruplex by 10 fold.

2.3.4. Selectivity for quadruplex-DNA structures

The most important requirement for an ideal quadruplex interactive agent is selectivity (Figure 19). Our goal was to find a new compound that binds selectively to quadruplex-DNA structure and not to ss-DNA, ds-DNA or triplex DNA.

As discussed, recently Chaires *et al* have developed a rapid competitive equilibrium dialysis method for studying drug selectivity to different DNA structures (82). In this method a solution of differing nucleic acid structures of identical concentration are dialysed against

the porphyrin of interest. After equilibrium, the amount of porphyrin bound to each DNA structure is determined by optical assay. More porphyrin accumulates in the dialysis tube containing the DNA structure for which the ligand has the highest binding affinity and selectivity.

We compared the binding affinity and selectivity of TMPyP4 (cationic), NMM (anionic) and Co(III)MPIX (anionic) to different DNA forms using this technique. Our data show that TMPyP4 can bind to all forms of DNA, although the binding affinity for quadruplex is almost two-fold greater than for double stranded DNA. This result is in agreement with previously published data (87) and demonstrates that the technique is reliable and valid for studying drug-DNA binding selectivity and affinity using different DNA forms.

In contrast to cationic TMPyP4, the anionic porphyrins, NMM and Co(III)MPIX showed high binding selectivity for quadruplex DNA over ss-DNA, ds-DNA and triplex (Figure 20), with Co(III)MPIX demonstrating the greater selectivity compared with NMM, as predicted by our previous Scatchard analysis.

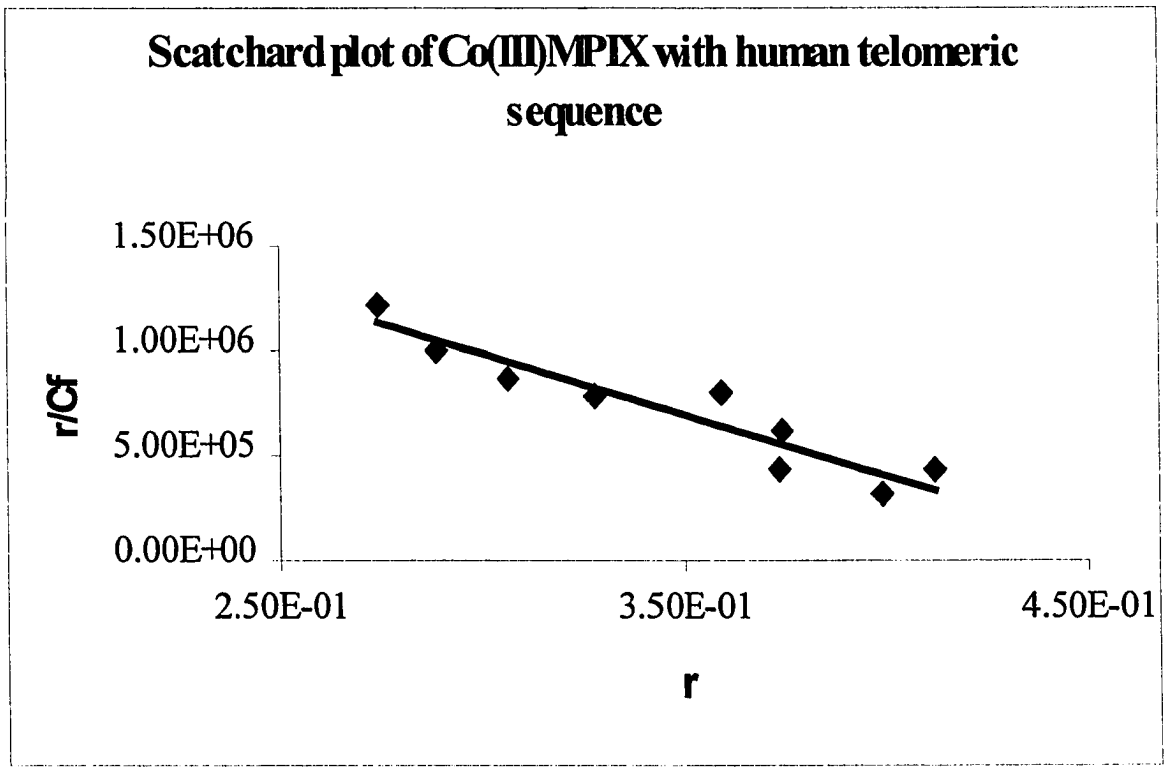

Figure 17. Scatchard plot analysis of Co(III)MPIX binding to human telomeric sequence. The values of r were calculated in terms of the concentration of quadruplex DNA. The data are represented by the points, and the fits, calculated with Scatchard equation [$r/C_f = K(n-r)$].

Oligomers	K (mol^{-1})	n
ds-DNA	No binding	No binding
Intermolecular quadruplex (T4G4)	3.0×10^{6}	1
Intramolecular quadruplex (HT4)	4.5×10^{6}	0.5

Table 3. Equilibrium binding constant properties of DNA sequences for Co(III)MPIX. The binding constant K calculated from the slop of the Scatchard plot and n represents the number of porphyrin molecules bound by duplex or quadruplex DNA. All titrations were performed at room temperature, and in buffer containing 10 mM sodium cacodylate and 0.1 M KCl. Samples were incubated for 10 min after each addition in the dark.

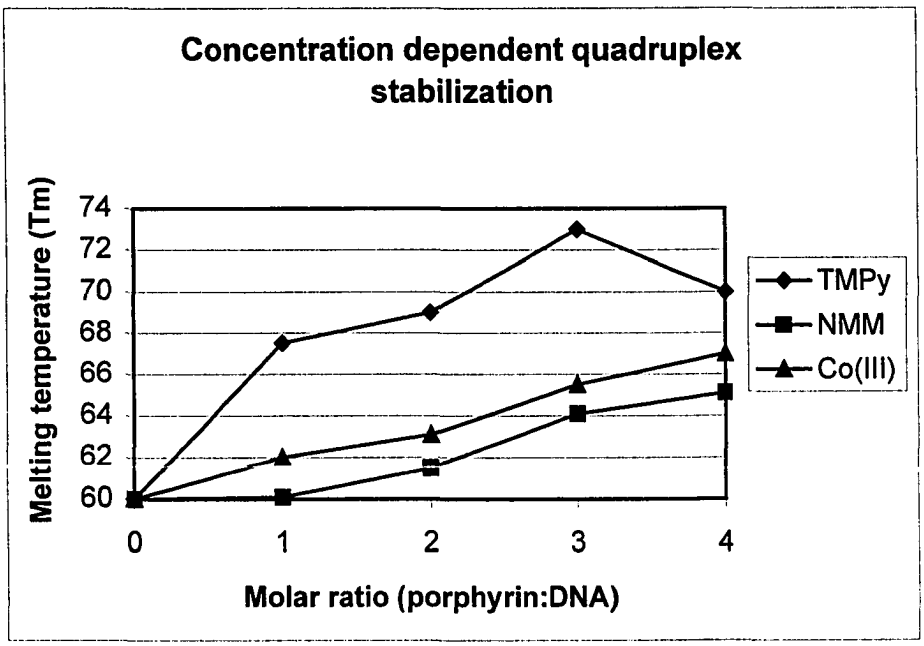

Figure 18. Comparing melting temperatures of quadruplex in presence of anionic and cationic porphyrins. HT4 DNA at 1.5 μM was suspended in buffer containing 10 mM sodium cacodylate (pH 8.0) and 100 mM KCl. Appropriate amounts of stock solutions of particular porphyrins were added sequentially to increase the molar ratio of porphyrin to DNA from 1:1 to 2:1, 3:1, 4:1. Melting curves were obtained by monitoring the absorbance at 295 nm as the temperature was ramped from 30 to 90°C at the rate of 1°C/min. The temperature corresponding to the maxima in the first derivative plots of the melting curves were selected as the melting temperatures (Tm).

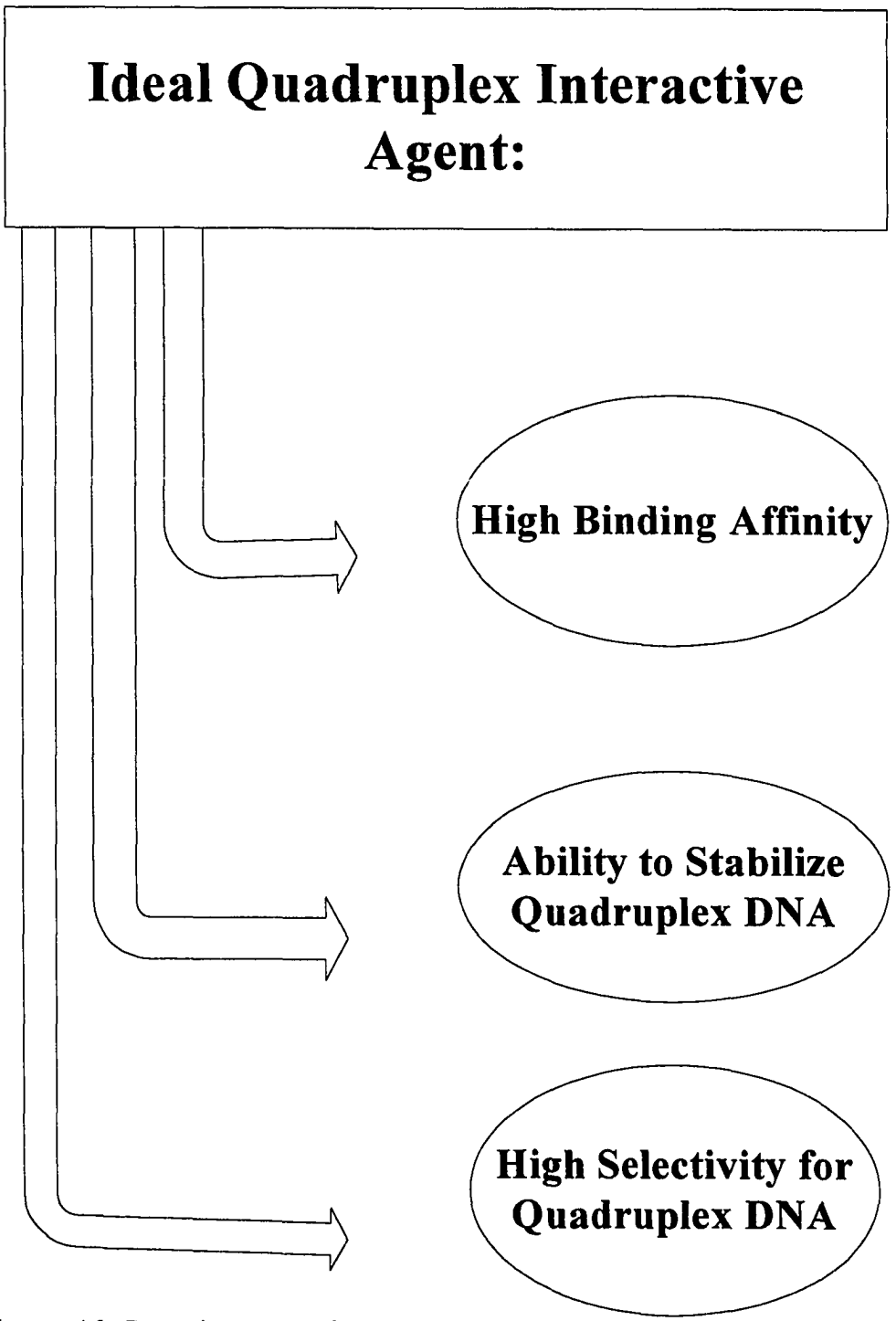

Figure 19. Requirements for ideal QIAs.

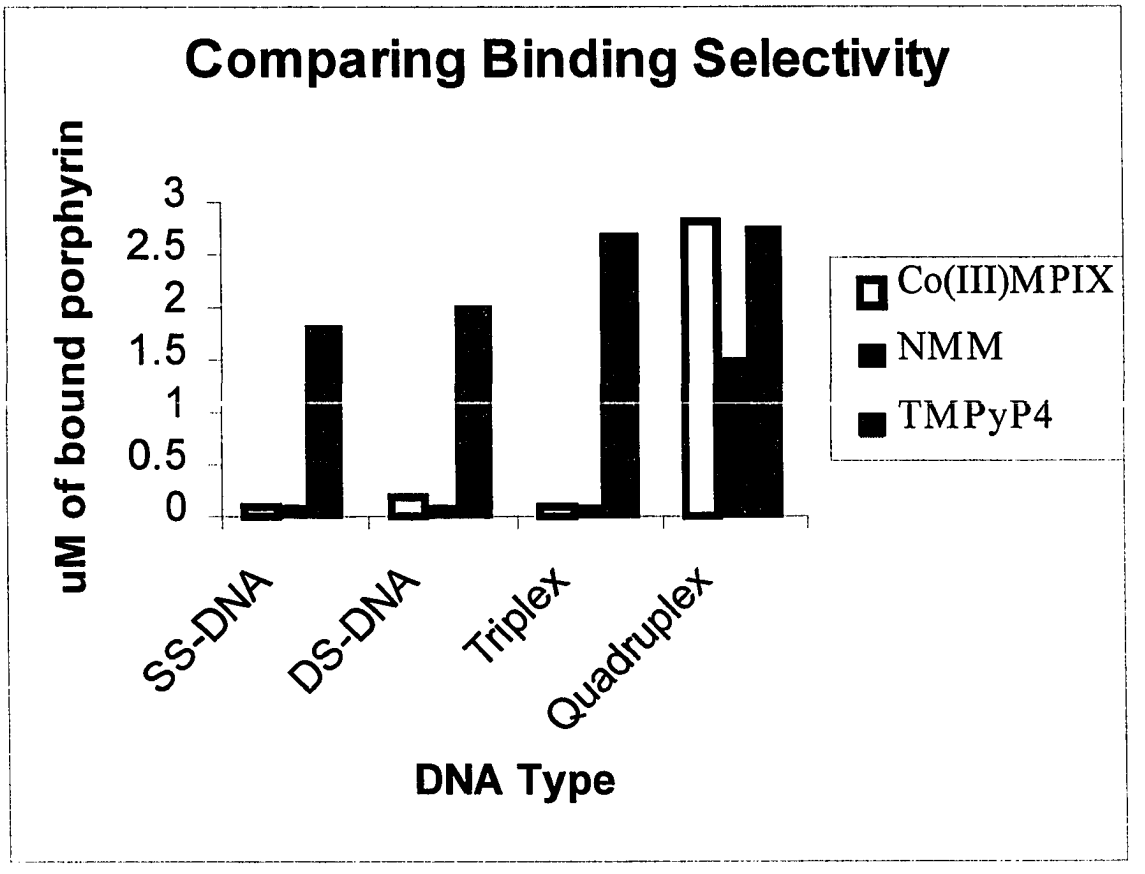

Figure 20. Comparing binding selectivity of anionic and cationic porphyrins. Selectivity of porphyrins is calculated by subtracting the μM of porphyrins found in the diasylate from the μM of porphyrin found in the dialysis bag containing 75 μM (in DNA bases) of one of the above species of DNA after 24 hr dialysis. Abbreviations: SS = single stranded DNA [poly(dT)], DS = double stranded DNA [poly (dA).poly (dT)], TS = triple stranded DNA [poly(dA)-poly$(dT)_2$], and Quad = quadruplex DNA $[(TTAGGG)_4]$.

porphyrin	$\Delta\lambda_s$	K(mol^{-1})	*n*	ΔT_m	μmoles bound	%hypochromicity
TMP	14	6.00E+06	0.67	12	2.74(low)	58.5
Co(III) MPIX	3	4.50E+06	1	3	1.32(high)	44.1
Co(III) PPIX	4	nd	nd	0	1.30(high)	46.0
NMM	18	2.00E+06	3	2.6	0.67(high)	60.6
Fe(III) PPIX	nd	7.00E+05	nd	nd	nd	nd
MPIX	nd	6.60E+05	nd	nd	1.2 (high)	nd
Ni(II) MPIX	nd	6.00E+05	nd	nd	nd	nd
Zn(II) MPIX	nd	5.50E+05	nd	nd	nd	nd
PPIX	16	4.59E+05	13	0	0.18	65.7
Fe(III) MPIX	nd	3.60E+05	nd	nd	nd	nd
Sn(IV) MPIX	0	3.08E+05	6.5	0	0.37(high)	19.3
Cr(III) PPIX	2	nd	nd	2.7	0.39(high)	38.8
Cr(III) MPIX	nd	2.06E+05	14.6	1.7	0.41(high)	35.7
Ru(II) MPIX	nd	nd	nd	nd	0	nd
Yb(III) MPIX	nd	nd	nd	nd	0	nd

Table 4. Porphyrins-quadruplex binding affinity and selectivity.
$\Delta\lambda$s is calculated as λ_b - λ_f, where λ_f is the wavelength of maximum absorbance of the Soret band for the free porphyrin and λ_b is the wavelength of maximum absorbance of the Soret band for the porphyrin in the presence of excess DNA. The binding constant, K is calculated from the slope of the Scatchard plot and n, the number of binding sites, is equal to the X intercept. The data were fit to the simple Scatchard equation: $r/C_f = K(n-r)$, where r is the ratio of molecules bound and C_f is the concentration of free porphyrin. ΔT_m is calculated as the difference between the T_m of the quadruplex DNA when the indicated porphyrin is present at a 3:1 molar ratio and when no porphyrin is present, respectively. μmoles bound indicates the level of porphyrin found associated with the quadruplex DNA following an equilibrium dialysis experiment to determine selectivity, it is calculated from $(A_{quad} - A_{dialysate})/(\varepsilon \times 10^{-6})$. The % hypochromicity was calculated using: $(\varepsilon_f - \varepsilon_b)/\varepsilon_f$, where ε_f and ε_b are the extinction coefficients at the Soret band of free and fully bound porphyrin, respectively. (nd = not determined).

2.3.5. Protoporphyrins

It was previously reported (91) that while certain G-rich sequences of ≈180 and 280 nucleotides bind to cationic NMM with sub-micromolar affinity, they exhibited lower binding affinities for mesoporphyrin IX (MPIX) as well as various metallo-MPIX derivatives. Furthermore, the same laboratory noted that hemin [iron (III) protoporphyrin IX; (PPIX)] binds to the G-rich sequences more tightly than some metallo-mesoporphyrin such as Ni(II)MPIX. Hence, we proposed that protoporphyrins might provide attractive candidates for further study, and the binding affinity and selectivity of protoporphyrin IX (PPIX), Co(III)PPIX, Fe(III)PPIX, and Cr(III)PPIX were examined. However, as shown in Table 4, all protoporphyrins used in this study revealed low binding affinity to quadruplex structures and were not further explored.

2.3.6. Saccharide-coated porphyrins

It is well known that hepatocytes express galactose receptors. It has been reported (83) that these receptors exhibit remarkable saccharide (galactoside) specificity for saccharide-coated porphyrins.

We tested whether incorporation of saccharide moieties to porphyrins exhibits any effect on quadruplex DNA recognition and binding affinity. We have studied four different sugar-porphyrins, modified by incorporation of glucose (or galactose) as the single substituent for a methyl group (mono-glucose TMPy, or mono-galactose TMPy, respectively) (Figure 21), or by the incorporation of four glucose (or galactose) molecules to substitute for the four peripheral methyl groups in the core TMPy (tetra-glucose TMPy, or tetra-galactose TMPy, respectively).

The presence of the sugar moiety only affects the binding affinity to a small extent, as determined from a Scatchard analysis for each individual sugar-modified porphyrin (Figure 22, and table 5). The binding constants of the four sugar modified porphyrins were on the

same order as the parent TMPy4 molecule. In addition, the selectivity of the four sugar-porphyrins for quadruplex over different DNA conformations is low (Figure 23). Indeed, all of the four sugar-modified porphyrins used in this study showed almost no preference for quadruplex DNA over single stranded DNA as demonstrated by dialysis experiments. These results suggest that the presence of such sugar moieties alone does not influence the binding affinity or binding selectivity to quadruplex DNA over other forms of DNA and that the relatively low selectivity arises from the core porphyrin.

Recently, few receptors such as lectins were shown to have 2 separate binding sites, one for porphyrin and a separate binding site for sugars. Several free-base porphyrins and their corresponding copper(II) and zinc(II) derivatives with the galactose-specific lectin from snake gourd seeds (*Trichosanthes anguina*) have been investigated by absorption and fluorescence spectroscopic techniques (93). The lectin dimer contains two apparently equivalent binding sites for porphyrins. The association constant obtained for the interaction of the various porphyrins with lectin were reported to be in the range 1.7

x 10^4- 6.2 x 10^5 M^{-1}, with the metalloporphyrins exhibiting higher affinity for the lectin compared with the free-base analogous. Both positively and negatively charged porphyrins bind to snake gourd seeds lectin (SGSL) with comparable affinities, suggesting that binding occurs primarily via hydrophobic interaction. Further, binding of porphyrins is found to be largely unaffected by the presence of the sugar ligand, lactose, indicating that the binding sites for the carbohydrate and porphyrins are different. This study (93) suggested that the lectin might serve as a receptor for some endogenous non-carbohydrate, hydrophobic ligand *in vivo*, in addition to the saccharide ligands. It also opens up the possibility of employing the SGSL in applications such as photodynamic therapy (PDT), which involve the use of porphyrins.

In PDT, porphyrins preferentially accumulate in dividing cells and as a consequence their concentration in tumor tissue is higher than in normal cells. Upon irradiation by light of an appropriate wavelength, porphyrins can react with molecular oxygen, sending it into its excited singlet state, which in turn cause irreversible tissue

damage. In many cases the ratio of the photoactive drug in tumor tissue to that of the surrounding normal tissue is as low as 2:1. Since several lectins exhibit a preferential agglutination of tumor cells, coupling porphyrins to lectins may result in an increased selectivity of the conjugate for the tumor cells. Thus, studies on porphyrin interaction with cell receptor can be useful from a therapeutic point of view. This study also highlights that although the presence of sugar attached to porphyrins can facilitate porphyrin cellular uptake in some cell, its presence is not important for all cells, and porphyrin can bind to the cell receptors independently. In another study, it has been shown that porphyrins by themselves can be used as novel drug delivery vehicles and indeed porphyrins have been successfully used to deliver antisense treatment to the cell (75).

In summary, we suggest that the use of saccharide directed cell recognition as a tool for porphyrin delivery could improve cellular uptake but more importantly, our data suggest that the presence of such sugar moieties will not adversely influence the binding of the porphyrins to DNA once inside the cell.

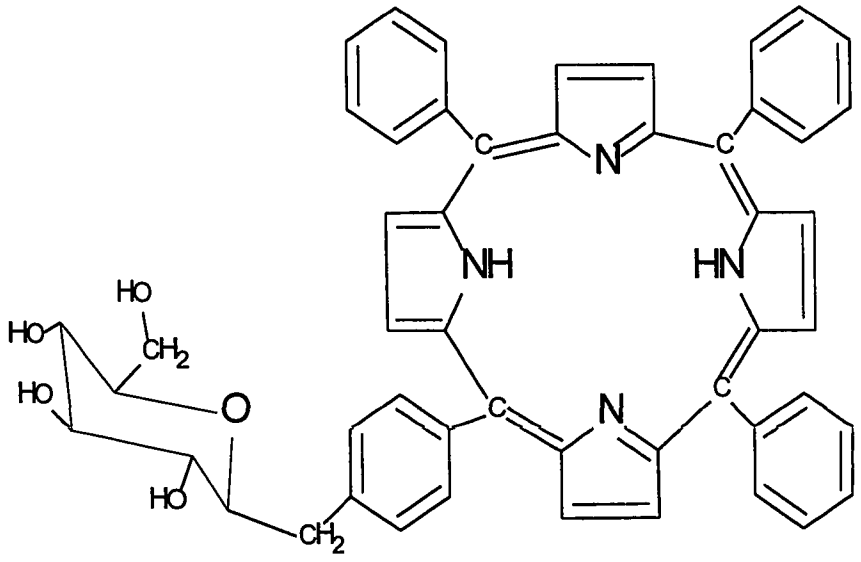

Figure 21. Structure of sugar porphyrin.

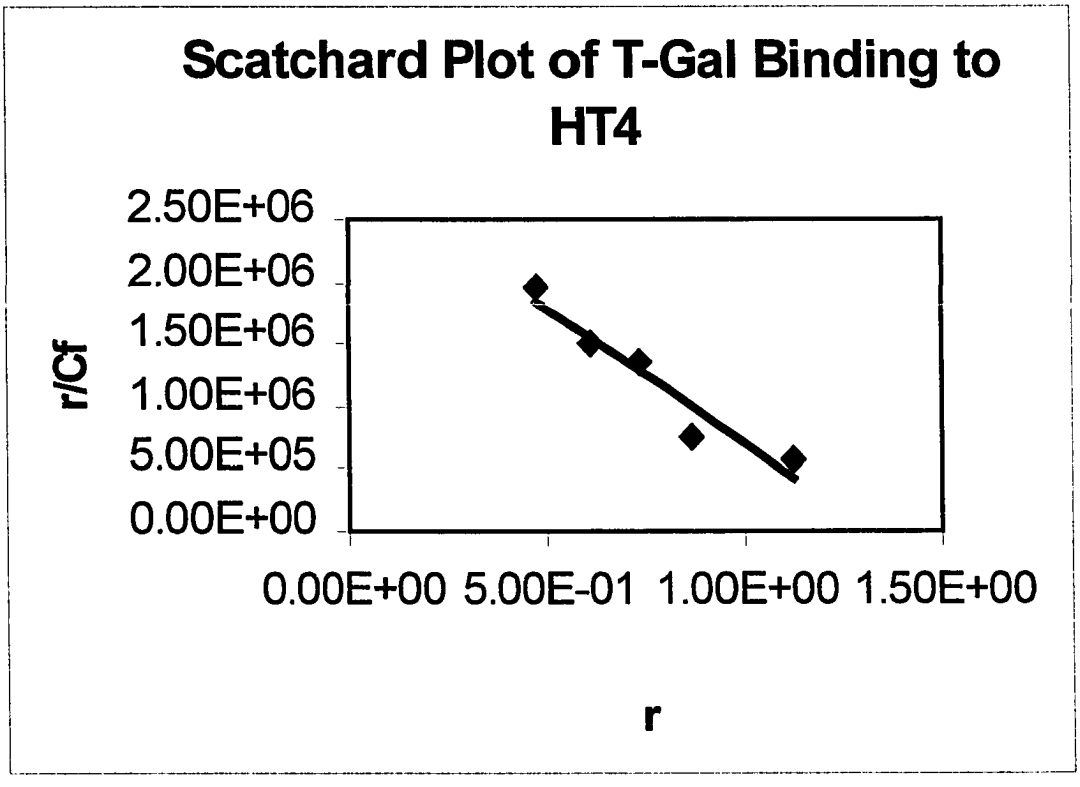

Figure 22. Scatchard plot analysis of T-galactose binding to quadruplex DNA. The data are represented by points, and the fits, calculated with Scatchard equation [r/Cf = K (n-r)], are represented by the line.

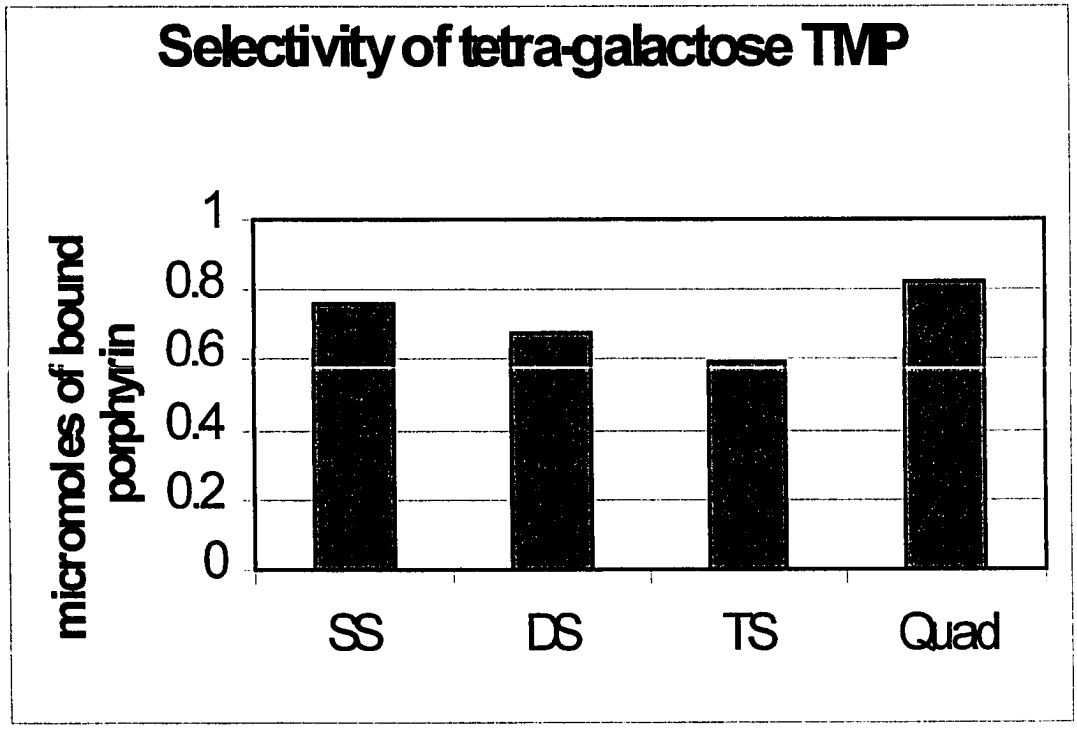

Figure 23. Selectivity of T-galactose to different DNA structures.

Results obtained by the competition dialysis method. Numbers are expressed as μM of bound porphyrin. Selectivity is calculated by subtracting the μM of porphyrin found in the dialysate from the μM of porphyrin in the dialysis bag containing 75 μM (in DNA bases) of one of the above species of DNA following a 24 hr dialysis. Abbreviations: SS = single stranded DNA [poly(dT)], DS = double stranded DNA [poly (dA).poly (dT)], TS = triple stranded DNA [poly(dA)-poly$(dT)_2$], and Quad = quadruplex DNA [$(TTAGGG)_4$].

Porphyrin	Binding Constant K (mol^{-1})	Selectivity for G-tetrads
Mono-Glu-TMPy	6.0×10^6	Low
Tetra-Glu-TMPy	2.0×10^6	Low
Mono-Gal-TMPy	4.5×10^6	Low
Tetra-Gal-TMPy	3.0×10^6	Low

Table 5. Sugar-porphyrins binding affinity and selectivity for quadruplex DNA. The binding constant, K is calculated from a Scatchard plot. The data were fit to the simple Scatchard equation:

$r/C_f = K(n-r)$, where r is the ratio of molecules bound and C_f is the concentration of free porphyrin. Low selectivity means that there was no appreciable difference of porphyrin concentration associated with quadruplex DNA and other DNA forms (ss, ds, and triplex DNA) after 24 hr dialysis.

2.3.7. Screening porphyrin libraries

We have screened different porphyrin libraries built on the cationic TMPyP as the core structure. The goal of this screening was to find a compound with high binding affinity and improved binding selectivity for quadruplex DNA by modifying the side chain of the TMPyP core compound.

Four pre-existing libraries of meso-substituted porphyrins (LA (1540 compounds), L1A (120 compounds), L2A (120 compounds) and L3A (21 compounds) were screened for their ability to bind quadruplex DNA with high selectivity for the human telomeric sequence (Figure 24). A sample of each of these libraries, which are eluted in the void volume after passing over a column consisting of ds-calf thymus DNA attached to glass beads, were assayed for quadruplex binding by the equilibrium dialysis assay (Figure 25).

None of the libraries investigated revealed high binding affinity or significant selectivity for quadruplex DNA over other DNA conformations. Some members of these libraries were investigated more closely after they revealed low binding affinity to double

stranded DNA, or alternatively showed no photocleavage ability of double stranded DNA. These porphyrins were named L3A reject (12 through 18). However, dialysis and binding studies revealed that none of these compounds have potential to bind specifically to quadruplex DNA (Table 6). One limitation of this approach is that no meso-substituted cationic porphyrins have yet demonstrated high levels of selectivity to quadruplex DNA. The results suggest that a more rationale approach, based on our binding and selectivity data, would be to synthesize a new library based on N-substituted anionic porphyrins that have already shown a high-degree of selectivity for quadruplex DNA. This pyrrole N-substituted library can then be screened for the ability to bind tightly to quadruplex DNA. It is unlikely that this library will need to be passed over a column containing calf thymus DNA as in the case of the meso-substituted libraries, due to the intrinsic selectivity for quadruplex DNA associated with this class of porphyrins.

We suggest that screening a library based on N-substituted anionic porphyrin will indeed lead to new porphyrins with improved

binding affinity and selectivity for quadruplex DNA structures. In addition, the traditional screening techniques for analyzing the selectivity and binding of a target ligand for quadruplex, as used here, are time consuming and not practical for analyzing vast numbers of molecules. As a consequence, we have developed a new fast, sensitive approach for drug screening many ligands (and not limited to porphyrin derivatives) based on fluorescence techniques.

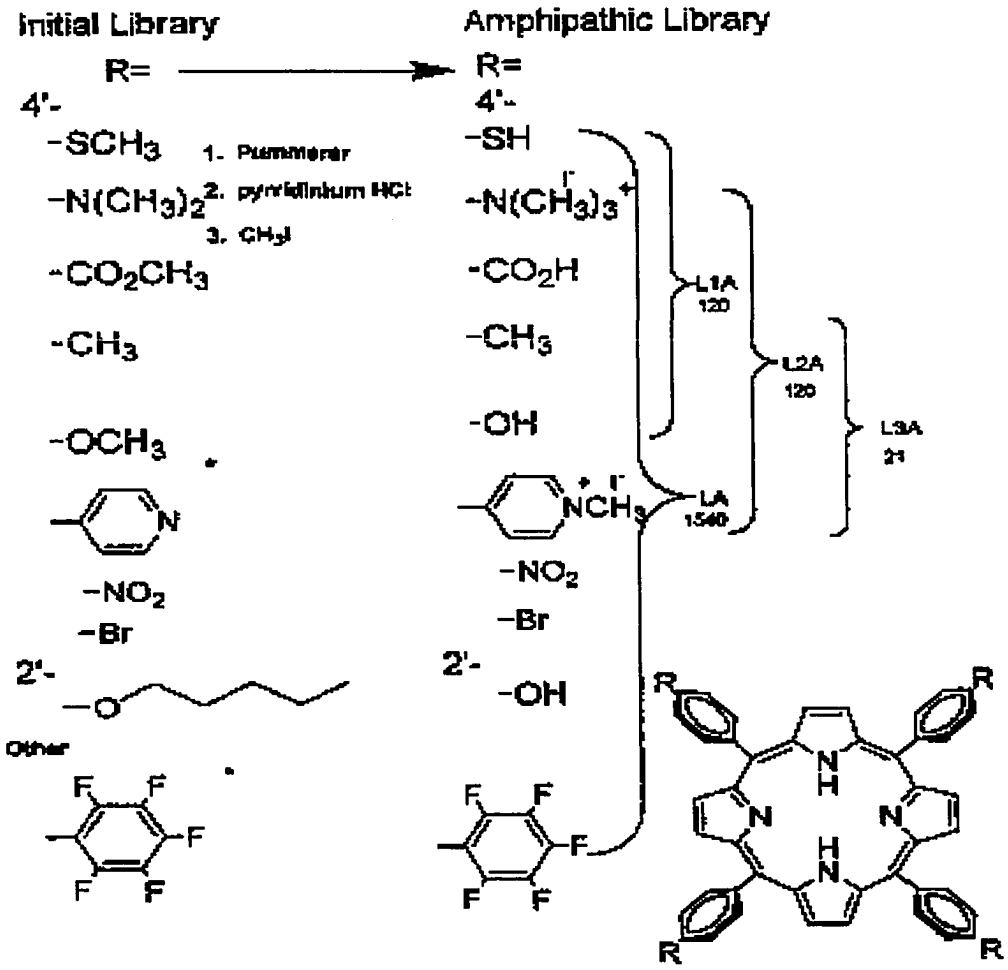

Figure 24. Structure of different porphyrin libraries. The number of compounds in each library indicated under the library name. Figure derived from Drain *et al* J. Comb. Chem. 1999, 1, 286-290.

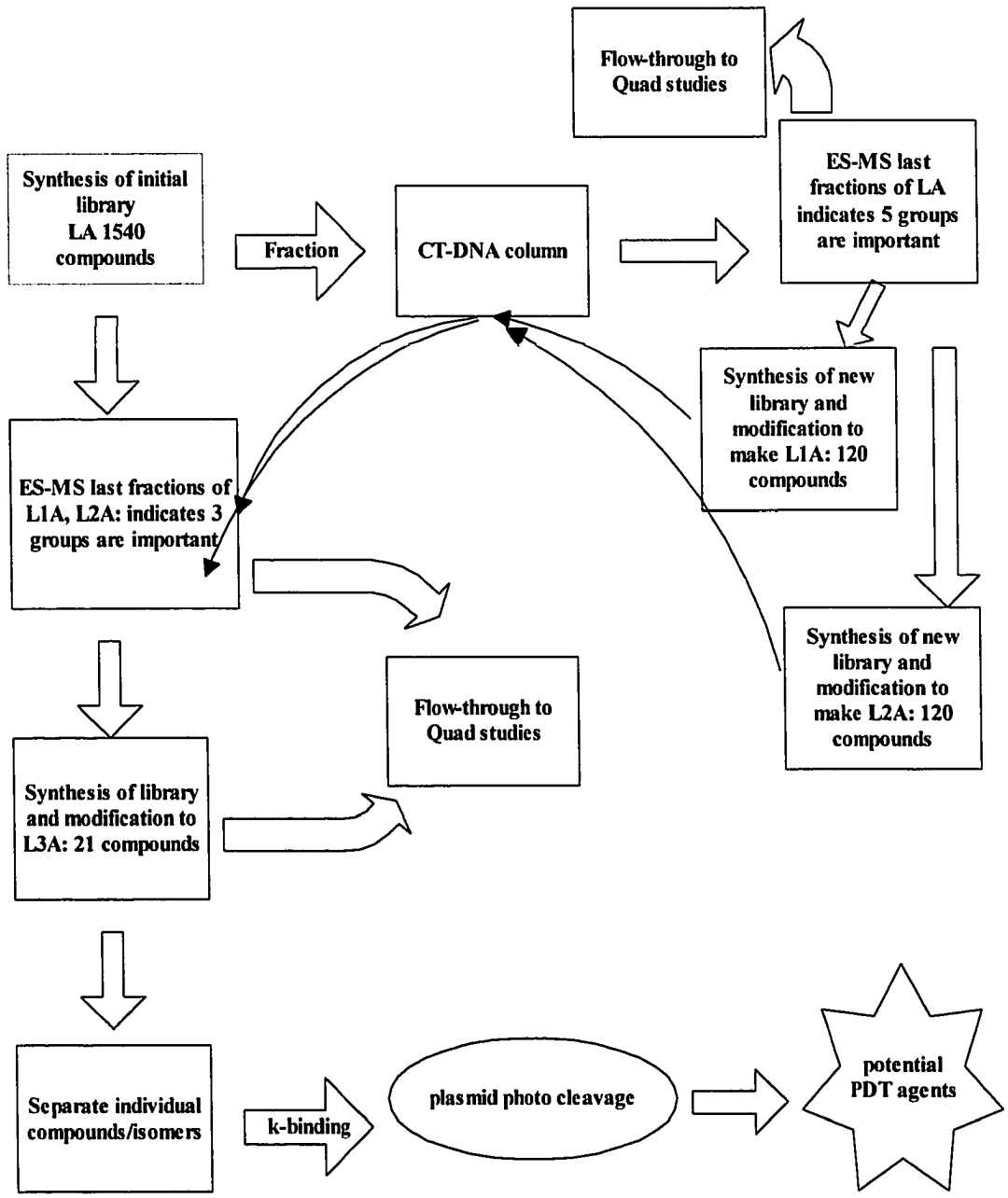

Figure 25. Scheme of library screening.

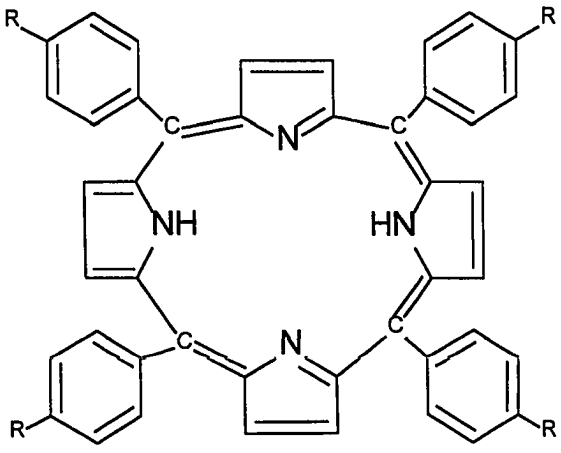

L3 rejects (no ØX174 photocleavage)					μMoles bound			
porphyrin	R	R'	R"	R"'	SS	DS	TS	Quad
12	PyMe	OH	OH	Me	0.03	1.17	0	0.37
13	PyMe	OH	Me	Me	0	0	0	0
14	PyMe	Me	OH	Me	0	0	0	0
15	PyMe	PyMe	OH	Me	0	0	0	0
16	PyMe	PyMe	Me	Me	nd	nd	nd	nd
17	PyMe	Me	PyMe	Me	0.5	0.18	0.43	0.05
18	PyMe	PyMe	OH	OH	nd	nd	nd	nd

Table 6. Structure and selectivity of L3 reject porphyrins. Numbers are expressed as μM of bound porphyrin. (nd = not determined)

3. Chapter II

Porphyrin-DNA Interaction:

Fluorescence Studies

3.1. Introduction:

3.1.1. DNA probes:

While very weak intrinsic fluorescence has been observed from DNA, the emission is too weak and too deep in the UV for practical applications. Fortunately, there are numerous probes that spontaneously or covalently bind to DNA and display enhanced fluorescence emission.

One of the most widely used fluorescence dyes for DNA detection is ethidium bromide (EB). EB is weakly fluorescent in water, whereas its fluorescence intensity increases about 30-fold upon binding to DNA. The fluorescence life-time of EB is about 1.7 ns in water and increases to about 20 ns upon binding to double-helical DNA. The mode of binding appears to be intercalation of the planar aromatic ring of the dye between the base pairs of double-helical DNA. Many DNA probes, such as Acridine Orange, bind to double-helical DNA by intercalation. However, other types of fluorescence probes bind into the minor groove of the DNA, such as 4', 6-

diamidino-2-phenylindole (DAPI) and Hoechst 33342. The fluorescence of DAPI appears to be most enhanced when adjacent to adenine-thymine (AT) rich regions within the DNA.

Fluorescent DNA probes for *in situ* hybridization are now commonly used for a wide spectrum of applications including the determination of mRNA distribution on the cellular and subcellular levels, monitoring gene expression, detection of gene and chromosome deletion and translocation, mapping and sequencing of genes (94, 95).

Factors that determine the sensitivity of fluorescent DNA probes include the quantum yield, target specificity and stability (96). Previously, DNA or RNA was either chemically labeled with only a single fluorophore on the 5' end of the oligonucleotides or alternatively, labeled by enzymatic means, such as nick translation, which incorporates (4% on average) dye-modified nucleotides for the bases (97). Current technology allows multiple fluorescent labels to be directly attached to the oligomers by chemical means leading to an enhanced labeling and brighter samples. However, increasing the label density of the fluorophore does not necessarily increase the

fluorescence sensitivity, since it may also quench the fluorescent signal by reducing the extinction coefficient of the dye and/or decreasing the stability of the target DNA. The amount of destabilization is dependent on the site used for attaching the dye. Some locations used for covalent dye attachment, such as the sugar, *via* a modified 2'-aminonucleoside, or the phosphate backbone, *via* the use of phosphorothioates, have been shown to result in significant duplex destabilization even at a low degree of dye incorporation (98).

Ideally, a fluorescent probe should closely resemble the naturally occurring purine or pyrimidine base structure, especially as hydrogen bonding sites are critical to base pairing. The fluorophore should be available as a phosphoramidite to allow site-specific insertion with automated DNA synthesizers. It should also have a reasonable quantum yield under physiologically relevant conditions (e.g., aqueous buffer, pH 6 to 8).

Recently, Hawkins *et al.* have developed pteridine nucleoside analogs that are highly fluorescent and structurally similar to the native nucleosides. In addition, these analogs have fluorescence properties,

such as excitation and emission maxima that differ from that of native DNA (99). In monitoring binding through anisotropy measurements, these analogs display relatively little movement that is unrelated to the motion of the DNA. In the case of conventionally attached probes, flexibility of linker arms allows movement of the fluorophore in ways that are independent of the movement of the DNA being studied. This level of independent motion leads to more complex interpretation of the results.

3.1.2. Pteridine nucleoside analog:

Pteridines are naturally occurring, highly fluorescent bicyclic planer compounds that were first isolated from butterfly wings in 1889.

The development of pteridines for DNA applications has focused on those compounds that are similar in structure to native nucleosides, are stable enough to withstand the caustic treatment used in the automated DNA synthesis, and are highly fluorescent (100).

Pteridines are incorporated into DNA through a deoxyribose moiety identical to that of native DNA with no "linker-arm" attachment involved. Because of this native-like linkage to DNA, these probes are very closely associated with neighboring bases rendering them exquisitely sensitive to subtle changes that occur in the DNA structure surrounding them. Changes in base stacking of base pairing in the vicinity of these probes are reflected by distinct changes in fluorescence properties of the pteridine. This sensitivity to neighboring bases is not duplicated by conventional linker-attached probes, which

are more removed from these interactions by the length of the carbon chain connecting them to the DNA. Probes that are different to nucleosides in size or structure can only be attached to DNA through the deoxyribose moiety using a linker, since they are more likely to disrupt the DNA tertiary structure and therefore not allow native-like interactions.

Fluorescent pteridine nucleoside analogs have an additional advantage in that they are quenched when incorporated into oligonucleotides sequences (sometimes referred to as self-quenching). This feature can be used in many ways to monitor the changing in tertiary structure occurring within the DNA as the bases interact with other molecules. Because quenching of pteridine probes in oligonucleotides is mostly due to base stacking interactions, events that affect base stacking are reflected directly by changes in fluorescence properties. It has been demonstrated experimentally that disruptions in the tertiary structure of DNA can be clearly monitored through changes in fluorescence intensity using pteridine nucleoside analogs (100).

3.1.3. Fluorescence properties of pteridine probes

Previously the fluorescence properties of four pteridine probes have been extensively studied (101). Two are guanosine analogs: 3-methyl-8- (2-deoxy-D-ribofuranosyl) isoxanthopterin, and 6-methyl-8-(2-deoxy-D-ribofuranosyl) isoxanthopterin, (3MI and 6MI, respectively), and two are pteridine-based adenosine analogs, 4-amino-8-(2-deoxy-ß-D-ribofuranosyl) 5'-O-dimethoxy-trityl-6-methyl-7(8H)-pteridone (6MAP), and 4-amino-8-(2-deoxy-ß-D-ribofuranosyl) 5'-O-dimthoxy-trityl 1,2,6-dimethyl-7(8H)-pteridone (DMAP). The chemical structure of the probe used in this study (6-MI) is shown in Figure 28. The fluorescence from all four of the pteridine-derived probes (3MI, 6MI, 6MAP, and DMAP) is quite blue with excitation wavelength maxima ranging from 310 to 348 nm and emission wavelength maxima ranging from 430 to 431 nm. Of the two-guanosine analog probes, 3MI has the highest quantum yield (0.88 for 3MI compared to 0.70 for 6MI). For the two-adenosine analogs, DMAP ($Q_{rel} = 0.48$) is slightly brighter than 6 MAP ($Q_{rel} = 0.39$).

The effects of incorporation of all four pteridine probes into oligonucleotides are quite similar, although the guanosine analog probes do not appear to be as heavily quenched as the adenosine analogs. The first fluorescence evaluation of pteridine nucleoside analog-containing nucleotides was performed using a series of 3MI-containing nucleotides where 3MI was substituted for guanosine at various sites (101). The study showed that incorporation of 3MI into oligonucleotides substantially quenches its fluorescence intensity. The fluorescence was maximally quenched when the fluorophore was positioned next to purine residues and least quenched when located next to pyrimidines. For each of the four probes, the quenching of the fluorescence caused by incorporation into oligonucleotides was fully reversed after digestion of the single strand with P1 nuclease, a strong indication that these probes do not themselves undergo measurable degradation during DNA synthesis and purification. The recoverability of the fluorescence intensity is also an indication of the value of each of these probes for monitoring events that affect the tertiary structure of DNA. If a probe-containing strand is bent or cleaved in the process

of interaction, the potential relief of quenching and subsequent increase in fluorescence intensity is considerable.

Data from the measurement of melting temperature profiles (Tm) suggest that 6MI and 6MAP are the most native like in double strand formation. 3MI, because of the 3-position methyl group is not expected to anneal very efficiently. Indeed, 3MI-containing oligonucleotides showed a Tm depression approximately equivalent to that of a single base pair mismatch. In contrast, the Tm values of double stranded 6MI-containing oligonucleotides are very similar to control values, strongly suggesting that 6MI may participate in base-pairing. Melting temperature measurements of DMAP-containing strands are slightly more depressed than those of the 6MAP-containing strands but the double strands are still somewhat less perturbed than a single base pair mismatch in the same position (101).

In terms of stability, the fluorescence signal from 3MI appears to be the most unaffected by continuous exposure to the excitation maximum. 3MI was tested in a time-based intensity experiment with exposure to 350 nm excitation for 2 hours at 37°C. No detectable loss

of fluorescence intensity was observed. 6MI, 6MAP, and DMAP all display a very slow rate of degradation (evidenced by a loss of fluorescence intensity) under time-based acquisition conditions, irradiating at their respective excitation maxima.

3.1.4. Use of pteridine DNA probes for G-quadruplex interactions

In this study we have used the pteridine analog, 6MI (Figure 26), as a fluorescent probe to investigate the interaction between G-quadruplexed DNA and porphyrin. 6MI has structural similarity to guanine, is involved in base pairing and expected to form G-quadruplex structures. In addition, the fluorescence properties, such as excitation and emission wavelength maxima, differ from that of native DNA and porphyrins, and therefore easily differentiated.

The use of fluorescence for investigating drug-DNA interaction provides an extremely sensitive and less time consuming tool when compared with more conventional optical methods. The use of fluorescent pteridine nucleotide analogs can provide valuable information regarding DNA interactions using a wide range of ligands,

regardless of whether the ligand itself is fluorescent. Furthermore, altered fluorescent signals from the pteridine labeled DNA can provide valuable information regarding DNA-quadruplex conformation during binding.

In the current study the majority of the porphyrins used are fluorescent; thus one may follow the interaction of porphyrin either from increased fluorescent signal of the porphyrin resulting from binding, or alternatively from a decrease in pteridine fluorescence intensity. Following both fluorescence emission spectra can thus lead to accurate and over-determination of values for the ligand binding constants.

We have used oligonucleotide sequences identical to those of the human telomeric repeat, with the exception that we have incorporated the pteridine analogs at different positions by replacing specific guanine residues (guanine residues 5 or 11) with 6MI. The effects of the presence of the pteridine nucleoside analogs on G-quadruplex formation and on the quadruplex-porphyrin interaction have been investigated.

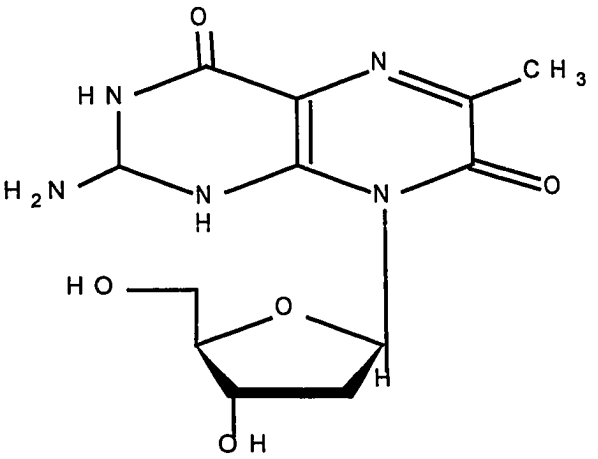

Figure 26. Structure of 6MI

3.2. Materials and Methods

3.2.1- DNA Oligomers and Porphyrins

Human telomeric $(TTAGGG)_4$ and *Oxytricha* telomeric (TTTTGGGG) sequences were purchased from Oligos etc, (HPLC purified). ss-DNA (polyA) and ds-DNA {poly (dA)-poly (dT)} were purchased from Amershem Inc. Quadruplex structures were formed by heating the DNA at 90°C for 10 minutes followed by cooling slowly to room temperature in a buffer containing 100 mM KCl and 10 mM cacodylate or in buffer containing 10 mM cacodylate only. Porphyrins were purchased from Porphyrin products (Logan, UT) and were used with no further purification.

The following pteridine-substituted sequences were provided by Dr. Mary E. Hawkins (Pediatric Division, NIH, Bethesda, Maryland).

A) TTAGGGTTAGF(6MI)GTTAGGGTTAGGG (5-tet)

B) TTAGGGTTAGGGTTAGGGTTAGF(6MI)G (11-tet)

3.2.2. Fluorescence Measurements

All fluorescence measurements were carried out using a SPEX Tau-3 spectrofluorimeter. Excitation and emission wavelengths of 399 nm and 614 nm for NMM and 429 nm and 655 nm for TMPyP4 and 340 nm and 420 nm for 6MI were used, respectively.

3.3. Results and Discussion

3.3.1. G-quadruplex formation

The use of fluorescence techniques to study quadruplex formation has been reported previously by several investigators (102-104). However, the incorporation of pteridine nucleoside analogs into oligonucleotides has not been explored. These probes are very closely associated with neighboring bases rendering their fluorescent signal very sensitive to any changes that occur in the DNA surrounding them. This sensitivity to neighboring (native) bases is not duplicated by the more conventional linker-attached probes.

The effect of incorporating the pteridine nucleoside analog (6MI) on quadruplex formation was examined by following the melting temperature of the DNA sequence containing the probe at two different positions, as measured from absorbance at 295 nm. The telomeric sequence containing the probe exhibited high melting temperatures similar to those measured for the corresponding telomeric sequence without the 6MI probe. Thus,

we concluded that incorporation of 6MI within telomeric DNA appears to have no appreciable effect on quadruplex formation. Additionally, G-quadruplex formation was examined by gel electrophoresis (DNA shadowing). The sequence containing 6MI runs as two separate bands (one band is single-stranded DNA, and the other is quadruplex DNA as compared to 24mer ss-DNA control). Formation of quadruplex structure was particularly noted in the presence of KCl, which is known to stabilize formation of G-quadruplex structures (Figure 27).

Incorporation of 6MI in position G5 (5tet) appears to form a more stable quadruplex structure when compared to substituting the same probe in position G11 (11tet), as shown by gel electrophoresis and the higher melting temperature of this sequence. No clear explanation for this observation can be made. However, it may reflect the ability of 6MI to form Hoogsteen base-pairing with neighboring guanine bases when the 5^{th} guanine is replaced resulting in formation of stable quadruplex structures. In contrast, replacement of the 11^{th} guanine with 6MI leads to formation of a

less stable quadruplex structure. This is further suggested from fluorescence quenching studies. With increasing concentrations of KCl to 100 mM, a decrease in the observed fluorescence intensity of 6MI labeled DNA was observed concurrent with quadruplex structure formation. For the 5-tet tetrad DNA sequence (fluorophore inserted at position G5) a higher degree of quenching was observed compared to the 11-tet sequence (incorporation of 6MI in the G11 position). The enhanced quenching observed for 5-tet is believed to arise from the fact that position G5 is actively involved in formation of the quadruplex structure with a resultant decrease in distance between the bases and 6MI arising (Figure 28). In contrast, position G11 is predicted to be less involved in quadruplex formation, giving rise to less quenching of 11-tet fluorescence by neighboring bases.

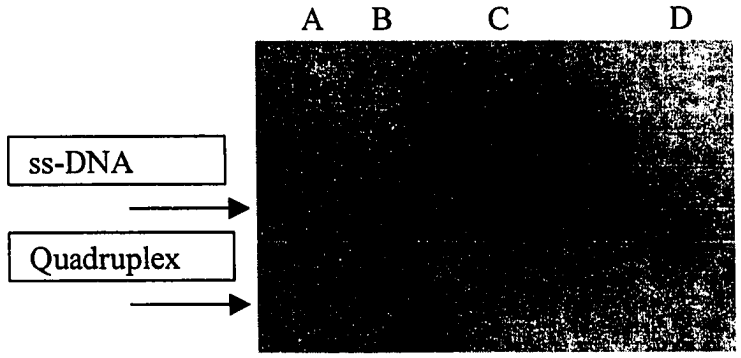

Figure 27. Gel electrophoresis of telomeric sequence containing 6MI.
A. 11tet in presence of 100 mM K^+.
B. 5tet in presence of 100 mM K^+.
C. 24-mer non-fluorescent ss-DNA.
D. 5 tet in 10 mM cacodylate buffer.

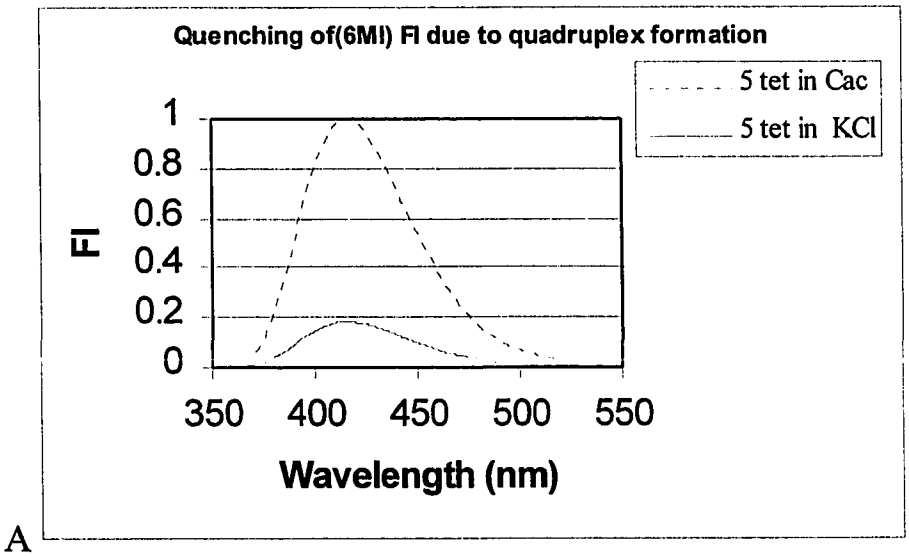

A

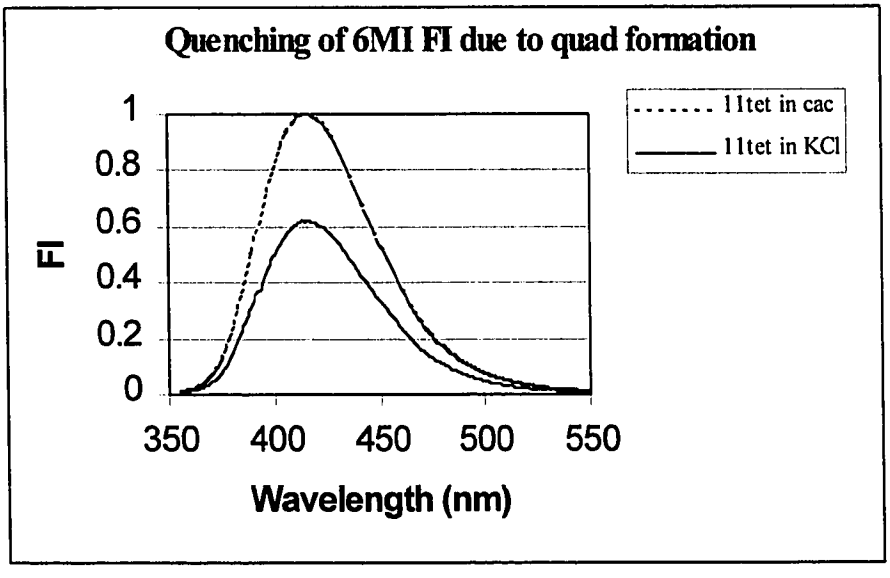

B

Figure 28. Quenching of 5-tet and 11-tet due to quadruplex formation. All fluorescence measurements were performed at 20°C. 5 and 11 tet represent the fluorescent oligonucleotides after substitution of guanine at the 5^{th} and 11^{th} position with 6MI, respectively. DNA was incubated in 10 mM sodium cacodylate, and quenching was evaluated after incubation in 10 mM cacaodylate, 0.1 M KCl, pH 7.5 buffer.

3.3.2. Use of Intrinsic Porphyrin Fluorescence to Measure Porphyrin-DNA Interactions

As a great many porphyrins exhibit intrinsic fluorescence, easy measurement and monitoring of their interactions with DNA is possible using standard fluorescence techniques.

The interaction between DNA and fluorescent porphyrins can simply be followed by monitoring the increase in fluorescence intensity of the dye as the concentration of the DNA increases. This was particularly noticeable for the titration of TMPy with double stranded DNA, single stranded DNA and quadruplex DNA. From the increase in fluorescence intensity observed the binding constant can be determined using Scatchard type analyses.

From fluorescent titration studies (summarized in Table 7), TMPy showed a somewhat higher affinity for quadruplex DNA, over double and single stranded DNA. Although, TMPyP4 binds to all forms of DNA, no high selectivity for quadruplex DNA was observed.

On the other hand, NMM showed absolute selectivity for quadruplex DNA and did not bind to double or single stranded DNA.

This was demonstrated by the increase in fluorescence intensity of NMM as the concentration of added telomeric (non fluorescent) quadruplex DNA was increased (Figure 29 and 30). In contrast, there was no increase in fluorescence intensity observed when single or double stranded DNA was titrated into a solution of NMM (Figure 30).

These data suggest that NMM has absolute selectivity and binds only to quadruplex DNA and not to other DNA conformations. This selectivity suggests that NMM can be used as a tool for detecting quadruplex formation; an increase in NMM fluorescence may be used as a signature for quadruplex presence.

Hence, the ability of the pteridine-labeled DNA sequences to form quadruplex structures was further confirmed (in addition to electrophoresis and melting temperature experiments discussed above) from titration using NMM. By observing the fluorescence intensity of NMM, as predicted for quadruplex formation, a dramatic enhancement in porphyrin fluorescence was observed as the concentration of labeled (tet-5) telomeric sequence was increased. The increase in porphyrin fluorescence intensity strongly suggests that the presence of pteridine

analogs incorporated within the DNA sequence has no appreciable effect on quadruplex formation.

3.3.3. Use of fluorescently-labeled quadruplex structure to study porphyrin binding

The incorporation of a pteridine analog into the DNA sequence is an elegant approach for studying drug binding to quadruplex when the drug of interest is neither fluorescent nor demonstrates any appreciable measurable optical properties in response to binding. By following the decrease (quenching) in fluorescence intensity of the pteridine analogs with addition of a particular ligand, one can determine the binding affinity and selectivity of a ligand for quadruplex DNA irrespective of whether the target molecule is fluorescent or not.

In this study, human telomeric sequences with G5 or G11 positions substituted using 6MI (tet-5 and tet-11, respectively), were synthesized for studying the interactions of both fluorescent (as a control) as well as non-fluorescent porphyrins with quadruplex-DNA.

Using NMM, which is known to selectively bind to quadruplex-DNA, we noted a decrease in pteridine fluorescence intensity of both tet5 and tet11 (Figure 32) with increasing NMM concentrations, suggesting that the fluorescence signal of 6MI is sensitive to quadruplex-ligand interactions with a decrease in intensity resulting from enhanced base-pairing through stabilization of the tetrad conformation. These data confirm our previous results that the increase in intrinsic NMM fluorescence intensity as the signature of binding to quadruplex DNA (Figure 33).

The quenching of the pteridine fluorescence signal may be used to determine the ligand-quadruplex binding constants. Table 7 summarizes binding constants for porphyrin-quadruplex interactions determined either from the enhanced intrinsic porphyrin fluorescence or from the decrease in 6MI labeled quadruplexed-DNA.

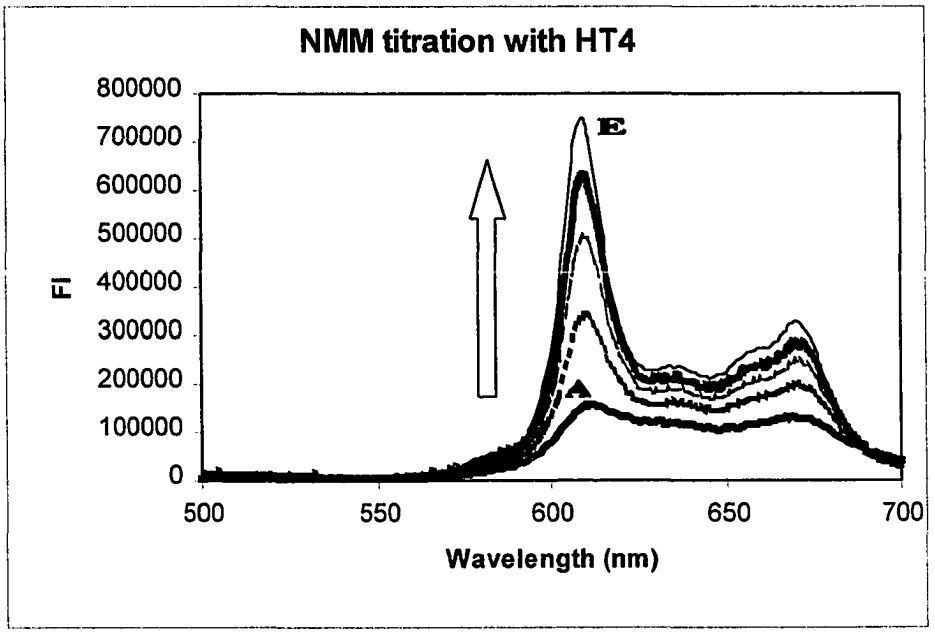

Figure 29. NMM titration with human non-fluorescent telomeric sequence. All measurements were performed at 20°C. The DNA concentration was increased from 10^{-7} to 10^{-6} M. After each addition samples were incubated in dark for 10 min. All measurements were performed in a buffer containing 10 mM cacodylate and .1 M KCl. 'A' represents NMM only, while, 'E' represents NMM and HT4 at saturation. Excitation was set at 410 nm and fluorescence emission was recorded at 610 nm.

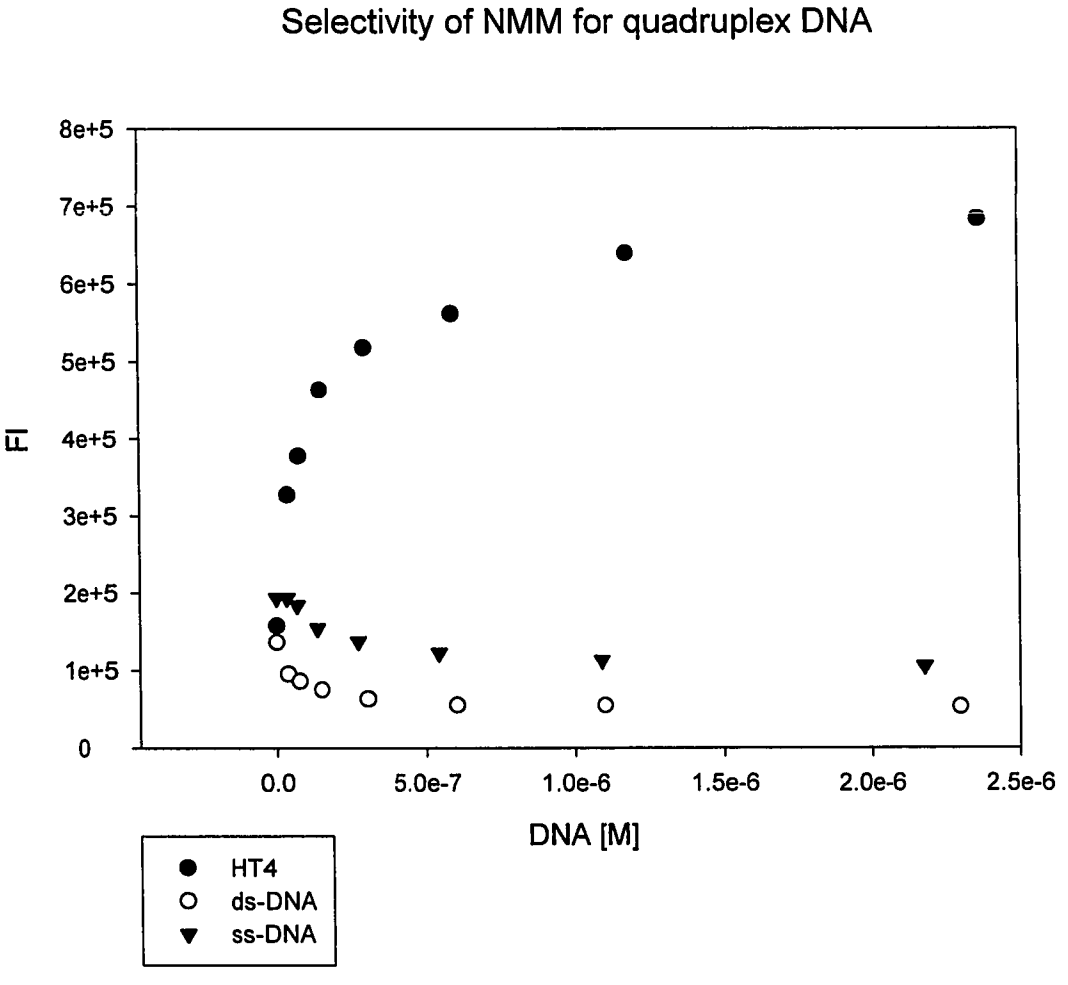

Figure 30. Selectivity of NMM for quadruples structures: Increased fluorescence intensity of NMM with increasing concentration of human telomeric sequence (non-fluorescent DNA). There was no fluorescence increase observed for ss-DNA or ds-DNA. Excitation was set at 410 nm and fluorescence emission was recorded at 610 nm. All measurements were performed in a buffer containing 10 mM cacodylate and 100 mM KCl.

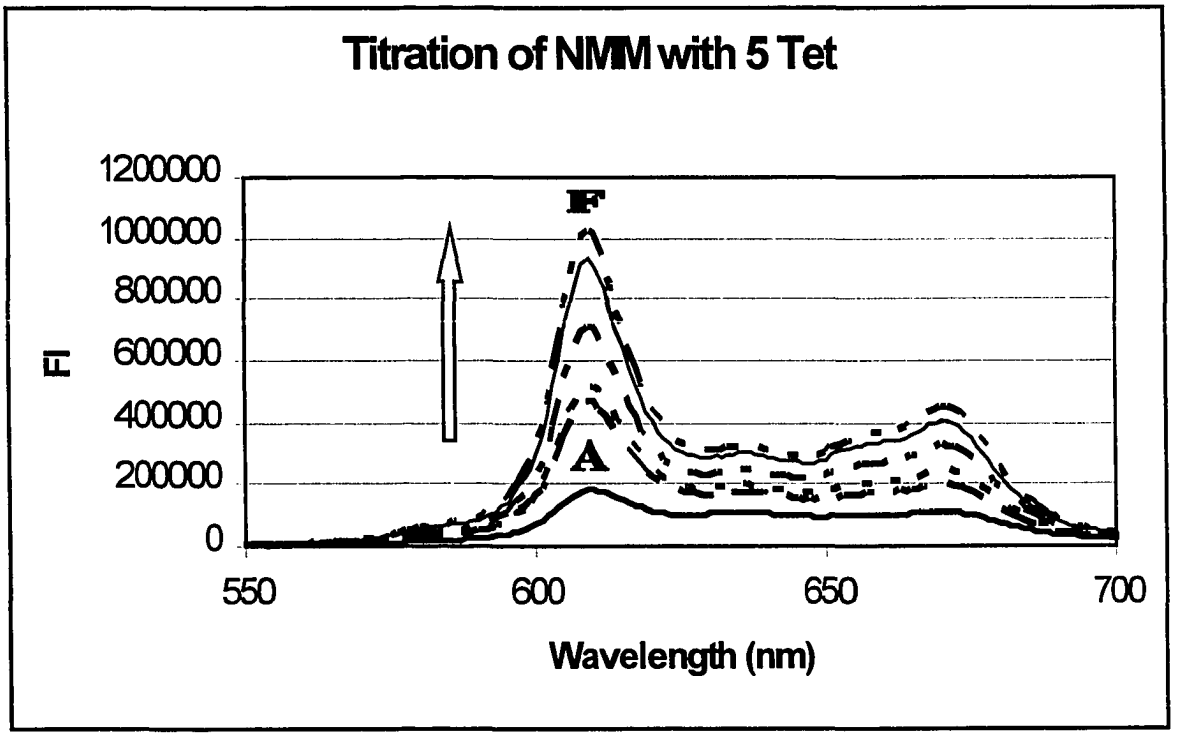

Figure 31. NMM titration with 5-tet labeled human telomeric DNA. 'A' represents the fluorescence intensity of NMM in the absence of 5-tet. The fluorescence intensity of NMM increases as the concentration of 5-tet is increased, and reaches saturation (F). Samples were incubated for 10 mins after each addition. All measurements were performed at 20°C and in buffer containing 10 mM cacodylate and 0.1 M KCl, pH 7.5. Excitation was set at 410 nm and fluorescence emission was recorded at 610 nm.

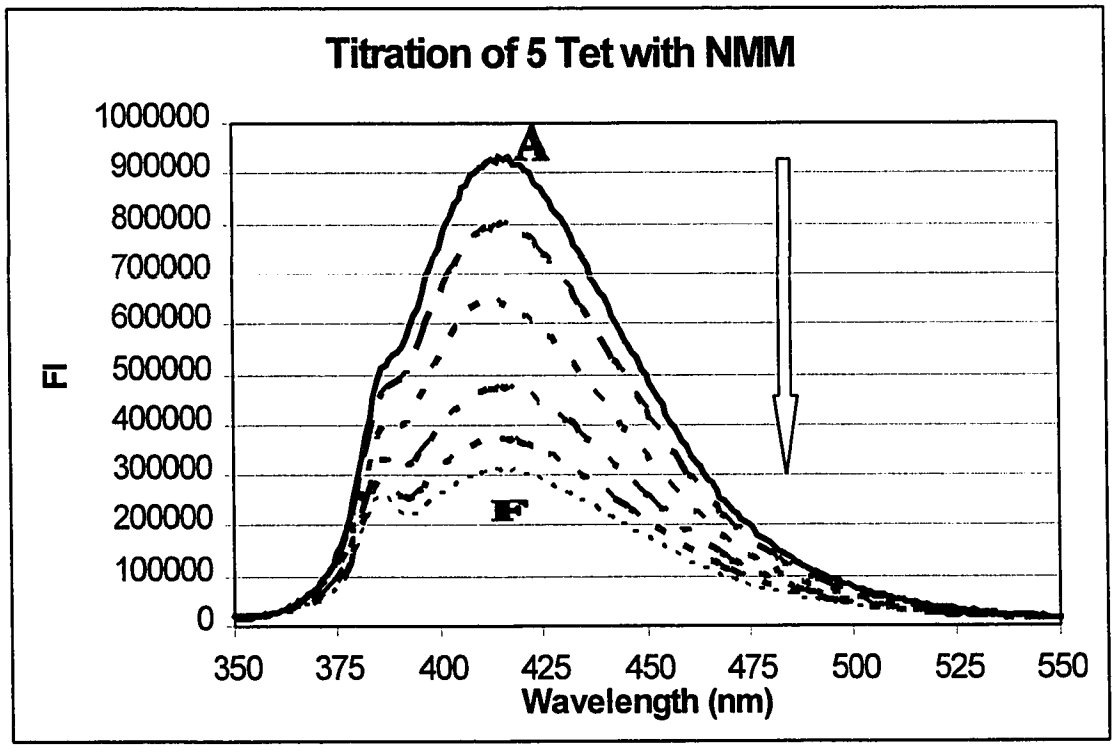

Figure 32. Titration of 5tet with NMM.
Fluorescence intensity of 5-tet decreases as the concentration of added NMM is increased (A to F). The porphyrin concentration was increased from 10^{-7} to 10^{-6} M. All measurements were performed at 20°C in a buffer containing 10 mM cacodylate and 0.1 M KCl, pH 7.5. Excitation was set at 340 nm and fluorescence emission was recorded at 420 nm.

In a comparative study, the decrease in fluorescence intensities reported using tet 5 or tet 11 was monitored as the concentration of NMM was increased (Figure 34). As expected, the data confirm that NMM binds to both sequences. However, a somewhat tighter binding is reported at the tet 5 position, which may be expected since the 5^{th} guanine is located well within the quadruplex conformation compared to the tet 11 position. In addition, our previous studies suggested that the tet 5 sequence was somewhat more stable than the tet 11 sequences as reported from melting temperature and gel electrophoresis experiments.

We have also examined the binding of Co(III)MPIX to fluorescently labeled DNA. Co(III)MPIX is only weakly fluorescent. Our ultraviolet spectroscopy binding data have suggested that Co(III)MPIX is an excellent candidate for telomerase inhibition as shown by relatively high binding affinity, high selectivity and enhanced quadruplex-stabilization. Binding of Co(III)MPIX to fluorescently labeled quadruplex DNA was carried out by using a telomeric sequence with 6MI probe in position G5, and by following

the decrease in fluorescence intensity of the pteridine analog as the concentration of the drug was increased (Figure 35). The binding constant of Co(III)MPIX to quadruplex DNA was found to be (10^7) higher than that of NMM to the same telomeric sequence (10^6). Binding affinity and selectivity of quadruplex DNA to different porphyrins are summarized in table 7. These results are in agreement with the UV studies reported in Chapter I.

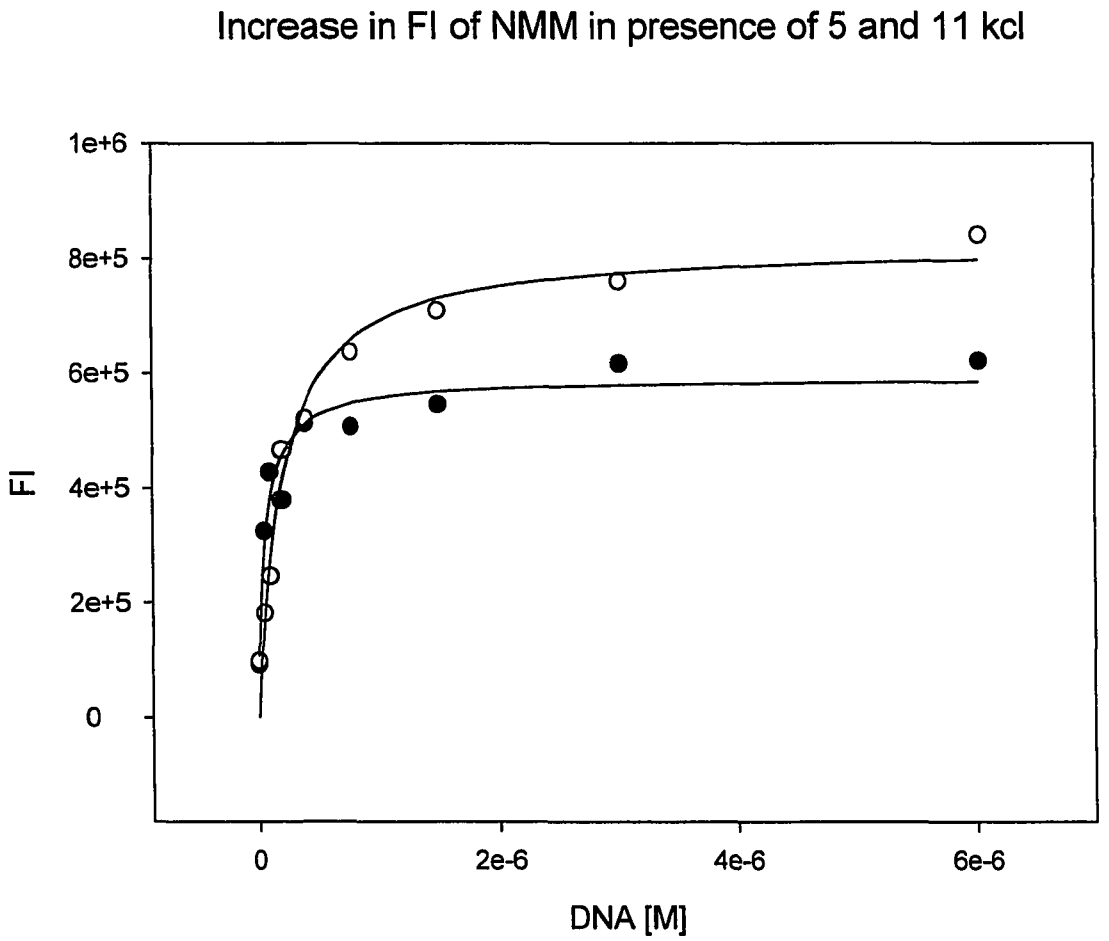

Figure 33. Increase in fluorescence intensities of 5tet and 11tet with increasing NMM concentration. Excitation was set at 410 nm and fluorescence emission was recorded at 610 nm.

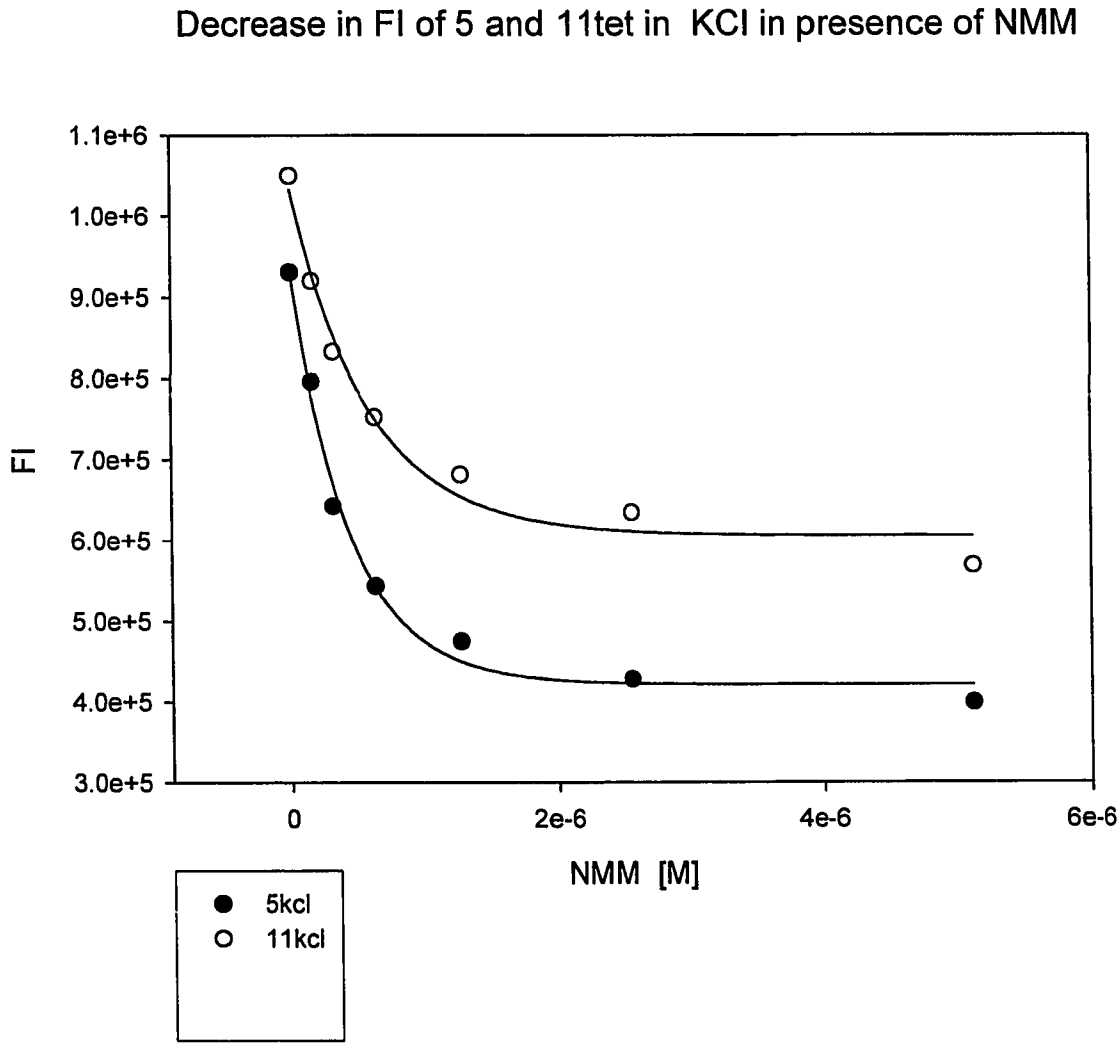

Figure 34. Decrease in FI of 5tet and 11tet as the concentration of NMM increases. Excitation was set at 340 nm and fluorescence emission was recorded at 420 nm.

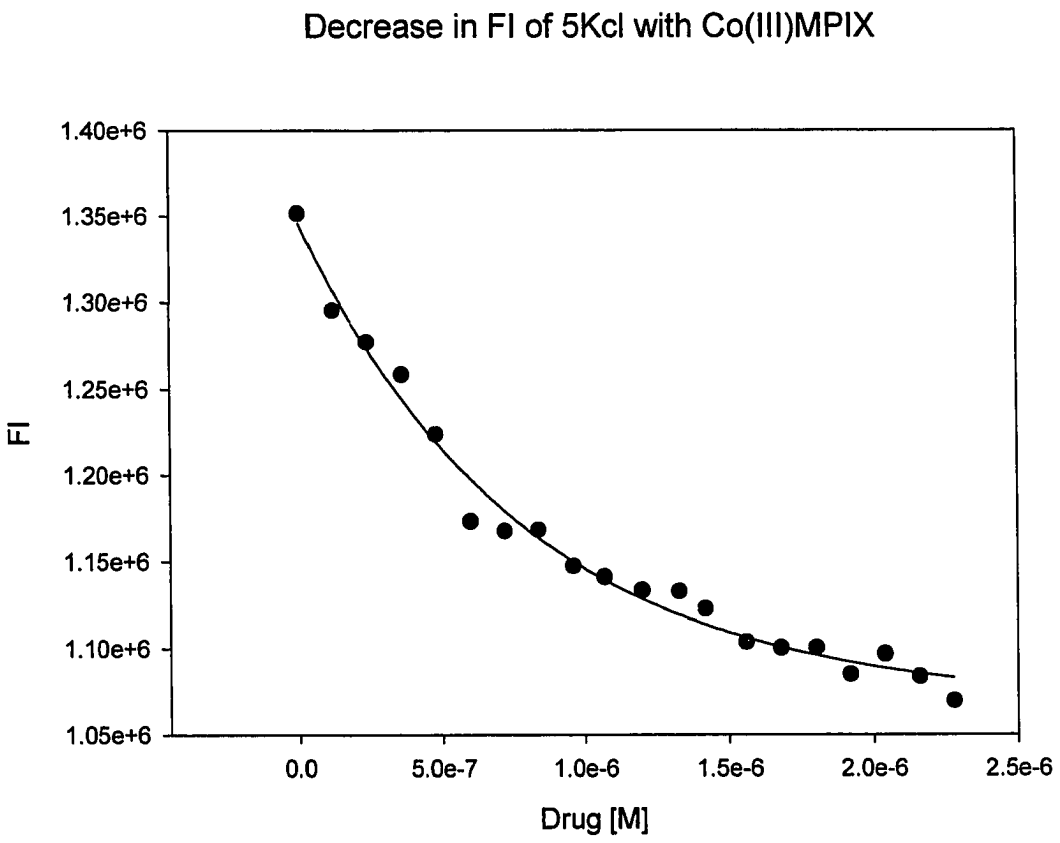

Figure 35. 5tet titration with Co(III)MPIX.
All measurements were performed in buffer solution containing 10 mM cacodylate and 0.1 M KCl. Excitation was set at 340 nm and fluorescence emission was recorded at 420 nm.

Porphyrin	Binding constant K (mol^{-1})	Selectivity for quadruplex DNA
TMPyP4	8.0×10^{7}	Low
NMM	1.8×10^{6}	High
Co(III)MPIX	6.0×10^{7}	High

Table 7. Summary of porphyrin binding affinity and selectivity for quadruplex DNA using fluorescence studies. Binding constant, K, was calculated by following the increase in intrinsic porphyrin fluorescence for TMPy and NMM and the decrease in fluorescence intensity of 6MI in case of Co(III)MPIX. High selectivity means the porphyrin showed binding affinity to quadruplex DNA only, while , low affinity means that the drug showed binding affinity for ss-DNA, ds-DNA, and quadruplex DNA.

3.3.4. Potential assay for drugs-quadruplex binding

The sensitivity of fluorescently labeled, pteridine containing, tetrad oligonucleotides suggest that a new drug-screening assay may be developed based on monitoring changes of fluorescence properties of the pteridine nucleoside analogs. This assay may overcome the complications of the conventional screening techniques known to date. By incorporation of 6MI into telomeric sequences, one can screen for drug-DNA interactions and quadruplex stabilization by monitoring the changes of the fluorescence intensity of the pteridine nucleoside analogs and not be limited to measurable spectroscopic properties of the drug. This approach may be ultimately extended to using a 96-well or 384-well microplate and a special microplate fluorescence reading detection system. The decrease of fluorescence intensity of the pteridine nucleoside analog is an indication of quadruplex stabilization, while an increase in fluorescence intensity may suggest destabilization or DNA cleavage.

Using this approach, screening of drugs used in pure form or libraries of different drugs is possible. The assay is less time

consuming than current approaches and is believed to be sensitive to changes in DNA tertiary structure.

4. Summary:

In this study, we have shown that N-substituted anionic porphyrins have a higher selectivity for quadruplex DNA than the more commonly studied meso-substituted cationic porphyrin, TMPyP4. In addition, porphyrins such as Co(III)MPIX, which show a high selectivity for quadruplex DNA structures over ss-DNA and ds-DNA accompanied by relatively high binding affinity, are predicted to be ideal agents for use in therapeutic approaches aimed to inhibit telomerase and thus inhibit the growth of cancer cells.

Finally, from our fluorescence studies a potential new drug-screening assay based on fluorescence measurement and the use of pteridine nucleoside analogs as DNA probes is proposed. This sensitive approach may allow rapid screening of massive libraries of drugs.

Bibliography:

1. Blackburn, E. H., 1991. Structure and function of telomeres. *Nature*, 350:569-573.

2. Lansdrop, P. M., Verwoerd, F. M. and H. J. Tanke, 1996. Heterogeneity in telomere length of human chromosomes. *Human molecular genetics,* 5:685-691.

3. Sandell, L.L. and V. A. Zakian, 1993. Loss of a yeast telomere: arrest, recovery and chromosome loss. *Cell,* 75:729-739.

4. Blasco, M. A., H.W. Lee, P. Hande, E. Samper, Landsdrop and C.W. Greider, 1997. Telomere shortening and tumor formation by mouse cells lacking telomerase RNA. *Cell,* 91:25-34.

5. Nakamura, T. M., J. P. Cooper, and T. Cech, 1998. Two models of survival of fission yeast without telomerase. *Science,* 282:493-496.

6. Greider, C.W., 1996. Telomere length regulation. *Annu. Rev. Biochem.,* 65:337-365.

7. Shay, J. W., Wright, W. E., and Werbin, H., 1991. Defining the molecular mechanism of human cell immortalization. *Biochim. Biophys. Acta.,* 1072:1-7.

8. Huschtscha, L. I., Holliday, R., 1983. Limiting and unlimited growth of SV40-transformed cells from human diploid MRC-5 fibroblasts. *J.Cell. Sci.*, 63:77-99.

9. Bryan, T. M., Reddel, R. R., 1997. Telomere dynamic and telomerase activity in in vitro immortalized human cells. *Eur. J. Cancer*, 33:767-773.

10. Nakamura, T. M., J. B. Morin, K. B. Chapman, S. A. Weinrich, W. H. Andrew, J. Linger, C. B. Harley and T. Cech., 1997. Telomerase catalytic subunit homologs from fission yeast and human. *Science,* 277:955-959.

11. Linger, J., Hughes, T. R., Shevchenko, A., Mann, M., Lundblad, V., and Cech, T., 1997. Reverse transcriptase motifs in the catalytic subunit of telomerase. *Science,* 276:561-567.

12. Nugent, C. I., Lundblad, V., 1998. Telomerase reverse transcriptase: components and regulation. *Genes Dev.,* 12:1073-1085.

13. Chen, J. L., Blasco, M. A., Greider, C. W., 2000. Secondary structure of vertebrate telomerase RNA. *Cell,* 100:503-514.

14. Nakamura, T. M., Cech, T.R., 1998. Reversing time: origin of telomerase. *Cell,* 92:587-590.

15. Bondar, A. G., Ouellette, M., Frolkins, M., Holt, S. E., Chiu, C. P., Morin, G.B., Harley, C.B., Shay, J.W., Linchtsteiner, S., Wright,W. E., 1998. Extension of life span by introduction of telomerase into normal human cells. *Science*, 279:349-352.

16. Morales, C. P., Holt, S. E., Quellette, M., Kaur, K. J., Yan, Y., Wilson, K. S., White, M. A., Wright, W. E., Shay, J. W., 1999. Absence of cancer-associated changes in human fibroblasts immortalized with telomerase. *Nat. Genet.*, 21:115-118.

17. Gandhi, L., Collins, K., 1998. Interaction of recombinant *Tetrahymena* telomerase proteins p80 and p95 with telomerase RNA and telomeric DNA substrates. *Genes Dev.*, 12:721-733.

18. Harrington, L., McPhail, T., Mar, V., Zhou, W., Oulton, R., Bass, M. B., Arruda, I., Robinson, M. O., 1997. A mammalian telomerase-associated protein. *Science*, 275:973-977.

19. Holt, S. E., Aisner, D. L., Baur, J., Tesmer, V. M., DY, M., Ouellette, M., Trager, J. B., Morin, G. B., Toft, D. O., Shay, J. W., Wright, W. E., White, M. A., 1999. Functional requirement of p23 and Hsp90 in telomerase complexes. *Genes Dev.*, 13:817-826.

20. Havlir, D. V., Lange, J. M., 1998. New antiretrovirals and new combinations. *AIDS*, 12 (Supp. A), S165-S174.

21. Helder, M. N., de Jong, S., de Vries, E. G. E., van der Zee, A. G. J., 1999. Telomerase targeting in cancer treatment: new developments. *Drug Resistance Updates*, 2: 104-115.

22. Peter, K., Gambertoglio, J. G., 1998. Intracellular phosphorylation of Zidovudine (ZDV) and other nucleoside reverse transcriptase inhibitors (RTI) used for human immunodeficiency virus (HIV) infection. *Pharm. Res.*, 15:819-825.

23. Cong, Y. S., Wen, J., Bacchetti, S., 1999. The human telomerase catalytic subunit hTERT: organization of the gene and characterization of the promoter. *Hum. Mol. Genet.*, 8:137-142.

24. Horikawa, I., Cable, P. L., Afshari, C., Barrett, J. C., 1999. Cloning and characterization of the promoter region of human telomerase reverse transcriptase gene. *Cancer Res.*, 59:826-830.

25. Devereux, T. R., Horikawa, I., Anna, C. H., Annab, L. A., Afshari, C. A., Barrett, J. C., 1999. DNA methylation analysis of

the promoter region of the human telomerase reverse transcriptase (hTERT) gene. *Cancer Res.*, 59:6087-6090.

26. Kanaya, T., Kyo, S., Hamada, K., Takakura, M., Kitagawa, Y., Harada, H., Inoue, M., 2000. Adenoviral expression of p53 represses telomerase activity through down-regulation of human telomerase reverse transcriptase transcription. *Clin. Cancer Res.*, 6:1239-1247.

27. Fujimoto, K., Takahashi, M., 1997. Telomerase activity in human leukemic cell lines is inhibited by antisense pentadecadeoxynucleotides targeted against c-myc mRNA. *Biophys. Res. Commun.*, 241:775-781.

28. Wang, J., Xie, L. Y., Allan, S., Beach, D., Hannon, G.J., 1998. Myc activates telomerase. *Genes. Dev.*, 12:1769-1774.

29. Oh, S., Song, Y.H., Yim, J., Kim, T. K., 2000. Identification of Mad as a repressor of the human telomerase (hTERT) gene. *Oncogene*, 19:1485-1490.

30. Kyo, S., Takakura, M., Taira, T., Kanaya, T., Itoh, H., Yutsudo, M., Ariga, H., Inoue, M., 2000. Sp1 cooperates with c-myc to activate transcription of the human telomerase reverse transcriptase gene (hTERT). *Nucleic Acids Research*. 28:669-677.

31. Feng, J., Funk, W., Wang, S., 1997. The RNA component of human telomerase. *Scienc,*. 269:1236-1241.

32. Kondo, S., Tanaka, Y., Kondo, Y., 1998. Antisense telomerase treatment: induction of two distinct pathways, apoptosis and differentiation. *FASEB J*, 12:801-811.

33. Kanazawa, Y., Ohkawa, K., Ueda, K., 1996. Hammerhead ribozyme-mediated inhibition of telomerase activity in extracts of human hepatocellular carcinoma cells. *Biochem. Biophys. Res. Commun,* 225:570-576.

34. Beattie, T. L., Zhou, W., Robinson, M. O., and Harrington, L., 2001. Functional multimerization of human telomerase reverse transcriptase. *Mol. Cell. Biol.*, 21:6151-6160.

35. Wenz, C., Enenkel, B., Amacker, M., Kelleher, C., Damm, K. and Lingner, J., 2001. Human telomerase contains two cooperating telomerase RNA molecules. *EMBO J.*, 20:3526-3534.

36. Smith, S., de Lange, T., 2000. Tankyrase promotes telomere elongation in human cells. *Curr. Biol.*, 10:1299-1302.

37. Rha, S. Y., Izbicka, E., Lawrence, R., Davidson, K., Sun, D., Moyer, M. P., Roodman, G. D., Hurley, L., Von Hoff, D., 2000. Effect of telomere and telomerase interactive agents on human tumor and normal cell lines. *Clin. Cancer Res.*, 6:987-993.

38. Izbicka, E., Nishioka, D., Marcell, V., Raymond, E., Davidson, K.K., Lawrence, R. A., Wheelhouse, R. T., Hurley, L., Wu, R. S., Von Hoff, D., 1999. Telomere interactive agents affect proliferation rates and induce chromosomal destabilization in Sea Urchin embryos. *Anticancer Drug Des.*, 14:355-356.

39. Izbicka, E., Wheelhouse, R.T., Raymond, E., Davidson, K.K., Lawerence, R. A., Sun, D., Windle, B .E., Hurley, L., Von Hoff, D., 1999. Effect of cationic porphyrins as G-quadruplex interactive agents in human tumor cells. *Cancer Res.*, 59:639-644.

40. Han, H., Bennett, R. J., Hurley, L., 2000. Inhibition of unwinding of G-quadruplex structures by sgs1 helicase in the presence of N,N(-bis[2-(1-Piperidino)ethyl]-3,4,9,10-Perylenetetracarboxylic Diimide, a G-quadruplex-interactive ligand. *Biochemistry,* 39:9311-9316.

41. Zahler, A. M., Williamson, J.R., Cech, T. R., Prescott, D. M., 1991. Inhibition of telomerase by G-quartet DNA structures. *Nature,* 350:718-720.

42. Henderson, E., Hardin, C. C., Walk, S. K., Tinoco, I., Blackburn, E. H., 1987. Telomeric DNA oligonucleotides form novel intramolecular structures containing guanine-guanine base pairs. *Cell,* 51:899-908.

43. Sundquist, W. I. and Klug, A., 1989. Telomeric DNA dimerizes by formation of guanine tetrads between hairpin loops. *Nature,* 342:825-829.

44. Sen, D. and Gilbert, W., 1988. Formation of parallel four stranded complexes by guanine-rich motifs in DNA and its implications for meiosis. *Nature,* 334:364-366.

45. Wang, Y., and Patel, D. J., 1994. Solution structure of *Tetrahymena* telomeric repeat $d(T_2G_4)_4$ G-tetraplex. *Structure,* 2:1141-1156.

46. Laughlan, G., Murchie, A. I., Norman, D.G., Moore, M. H., Moody, P.C., Lilley, D. M. and Luisi, B., 1994. The high-resolution crystal structure of a parallel-stranded guanine tetraplex. *Science,* 265:520-524.

47.Smith, F. W., and Feigon, J., 1992. Quadruplex structure of Oxytricha telomeric DNA oligonucleotides. *Nature,* 356:164-168.

48. Mohanty, D. and Bansal, M., 1993. Conformational polymorphism in G-tetraplex structures: strand reversal by base flibover or sugar flibover. *Nucleic Acids Res.*, 21:1767-1774.

49. Aboul-ela, F., Murchie, A. I., and Lilley, D. M., 1992. NMR study of parallel-stranded tetraplex formation by the hexadeoxynucleotides d(TG_4T). *Nature,* 360:280-282.

50. Kang, C., Zhang, X., Ratliff, R., Moyzis, R. and Rich, A., 1992. Crystal structure of four-stranded *Oxytricha* telomeric DNA. Nature, 356, 126-131.

51. Strahan, G. D., Shafer, R. H. and Keniry, M. A., 1994. Structural properties of the [d($G_3T_4G_3$)]2 quadruplex: evidence for sequential syn-syn deoxyguanosines. *Nucleic Acids Res.*, 22:5447-5455.

52. Schultze, P., Smith, F.W., and Feigon, J., 1994. Refined solution structure of the dimeric quadruplex formed from the *Oxytricha* telomeric oligonucleotides. *Structure*, 2:221-233.

53. Murchie, A. I. and Lilley, D.M., 1994. Tetraplex folding of telomere sequences and the inclusion of adenine bases. *EMBO J.*, 13:993-1001.

54. Ashley, C. T., and Warren, S. T., 1995. Trinucleotide repeat expansion and human disease. *Annu. Rev. Genet.*, 29:703-728.

55. Howell, R. M., Woodford, K.J. Weitzmann, M. N., and Usdin, K., 1996. The chicken beta-globin gene promoter forms a novel "cinched" tetrahelical structure. *J. Biol. Chem.*, 271:5208-5214.

56. Guschlbauer, W., Chantot, J. F., and Thiele, D., 1990. Four-stranded nucleic acid structures 25 years later: from guanosine gels to telomere DNA. *J. Biomol. Struct. Dyn.*, 8:491-511.

57. Walsh, K., and Gualberto, A., 1992. Myo D binds to the guanine tetrad nucleic acid structure. *J. Biol. Chem.*, 267:13714-13718.

58. Fang, G., and Cech, T. R., 1993. The beta subunit of *Oxytricha* telomere-binding protein promotes G-quartet formation. *Cell*, 74:875-885.

59. Konig, P., Giraldo, R., Chapman, L. and Rhodes, D., 1996. The crystal structure of the DNA-binding domain of yeast RAP1 I complex with telomeric DNA. *Cell*, 85:125-136.

60. Arimondo, P.B., Riou, J. F., Mergny, J. L., Tazi, J., Sun, J. S., Garestier, T. and Helene, C., 2000. Interaction of human DNA topoisomerase I with G- quartet structures. *Nuclei Acids Res.* 28: 4832-4838.

61. Harrington, C., Lan, Y. and Akman, S. A., 1997. The identification and characterization of a G4-DNA resolvase activity. *J. Biol. Chem.*, 272:24631-24636.

62. Fry, M. and Loeb, L. A., 1999. Human Werner syndrome DNA helicase unwinds tetrahelical structures of the fragile X syndrome repeat sequence $d(CGG)_n$. *J. Biol. Chem.*, 274:12797-12802.

63. Baran, N., Pucshansky, L., Marco, Y., Benjamin, S. and Manor, H., 1997. The SV40 large T-antigen helicase can unwind four stranded DNA structures linked by G-quartets. *Nucleic Acids Res.* 25:297-303.

64. Mergny, J. L., Phan, A. T., Lacroix, L., 1998. Following G-quartet formation by UV-spectroscopy. *FEBS Letters*. 435:74-78.

65. Siddiqui-Jain, A., Gran, C. L., Bearss, D. J., Hurley, L. H., 2002. Direct evidence for a G-quadruplex in a promoter region and its targeting with a small molecule to repress c-MYC transcription. *PNAS*. 99(18):11593-11598.

66. Perry, P. J., Jenkins, J. C., 2001. DNA tetraplex-binding drugs: structure-selectivity targeting is critical for antitumour telomerase inhibition. *Mini. Rev. Med. Chem.* 1(1):31-41.

67. Harrison, R. J., Gowan, S. M., Kelland, L. R., Neidle, S., 1999. Human telomerase inhibition by substituted acridine derivatives. *Bioorg. Med. Chem. Lett.* 9(17):2463-2468.

68. Kim, M. Y., Vankayalapati, H., Shin-Ya, K., Wierzba, K., Hurley, L. H., 2002. Telomestatin, a potent telomerase inhibitor that interacts quite specifically with the human telomeric intramolecular G-quadruplex. *J. Am. Chem. Soc.* 124(10):2098-2099.

69. Shibutani, S., Margulis, L. A., Geacintov, N. E., Grollman, A. P., 1993. Translesional synthesis on a DNA template containing a single stereoisomer of dG-(+)- or dG-(-)-anti-BPDE (7,8-dihydroxy-anti-9,10-epoxy-7,8,9,10-tetrahydrobenzo[a]pyrene). *Biochemistry*. 32:7531-7541.

70. Xie, X. M., Geacintove, N. E., Broyde, S., 1999. Stereochemical origin of opposite orientations in DNA adducts derived from enantimoeric anti-benzo[a]pyrene diol epoxides with different tumorigenic potentials. *Biochemistry*. 38:2956-2968.

71. Perry, P. J., Gowan, S. M., Reszka, A. P., Polucci, P., Jenkins, T. C., Kelland, L. R., Neidle, S., 1998. 1,4- and 2,6-disubstituted aminoanthracene-9,10-dione derivatives as inhibitors of human telomerase. *J. Med. Chem.* 41(17):3253-3260.

72. Han, H., Cliff, C. L., Hurley, L. H., 1999. Accelerated assembly of G-quadruplex structures by a small molecule. *Biochemistry.* 38(22):6981-6986.

73. Marzilli, L. G., 1990. *New J. Chem.* 14:409-420.

74. Fiel, R. J., 1989. *J. Biomol. Struct. Dyn.* 6:1259-1283.

75. Benimetskaya, L., Takle, G. B., Vilenchik, M., Lebedeva, I., Miller, P. and Stein, C. A., 1998. Cationic Porphyrins: novel delivery vehicles for antisense oligodeoxynucleotides. *Nucleic Acids Res.*, 26:5310-5317.

76. Fiel, R. J., and Munson, B. R., 1980. *Nucleic Acids Res.*, 8:2835.

77. Hui, X., Gresh, N. and Pullman, B., 1990. *Nucleic Acid Res.*, 18:1109.

78. Strahan, G. D., Lu, D., Tsuboi, M., and Nakamoto, K., 1992. *J. Phys. Chem.*, 96:6450.

79. Lu, D., Guo, Q., Pasternack, R. F., Wink, D. J., Seeman, N. C., and Kallenbach, R., 1990. *Biochemistry.* 29:1614.

80. Han, H., Langley, D. R., Rangan, A. and Hurley, L., 2001. Selective interaction of cationic porphyrins with G-quadruplex structures. *J. Am. Chem. Soc.*, 123:8902-8913.

81. Han, F. X., Wheelhouse, R.T. and Hurley, L., 1999. Interaction of TMPyP4 and TMPyP2 with quadruplex DNA. Structural basis for the differential effects on telomerase inhibition. *J. Am. Chem. Soc.,* 121:3561-3570.

82. Ren, J., and Chaires, J. B., 1999. Sequence and structural Selectivity of nucleic acid binding ligands. *Biochemistry.* 38:16067-16075.

83. Fujimoto, K., Miyata, T. and Aoyama, Y., 2000. Saccharide-directed cell recognition and molecular delivery using macrocyclic saccharide clusters: masking of hydrophobicity to enhance the saccharide specificity. *J. Am. Chem. Soc.*, 122:3558-3559.

84. Terrett, N. K. *Combinatorial chemistry*, Oxford University Press: New York, 1998.

85. Stemberg, E. D., Dolphin, D., Brucker, C., 1998. Porphyrin-based photosensitizers for use in photodynamic therapy. *Tetrahedron.* 54:4151-4202.

86. Drain, C. M., Gong, X., Ruta, V., Soll, E. and Chicoineau, P. F., 1999. Cominatorial synthesis and modification of fubctional porphyrin libraries: identification of new, amphipathic motifs for biomolecule binding. *J. Comb. Chem.*, 1:286-290.

87.Anantha, N. V., Azam, M. and sheardy, R. D., 1998. Porphyrin binding to quadruplexed T4G4. *Biochemistry.* 37:2709-2714.

88. Arthanari, H., Basu, S., Kawano, T. L., and Bolton, P. H., 1998. Fluorescent dyes specific for quadruplex DNA. *Nucleic Acid Res.* 26(16):3724-3728.

89. Wu, X., Maizels, N., 2001. Substrate- specific inhibition of RecQ helicase. *Nucleic Acids Research*, 29(8):1765-1771.

90. Brosh, R. M., Karow, J. K., White, E. J., Shaw, N. D., Hickson, I. D., and Bohr, V. A., 2000. Potent inhibition of Werner and Bloom helicases by DNA minor groove binding drugs. *Nucleic Acids Research*. 28:2420-2430.

91. Li, Y., Geyer, C. R., and Sen, D., 1996. Recognition of anionic porphyrins by DNA aptamers. *Biochemistry*. 35:6911-6922.

92. Koeppel, F., Riou, J. F., Laoui, A., Milliet, P., Arimondo, P. B., Labit, D., Petitgenet, O., Helene, C., and Mergney, J. L., 2001. Ethidium derivatives bind to G-quartets, inhibit telomerase and act as fluorescence probe for quadruplex. *Nucleic Acids Research*. 29(5):1087-1096.

93. Komath, S. S., Kenoth, R., Giribabu, L., Maiya, G., Swamy, M. J., 2000. Fluorescence and absorption spectroscopic studies on the interaction of porphyrin with snake gourd (Trichosanthes anguina) seed lectin. *J. Photochem. Photobiol. B: Biol.* 55:49-55.

94. Birchall, P. S., Fishpool, R. M., and Albertson, D. G., 1995. *Nature genet,* 11:314-320.

95. Lawerance, J. B., Villnace, C. A., and Singer, R.H., 1988. *Cell,* 52:51-61.

96. Randolph, J. B., and Waggoner, A. S. 1997. Stability, specificity and fluorescence brightness of multiply-labeled florescent DNA probe. *Nucleic Acids Research.* 25(14):2923-2929.

97. Folsom, V., Hunkeler, M. J., Haces, A., and Harding, J. D., 1989. *Anal. Biochem.* 182:309-314.

98. Ozaki, H., and Mclaughlin, L. W., 1992. *Nucleic Acids Research.* 20:5205-5214.

99. Hawkins, M. E., Pfleiderer, W., Balis, F. M., Porter, D. and Knutson, J. R., 1997. Fluorescence properties of pteridine nucleoside analogs as monomers and incorporated into oligonucleotides. *Analytical Biochemistry* 244:86-95.

100. Hawkins, M. E., Pfleiderer, W., Mazumder, A., Pommier, Y. G., and Balis, F. M., 1995. Incorporation of a fluorescent guanosine analog into oligonucleotides and its application to a real time assay for HIV-I integrase 3' processing reaction. *Nucleic Acids Research.* 23:2872-2880.

101. Hawkins, M. E., 2001. Fluorescent pteridine nucleoside analogs: a window on DNA interactions. *Cell Biochemistry and Biophysics.* 34:257-281.

102. Simonsson, T. and Sjoback, R., 1999. DNA tetraplex formation studies with fluorescence resonance energy transfer. *Journal of Biological Chemistry.* 274(24):17379-17383.

103. Mergny, J. L., 1999. Fluorescence energy transfer as a probe for tetraplex formation: the i-motif. *Biochemistry.* 38:1573-1581.

104. Mergny, J. L. and Maurizot, J. C. 2001. Flourescnce resonance energy transfer as a probe for G-quartet formation by a telomeric repeat. *Chem. Bio. Chem.* 2:124-132.